DISS. ETH NO. 24724

Defining key proteins of the primary carbohydrate metabolism in *Arabidopsis thaliana*

A thesis submitted to attain the degree of

DOCTOR OF SCIENCES of ETH ZURICH
(Dr. sc. ETH Zurich)

presented by

Dániel Árpád Carrera

Master's Degree, Eötvös Loránd University (Budapest, Hungary)

born on 01.09.1987
citizen of Hungary

accepted on the recommendation of

Prof. Samuel C. Zeeman (examiner)
Dr. Sebastian Streb (co-examiner)
Dr. Yves Gibon (co-examiner)

2017

Acknowledgement

There are so many people, who supported me and without whom I would have not been able to complete my work.

First, I would like to thank two persons. I am very grateful to **Sam Zeeman** for providing me this opportunity in his group, his door was always opened and his suggestions and feedbacks were always helpful. **Sebastian Streb** was a fantastic supervisor, who not only taught me many new techniques, but he was always full with new ideas. His out-of-the-box way of thinking is a skill, I can only hope to acquire once.

Simona Eicke was always happy to help me and I could turn to her, if I needed something in the lab. **Gavin George** was more than a postdoc, a very clever person and a good friend, who contributed to my FBA project significantly.

I would like to thank to **Martina Zanella**, **Tina Schreier** and **Federica Assenza**, our small group of PhD students, with whom I started together. They were a great company during my whole time even outside of the lab. **Barbara Pfister** and **Dave Seung** was always happy to help me.

I am equally thankful to **all the members of the group**.

I would also like to thank my friends and family, especially to my **mother**, who unconditionally supported me in my whole life. Finally, I would like to express my deepest gratitude to my incredible wife, **Eszter**, who has been always there for me, and without whom my life even with a PhD would be meaningless.

Table of content

Summary

Photosynthetic assimilation of atmospheric carbon dioxide (CO_2) is the major carbon fixation mechanism. Thereby the captured light energy is used to produce carbohydrates within the Calvin-Benson cycle. A portion of the synthesized carbohydrates is exported out of the chloroplast into the cytosol, where sucrose can be produced. Sucrose is a non-reducing, neutral disaccharide, which can be transported throughout the plant, providing the necessary carbon and energy for development.

The Calvin-Benson cycle and cytosolic sucrose metabolism build a complex network consisting of many highly regulated biochemical reactions. One characteristic of primary carbohydrate metabolism in plants is the apparent high level of genetic redundancy, especially among the cytosolic sucrose-metabolic enzymes. While the biochemical reactions are relatively well described, the role of the single isoforms is still unclear, and the apparent redundant isoforms might have a metabolic and physiological role. The aim of this work was to unravel and clarify the function of these (iso)enzymes and, if possible, attribute specific functions to them.

First, homozygous single knock-out mutants were screened for phenotypic differences under normal growth conditions. This rarely revealed significant alterations compared to the wild type, suggesting that the isoenzymes may actually be redundant. However, as plants are naturally constantly exposed to environmental fluctuations, the roles of the isoforms may become apparent during acclimation. We therefore established a hydroponic platform, where plants could be grown in well-defined nutrient-deficient media (either without nitrate or phosphate) and under mild long-term abiotic stresses (cold, warm, salt or osmotic stress). This allowed me to perform a comparative proteomic analysis in wild type plants, where the plants' stress responses to different treatments were examined in both the shoot and the root (Chapter 1). My results suggested that the plants response to the different stresses in a very specific manners. Furthermore, these responses were distinct in the root and the shoot.

To link the changes in the proteome with changes at the metabolic level, we also measured carbohydrates in the hydroponically grown plants (Chapter 2). Moreover, I selected promising candidates based on the proteomic analyses, i.e. sucrose-metabolic proteins that were either up- or downregulated in one of the stress responses. The corresponding single mutants were then grown under the stress treatments and analyzed for their growth and early development (Chapter 2).

One isoform among the four sucrose phosphate phosphatases (SPP2) and one fructokinase (FRK) turned out to be essential in seed development, the complete knock-out of them resulted in aborted seed development and non-viable plants. The knock-out mutant of another fructokinase (FRK7), which had been downregulated during the salt-stress treatment, grew slower under normal conditions, but was not further impaired during this stress. Further, a cytosolic fructose 1,6-bisphosphate aldolase (FBA8) appeared as the major isoform of its gene family in the cytosol.

In the final part of this work (Chapter 3), I characterized additional fructose 1,6-bisphosphate aldolases. The FBA family is known to have diverse functions in plant physiology (i.e. glycolysis, sucrose biosynthesis, Calvin-Benson cycle), but I focused on their role in the Calvin-Benson cycle and investigated the three plastidial isoforms (FBA1, FBA2 and FBA3). While the *fba1* mutant was indistinguishable from the wild type, the *fba2* and *fba3* single mutants grew considerably slower and displayed additional distinct phenotypes: The *fba2* mutant showed a marked decrease in total FBA activity and a low level of starch coupled with a high sugar content. The *fba3* mutant had an extremely high carbohydrate content, displaying five times elevated sugar and starch levels at the end of the day, but the total FBA activity was altered only little. GUS-reporter lines suggested that FBA3 was predominantly expressed in vascular tissues. This was in contrast to FBA1 and FBA2, which were expressed predominantly in the photosynthesizing cells of the leaf lamina. These data indicate that FBA1 and FBA2 catalyze the canonical reactions in the Calvin-Benson cycle, with FBA2 being the major isoform. By contrast, FBA3 is probably functional in non-photosynthesizing, heterotrophic tissues, especially in the vasculature. The knock-out of FBA3 created a barrier between the photosynthesizing source tissues and the heterotrophic sink tissues.

Zusammenfassung

Die photosynthetische Assimilation von atmosphärischem Kohlendioxid (CO_2) ist der wichtigster Mechanismus zur Kohlenstofffixierung. Hierbei dient die aufgefangene Lichtenergie der Synthese von Kohlenhydraten innerhalb des Calvin-Benson-Zyklus. Ein Teil dieser Kohlenhydrate wird aus dem Chloroplasten ins Zytosol exportiert, wo Saccharose synthetisiert werden kann. Saccharose ist ein nichtreduzierender ungeladener Zweifachzucker, welcher als Transportmolekül die Pflanze mit dem nötigen Kohlenstoff und Energie versorgt.

Der Calvin-Benson-Zyklus und der Saccharose-Metabolismus bilden ein komplexes Netzwerk aus vielen streng regulierten biochemischen Reaktionen. Typisch ist der hohe Grad an Redundanz, insbesondere unter den Enzymen, die im Zytosol Saccharose metabolisieren. Während die biochemischen Reaktionen gut beschrieben sind, ist die Rolle der einzelnen Isoformen noch unklar. Das Ziel dieser Arbeit war es deshalb, die Funktion dieser Isoformen zu enträtseln und, falls möglich, ihnen neue Funktionen zuzuordnen.

Als erstes haben wir homozygote Einzelmutanten auf phänotypische Veränderungen unter normalen Wachstumsbedingungen untersucht. Da diese Mutanten kaum signifikante Unterschiede zum Wildtyp aufwiesen, könnte man meinen, dass die Isoenzyme nutzlos wären. In der Natur sind Pflanzen allerdings diversen Umwelteinflüssen ausgesetzt, und möglicherweise treten die Funktionen der einzelnen Isoformen erst während der Anpassung an diese Einflüsse zu Tage. Um dies zu testen, haben wir eine Plattform für Hydrokulturen entwickelt, in der wir Pflanzen in wohldefinierten Mangel-Nährlösungen (entweder ohne Stickstoff oder ohne Phosphat) und unter milden abiotischen Stressen (Kälte-, Wärme-, Salz- oder osmotischer Stress) wachsen lassen konnten. Diese Plattform erlaubte mir anschliessend, das Proteom von Wildtyppflanzen unter diesen Stressbedingungen sowohl in der Wurzel als auch im Spross zu untersuchen (Kapitel 1). Meine Ergebnisse deuteten darauf hin, dass die Pflanze auf die Stressarten jeweils verschieden reagiert. Ausserdem unterschieden sich die Stressantworten in der Wurzel von jenen im Spross.

Um die Veränderungen im Proteom der Pflanze mit Veränderungen im Stoffwechsel zu verknüpfen, haben wir die Kohlenhydratmengen bestimmt (Kapitel 2). Basierend auf den Proteom-Analysen haben wir ausserdem vielversprechende Kandidaten für weitere Untersuchen ausgewählt, d.h. Saccharose metabolisierende Proteine, die unter Stressbehandlung entweder erhöht oder erniedrigt vorlagen. Die entsprechenden Einzelmutanten wurden anschliessend verschiedenen Stressen ausgesetzt und ihr Wachstum und ihre frühe Entwicklung analysiert.

Eine Isoform der Saccharosephosphat-Phosphatasen (SPP2) und eine Fructokinase (FRK) stellten sich als essentiell für die Samenentwicklung heraus. Die Mutante einer anderen Fructokinase (FRK7), welche unter Salzstress im Wildtyp verringert vorlag, wuchs zwar bereits unter Kontrollbedingungen verlangsamt, war unter Salzstress aber nicht zusätzlich beeinträchtigt. Weiters schien eine zytosolische Fructose-1,6-Bisphosphat-Aldolase (FBA8) die Hauptform im Zytosol zu sein. Diese Enzyme bilden nun interessante Kandidaten für weiterführende Untersuchungen des primären Kohlenhydratstoffwechsels.

Im letzten Teil dieser Arbeit (Kapitel 3) charakterisierte ich drei weitere Fructose-1,6-Bisphosphat-Aldolasen. Diese Enzymfamilie weist eine grosse funktionelle Bandbreite auf (i.e. Glykolyse, Saccharosebiosynthese, Calvin-Benson-Zyklus). Da ich jedoch primär an ihrer Rolle im Calvin-Benson-Zyklus interessiert war, konzentrierte ich mich auf die drei plastidären Isoformen (FBA1, FBA2 und FBA3). Während die *fba1*-Mutante nicht vom Wildtyp unterscheidbar war, wuchsen die *fba2*- und *fba3*-Mutanten deutlich langsamer und wiesen weitere spezifische Phänotypen auf: Die *fba2*-Mutante besass eine viel geringere FBA-Gesamtenzymaktivität, verringerte Stärkemengen und einen erhöhten Zuckerlevel. Die *fba3*-Mutante hingegen zeigte extrem hohe Kohlenhydratwerte (fünffach erhöhte Zucker- und Stärkelevels am Ende des Tages), aber nur geringfügig verringerte FBA-Enzymaktivität. GUS-Färbeexperimente deuteten darauf hin, dass FBA3 hauptsächlich im vaskulären Gewebe exprimiert ist. Im Gegensatz dazu schienen FBA1 und FBA2 primär in photosynthetisch aktiven Zellen der Blattspreite aufzutreten. Diese Daten weisen darauf hin, dass FBA1 und FBA2 die kanonischen Reaktionen im Calvin-Benson-Zyklus katalysieren, wobei FBA2 wohl die Hauptform bildet. FBA3 hingegen scheint hauptsächlich in photosynthetisch inaktivem, heterotrophen Gewebe zu wirken, vornehmlich im vaskulären Gewebe. Möglicherweise erleichtert es dort den Transport von Zuckern von ihrer Quelle zur Senke.

1) Introduction

Importance of improvement in primary carbohydrate metabolism and stress tolerance in terms of agricultural yield and future food production

Human nutrition relies almost entirely on agriculture and its productivity, but the sustainability of the system is doubtful; maintaining the productivity on the present level is already questionable. Conservative projections estimate that there will be approximately 9 (7-11) billion inhabitants on Earth in 2050 (FAO, 2012) and the increasing demand for food is coupled with limited land area. Based on this estimate, agricultural production will have to increase by 50 to 100% until 2050, but historical rates of yield growth for most crops are only half of what would be required to achieve this (Curtis and Halford, 2013). Increasing food production is technically very challenging (Raines, 2011; Dockter et. al 2014), and climate change further endangers the whole process. The annual improvements achieved since the Green Revolution are slowing down, stagnating or even reversing (Long et. al, 2015). A mild scenario suggests a 2°C rise in global temperature, and the present effects of global warming on food production are only partially and temporarily compensated by the ability of the existing crops to acclimate and adapt (Challinor et. al, 2013). Increased temperature will be coupled with further stresses. The frequency of disturbances (i.e. drought, floods, increased salt concentration in soil, nutrient limitations, etc.) will increase, and by the end of the 21st century, many densely populated areas will be seriously arid regions (Dai, 2012).

Due to their sessile lifestyle, plants cannot actively move and change position, they are inevitably exposed to the changing environmental conditions during their normal lifetime; hence, they have to cope with them directly in order to minimize or compensate for the loss in their fitness. Abiotic stress can be defined as the negative impact of a non-living agent. Biotic stressors include other living organisms such as bacteria, fungi, insects or even humans. Abiotic stress can include a great variety of very different stressors: temperature shift, drought, flooding, elevated salt, wind, fire, nutrient limitation, radiation, etc. It is basically unavoidable, and the simultaneous occurrence of different abiotic stressors, which is common in the natural environment, can even multiply their detrimental effect on aplant’s physiology.

There is still a huge gap between the maximum materialized and the average yield. The combination of biotic and abiotic stress can reduce the productivity by 65-87% depending on the crop (Shinozaki et. al, 2015), and this gap has to be reduced. The acclimation, resistance, avoidance and adaptation strategies have been extensively investigated, but the underlying mechanisms are very complex and still only partially understood. Improved knowledge about signaling pathways, transcription factors and regulated proteins of the cellular machinery would facilitate the efforts to optimize crop breeding.

Besides the incredible capabilities of plants to acclimate, tolerate and overcome suboptimal conditions, there are other physiological processes above stress resistance that can be exploited better to increase the agricultural yield. One way might be to improve the photosynthetic efficiency and modulate primary carbohydrate metabolism, but it is only one of many methods to improve agricultural yield. Every aspect of resource limitation can reduce growth and it should be optimized. Even if resources are not limited, their import and utilization can be. Plant anatomy and architecture can be altered or new varieties and species can be bred.

Carbohydrate metabolism is a good target, because in many crop plants they are the desired end products. The synthesis, utilization, transport, storage and remobilization of carbohydrates are tightly controlled and adapt to environmental disturbances and cope with changes in energy and supply demand (Bae et. al, 2005; Nishizawa et. al, 2008; Schmitz et. al, 2012, Thalmann et. al, 2016). Photoassimilates produced via the Calvin-Benson cycle are transported and used as building blocks for all organic compounds. The rate of photosynthesis influence biomass and elevated carbon assimilation results in higher biomass, which can directly or indirectly influence the yield (Zhu et. al, 2010; Long et. al, 2015). As a consequence, several approaches to manipulate photosynthesis were undertaken to increase plant yield (Simkin et. al, 2015; Ding et. al, 2016; Simkin et. al, 2016). Assimilated carbon is partitioned directly into sucrose and starch in most plants. During the night, they rely mostly on starch reserves in the leaf; small disturbances in leaf starch turnover affect metabolism and growth (Stitt and Zeeman, 2012) and vice versa. Starch and soluble sugar metabolism in plants is highly affected by changing environmental conditions and they play an active role in the plants' response to stress too (Krasensky and Jonak, 2012). Sugars can serve as

osmoprotectants and signaling molecules, and are usually accumulated in long-term stresses (Kempa et. al, 2008).

Primary carbohydrate metabolism

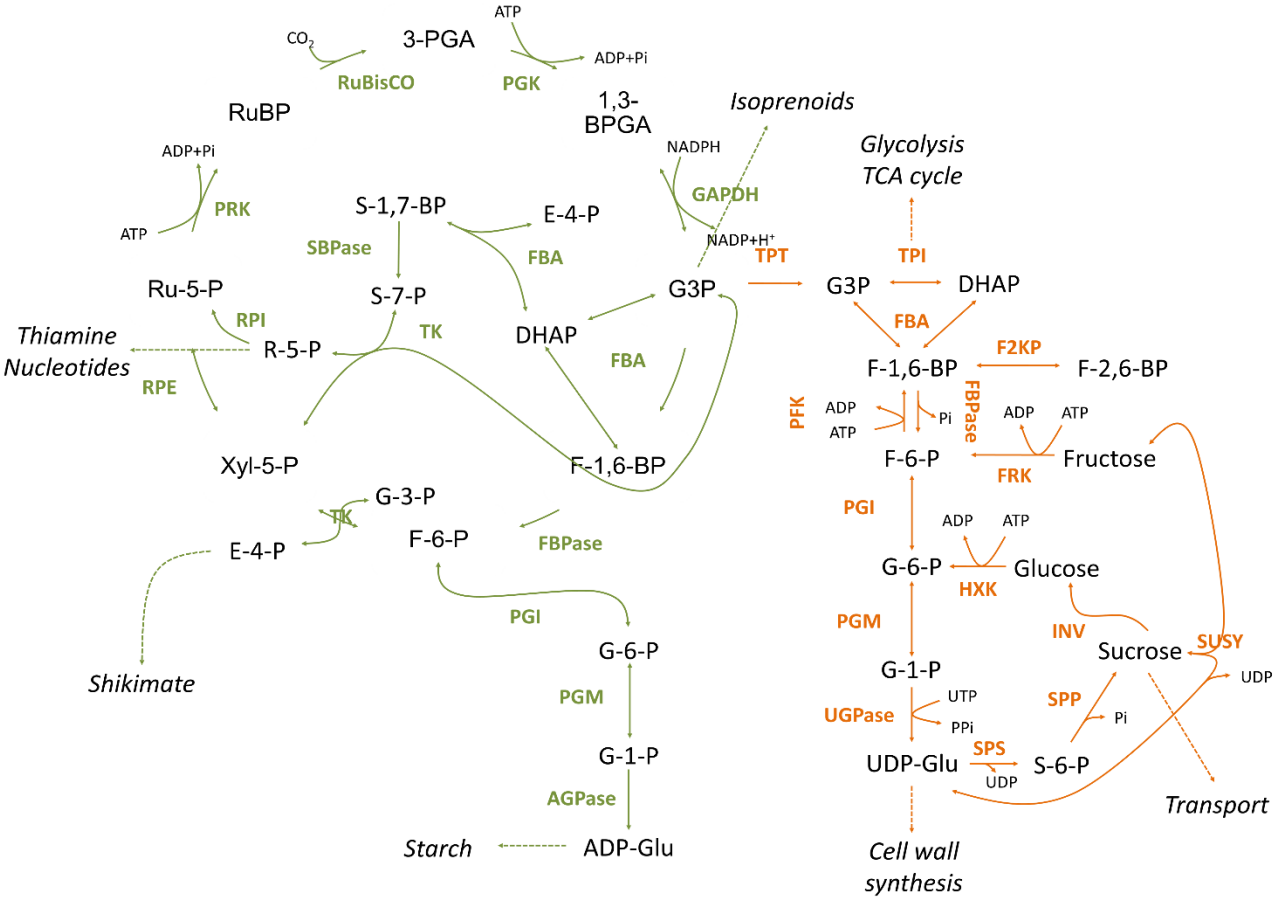

Figure 1-1. Schematic representation of the Calvin-Benson cycle and cytosolic sucrose metabolism. Pathways located in the plastid and the cytosol are depicted with green and orange respectively. Dashed lines represent exit point out of central carbohydrate metabolism. Metabolites are in black, enzymes are in color. PGI: phosphoglucoisomerase, PGM: phosphoglucomutase, TK: transketolase, TPT: triose phosphate/phosphate translocator, INV: invertases, SUSY: sucrose synthase, FRK: fructokinases, HXK: hexokinase, TPI: triose phosphate isomerase, PGK: phosphoglycerate kinase, PFK: ATP-dependent phosphofructokinases, SPS: sucrose-phosphate synthase, SPP: sucrose-phosphate phosphatase, UGPase: UDP-Glucose Pyrophosphorylase, AGPase: ADP-Glucose Pyrophosphorylase, FBA: Fructose 1,6-bisphosphate aldolase, SBPase: Sedoheptulose 1,7-bisphosphatase, FBPase: Fructose 1,6-bisphosphatase, F2KP: 6-phosphofructo-2-kinase/fructose- 2,6-bisphosphatase, PRK: Phosphoribulokinase, RuBisCO: Ribulose 1,5-bisphosphate carboxylase/oxygenase, RPI: phosphopentose isomerase, RPE: phosphopentose epimerase, F-1,6-BP: fructose 1,6-bisphosphate, F-2,6-BP: fructose 2,6-bisphosphate, E4P: erythrose 4-phosphate, SBP: sedoheptulose 1,7-bisphosphate, S-7-P: sedoheptulose 7-phosphate, F-6-P: fructose 6-phosphate, G-6-P: glucose 6-phosphate, G-1-P: glucose 1-phosphate, ADP-Glu: ADP-glucose, UDP-Glu: UDP-glucose, S-6-P: sucrose 6-phosphate, DHAP: dihydroxy acetone phosphate, G3P: glycerylaldehyde 3-phosphate, Ru-5-P: ribulose 5-phosphate, RuBP: ribulose 1,5-bisphosphate, R-5-P: ribose 5-phosphate, Xyl-5-P: xylose 5-phosphate, 3-PGA: 3-phosphoglycerate, 1,3-BPGA: 1,3-bisphosphoglycerate

The Calvin-Benson cycle

The principal CO_2 fixation pathway in plants is the Calvin-Benson cycle in the chloroplast stroma, where atmospheric CO_2 is incorporated into organic compounds through the ribulose 1,5-bisphosphate carboxylase/oxygenase (RuBisCO), which catalyzes the initial carboxylating reaction in the cycle (Fig. 1). The necessary energy and reducing power for the conversion of inorganic carbon into organic compounds is provided by the previously captured light. The cycle is organized in three phases: CO_2 fixation, reduction of 3-phosphoglycerate, regeneration of RuBP. At the end of the reduction phase triose-phosphates are produced, which are either metabolized further in the Calvin-Benson cycle, or exported out of the plastid into the cytosol. Five out of six triose phosphates produced by the cycle remain within, one-sixth exits the cycle. If they are exported out of the chloroplast, they can be used to produce into sucrose and transported throughout the plant.

The pathway was discovered and described thoroughly in 1950s (Melvin Calvin, 1962), the biochemical basis of the cycle is well investigated; Melvin Calvin was merited with the Nobel Price of Chemistry in 1961 for his work to unravel and characterize the process, he is one of the few Nobel Laureates, who came from the field of plant sciences. He conducted his research with his team (Andrew Benson and James Bassham) at the University of California, Berkeley.

The pathway of the Calvin-Benson cycle

The three phases of the Calvin-Benson cycle (carboxylation, reduction and regeneration) consist of several highly coordinated reactions:

1) Carboxylation
    a) Three CO_2, H_2O and ribulose 1,5-bisphosphate (RuBP) molecules are formed together to produce six 3-phosphoglycerate (3-PGA) by Ribulose 1,5-bisphosphate carboxylase/oxygenase (RuBisCO)
2) Reduction
    a) 3-PGA is further phosphorylated by 3-phosphoglycerate kinase
    b) Glyceraldehyde 3-phosphate (G3P) is produced by glyceraldehyde 3-phosphate dehydrogenase (GAPD)

3) Regeneration of RuBP
    a) Triose phosphate isomerase converts G3P into dihydroxyacetone phosphate (DHAP)
    b) Fructose 1,6-phosphate aldolase (FBA) catalyses the condensation of two bisphosphates. Fructose 1,6-bisphosphate (F-1,6-BP) and sedoheptulose 1,7-bisphosphate (S-1,7-BP) are produced out of G3P and DHAP and erythrose 4-phosphate (E-4-P) and DHAP respectively.
    c) F-1,6-BP is dephosphorylated by fructose 1,6-bisphosphatase (FBPase)
    d) S-1,7-BP is dephosphorylated by sedoheptulose 1,7-bisphosphatase (SBPase)
    e) The substrates of transketolase (TK) are S-7-P and G3P, which are converted into Xylulose 5-phosphate (Xyl-5-P) and ribose 5-phosphate (R-5-P).
    f) Xyl-5-P is transformed into ribulose 5-phosphate (Ru-5-P) by ribulose 5-phosphate epimerase (RPE)
    g) R-5-P is converted into ribulose 5-phosphate (Ru-5-P) by ribose 5-phosphate isomerase (RPI)
    h) The final regeneration step is the phosphorylation of the Ru-5-P by phosphoribulokinase (PRK), which generates the necessary RuBP donor for the incorporation of CO_2 by the RuBisCO.

The Calvin-Benson cycle and the flux through it are regulated very strongly. This regulation involves protein-protein interactions (i.e. Rubsico activase (Archie Portis, 2013), assembly of protein complex by the CP12 (Graciet et. al, 2004)), posttranslational modification (i.e. redox regulation via the ferredoxin-thioredoxin system (Michelet et. al, 2013), methylation (Minnino et. al, 2012)), allosteric control (ATP-dependent steps in the cycle) and the enzymes participating in the pathway can control the flux over the system (Zhu et. al, 2007). The enzymes, which catalyse irreversible reactions (i.e. PRK, FBPase, SBPase), were considered for a long time key enzymes of the cycle as an enzymatic bottlenecks, but this view turned out to be rather artificial than biologically relevant (Zhu et, al, 2007; Christine Raines, 2011). On one hand, the irreversibility does not automatically imply flux control, and on the other hand, all the enzymes of the Calvin-Benson cycle are key enzymes. The RuBisCO itself catalyses an oxygenation reaction next to the carboxylation (photorespiration), which provides another layer of control, but this complex process will not be discussed furtherhere.

Cytosolic sucrose metabolism, biosynthesis of sucrose

Sucrose is the major end product of photosynthesis. It is a non-reducing, neutral disaccharide and is transported throughout the plant from source to sink tissues via the phloem to supply energy and carbon (e.g. from photosynthesizing leaves to roots or seeds).

The sucrose metabolic network in the cytosol can be divided into different sub-processes, which represent the metabolic steps of synthesis, breakdown or transport of sucrose. First, triose-phosphates are transported out of the chloroplast by the triose phosphate/phosphate translocators (TPT), which in Arabidopsis has two isoforms (TPT1 and TPT2) (Schmitz et. al, 2012), and the loss of TPT in the *tpt2* homozygous single knock-out mutant results in a slow growth phenotype (Walters et. al, 2004), but is viable, because it can be bypassed and sugars can supplied from the chloroplast by different transporters. Transporters (MEX1, GPT1), which are responsible for the export of starch degradation products (maltose and glucose) during the night (Niittylä et al., 2004; Kunz et. al, 2010), can compensate partially the loss of TPT. Simultaneously, starch synthesis is also increased to compensate the lack of the transporters (Walters et. al, 2004).

Triose phosphates are interconverted reversibly into fructose-1,6-bisphosphate by fructose 1,6 bisphosphate aldolase (FBA), which also has several isoforms (Lu et. al, 2012, Cai et. al, 2016). There are three plastidial and five cytosolic FBAs annotated in *Arabidopsis thaliana*. The irreversible removal of the phosphate group from the FBP generates fructose 6-phosphate and is catalyzed by the single FBPase enzyme (Rojas-González et. al, 2015). This step is regulated by the level of fructose 2,6-bisphosphate, which is controlled by 6-phosphofructo-2-kinase/fructose- 2,6-bisphosphatase (F2KP), which allows further control over the whole sucrose production and carbon assimilation in the plant cell (McCormick and Kruger, 2010). Fructose 2,6-bisphosphate (F-2,6-P), which is a specific cytosolic signaling molecule, inhibits the FBPase, F-2,6-P levels depend on the status of the triose phosphate and hexose phosphate pools, which are monitored constantly. Next to the FBPase, two other enzymes are involved in the interconversion of fructose 6-phosphate to fructose 1,6-bisphosphate: ATP-dependent phosphofructokinases (PFK) and Pyrophosphate-dependent phosphofructokinases (PFP) (Mustroph et. al, 2007; Lim et. al, 2009). While PFK catalyzes the irreversible reaction of

phosphorylation of fructose 6-phosphate, PFP catalyzes the reversible interconversion between the phosphorylated sugars.

The hexose-phosphate pool consists of fructose 6-phosphate (F-6-P), glucose 6-phosphate (G-6-P) and glucose 1-phosphate (G-1-P). Two enzymes, PGM and PGI perform the reversible interconversion of the respective hexose phosphates (PGM: F-6-P ↔ G-6-P, PGI: G-6-P ↔ G-1-P). In Arabidopsis, PGI has one, PGM has two cytosolic isoforms and the complete knock-out of their activity results in an unviable plant showing the essential role of the hexose-phosphate pool (Egli et. al, 2010; Kunz et. al, 2014). Glucose 1-phosphate and UTP are substrates of the UGPase, a gene family with three isoforms, which converts them to UDP-glucose and pyrophosphate (Park et. al, 2012). The hexose-phosphate pool is followed by the actual biosynthesis of sucrose. Sucrose-phosphate synthase (SPS) catalyzes the formation of sucrose 6-phosphate from fructose 6-phosphate and UDP-glucose (Sun et. al, 2011). Subsequently, as the final step, sucrose 6-P is hydrolyzed by a specific sucrose-phosphate phosphatase (SPP) to release sucrose, both the SPP and SPS gene families have four isoforms (Volkert et. al, 2014; Albi et. al, 2016).

Breakdown and transport of sucrose

Sucrose is produced in the mesophyll cells and can be transported out of the cell or into the vacuole, where it can be stored. Sucrose can be catabolized to hexose phosphates, which can follow two routes: the breakdown can be done by invertases or sucrose synthases. Invertases hydrolyze sucrose irreversibly to glucose and fructose, sucrose synthases catalyze the reversible conversion of sucrose to fructose and UDP-glucose (Barratt et. al, 2009). Invertase is a big family with many isoforms of a broad range of functions in different subcellular localizations (cell wall, cytosol, and vacuole) (Ruan et. al, 2010). Sucrose synthase might function primarily in non-photosynthetic cells (Fujii et. al, 2009). The generated hexoses (fructose and glucose) need to be phosphorylated to enter the hexose phosphate pool again, which is performed by kinases in an irreversible reaction. Fructose is phosphorylated by fructokinases (FRK) (Riggs et. al, 2017), glucose by hexokinases (HXK) (Claeyssen and Rivoal, 2007). HXK can phosphorylate fructose too. Some hexokinase isoforms fulfill only a catalytic function, but other plays a role in signaling as a glucose sensor too (Jang et. al, 1997).

In order to reach the sink tissues, sucrose has to be loaded into the phloem and subsequently unloaded. A broad family of sucrose transporters (SUTs, SWEETs, HXTs) is responsible for these crucial processes in the plasma membrane or the vacuole (Kühn and Grof, 2008; Li et. al, 2017), and recently new key transporters were discovered and characterized (Chen et. al, 2012). Sucrose is mainly transported into the apoplasm and then loaded into the phloem by highly controlled couple reactions of different transporters. The efflux into the apoplasm is facilitated by SWEET transporters, which is followed by the phloem loading by SUT sucrose-H+ cotransporters (Chen et. al, 2012).

Biosynthesis of starch

Fructose 6-phosphate in the Calvin-Benson cycle is the exit point for starch synthesis, first it is converted into glucose 6-phosphate by the plastidial phosphoglucoisomerase (Yu et. al, 2000), which is followed by the plastidial phosphoglucomutase, which produces glucose 1-phosphate (Caspar et. al, 1985). The next step is catalyzed by ADP-glucose pyrophosphorylases. This enzyme takes ATP as a substrate, and produces ADP-glucose and inorganic pyrophosphate (Ventriglia et. al, 2008). ADP glucose is the direct precursor of the starch biosynthesis.

Starch is also a primary carbohydrate product of photosynthesis. It is semi-crystalline, insoluble glucose polymer that serves as a storage molecule. In *Arabidopsis thaliana* leaves, transitory starch is synthesized during the day until the subsequent night, when starch is broken down in the dark providing carbon and energy for growth and metabolism when there is no photosynthesis (Streb and Zeeman, 2012). It is under a strong, but flexible diurnal regulation (Kölling et. al, 2015), the synthesized starch is used up gradually during the night almost completely, which ensures that the plant does not go into starvation even at the end of the night.

Metabolic pathways diverging form the primary carbohydrate metabolism

Primary carbohydrate metabolism establishes the entry points for further key metabolic processes, essentially all the carbon molecules of the plant were at least once channeled through it. Erythrose 4-phosphate can be fueled into the shikimate pathway, which is essential for synthesis of aromatic amino acids, like tryptophan, phenylalanine or tyrosine (Meade and Dudareva, 2012). Ribose 5-phosphate is a key metabolite in the metabolism of nucleotides

and thiamines (Stasolla et. al, 2003; Aymeric Goyer, 2010). In the cytosol, UDP-glucose is the precursor of cell wall biosynthesis (Park et. al, 2010), triose phosphates are channeled into the glycolysis, citric acid cycle (Muñoz-Bertomeu et. al, 2009). Glycolysis also produces some ATP and with the citric acid cycle, which uses some of the produced energy, many of their intermediates serves as substrates for numerous biosynthetic pathways (amino acids, nucleic acids, fatty acids, etc.).

Proteomic analysis of the plants' stress response

Proteomics has become a powerful high-throughput tool and technique in the last decades (Aebersold and Mann, 2003), which has had a broad application since the beginning in the field of plant biology (Sacha Baginsky, 2009). It provides us with quantitative and systematic information about the abundance of proteins and can also be used to investigate protein-protein interactions, posttranslational modifications, organelle specific proteomes, etc.

Proteomic approaches have contributed much to our present understanding about plant's response to stress. Due to their sessile lifestyle, the only way for plants to minimize their loss in an unfavorable environment is to adjust their metabolism and development. Whole plant responses are studied with transcriptomic approaches (Agarwal et. al, 2014), as that method promises to deliver the broadest overview. However, based on transcriptional changes, it is not always possible to explain the current metabolic status of a biological system. It is challenging to predict the protein level based on the mRNA level. Transcripts can be seen as snapshots, which are followed by protein changes, and therefore, a remodeling of the cellular machinery over time as mRNA is translated into peptides (Stitt et. al, 2010; Baerenfaller et. al, 2012; Guerreiro et. al, 2014). Major metabolic enzymes and their changes in protein level can be a good target of a proteomic analysis during the stress response, because they are quite abundant, although it can be a technically challenging. RuBisCO can contribute up to 50% of the total protein content in the green tissues, and together with other major catalytic enzymes, it can obscure the detection of other less abundant proteins, making it difficult to look deeper into the plant proteome in the photosynthesizing tissues (Fröhlich et. al, 2012; Gupta et. al, 2015). In the last years, proteomic experiments have been carried out in different stress conditions, tissues, organelles and plant species (Kosová et. al, 2011; Rodziewicz et. al, 2013; Ghosh and Xu, 2014; Jorrín-Novo et. al, 2015; Janmohammadi et. al, 2015). Abiotic

stress research focused mainly on early stress response to an unnaturally strong abiotic factor. However, these experiments may be less suitable to investigate how plants tolerate and acclimate to longer-term environmental changes. Indeed plants in nature are almost always exposed to suboptimal conditions with one or several biotic and abiotic stressors.

Nutrient limitation

Nutrient availability is another key factor that can substantially limit plant growth and, as a result, yield. Nitrogen (N) and phosphorus (P) are two essential macronutrients, and are often limiting in agriculture, which can only be augmented with the application of N and P fertilizers (Masclaux-Daubresse et. al, 2010; Ågren et. al, 2012). This creates serious environmental problems and, on the top of that, the long-term supply of the fertilizers is also not sustainable (Natasha Gilbert, 2009). Phosphorus is provided by mining, but the resources are limited and may be completely exhausted in the next decades. N- and P-metabolism are highly interconnected with carbohydrate metabolism, and they have an influence on each other (Nunes-Nesi et. al, 2010). Plants growing in a nutrient deficient environment accumulate carbohydrates and have a reduced growth (Stitt and Krapp, 1999; Rouached et. al, 2010).

Isoform redundancy of the primary carbohydrate metabolism

There is a high degree of apparent redundancy among the genes encoding enzymes of primary carbohydrate metabolism. Genome sequencing in the past decades revealed multiple genes corresponding to many of the metabolic steps (i.e. six isoforms of the sucrose-synthase family, eight isoforms of the fructose 1,6 bisphosphate aldolases, or more than 20 invertases). Plant genomes tend to evolve at a higher rate than other eukaryotic organisms, genome sizes vary and duplication events happen more frequently (Panchy et. al, 2016). There is no well-described explanation for the high number of isoforms, but there might not be a universal reason. The numerous isoforms might provide robustness, stability and flexibility simultaneously. While certain steps are catalyzed by several isoforms, other reaction are strictly catalyzed by enzymes encoded by single genes (i.e. PGI, FBPase), and knocking them out can be lethal for the plants (i.e. PGI (Kunz et. al, 2014), RuBisCO (Feiz et. al, 2012). The single isoforms tend to be highly conserved among plant species (Egli et. al, 2010). One explanation can be that multiple isoforms are simply redundant and are responsible for the

same enzymatic step. If there is no metabolic bypass, the right combination of the knock-outs can reveal the redundancy with multiple mutants being lethal; the *pgm2pgm3* and *ugp1ugp2* double mutants are good examples (Egli et. al, 2010; Park et. al, 2010). On the other hand, other multiple knock-out mutants do not show any growth defect. For instance, a knock-out of four out of six sucrose synthases (SuSy1-4) has no phenotypical impact on plant development in normal growth environment (Barratt et. al, 2009; Baroja-Fernández et. al, 2011).

Gene family	Number of plastidial isoforms	Number of cytosolic isoforms
TPT		2
GPT		2
FBA	3	5
FBPase	2	1
F2KP		1
PGM	1	2
PGI	1	1
UGPase	1	2
SPS		4
SPP		4
SuSy		6
INV		>17
HXK	1	2
FRK	1(?)	6(?)
PFK	1(?)	6
PFP		4
RuBisCO	1(?)	
PRK	1	
PGK	2(?)	1(?)
SBPase	1	
TK	2	
RPI	2	2
RPE	1	2
GAPDH	3	2

Table 1-1. Number of plastidial and cytosolic isoforms of the primary carbohydrate gene families in *Arabidopsis thaliana*. (?) the number and/or the localization of the different isoforms is unclear. In this artificial framework, transporters (TPT, GPT, INV) were considered cytosolic.

In some cases, mutations affecting enzymes for which there is no known metabolic bypass, cause a severe phenotype (i.e. pFBPase), and yet is not lethal. In such cases, there might be other proteins, which can take over to a certain level, even if they do not belong to the same

gene family (Martina Zanella unpublished). Despite the unclear significance of the high level genetic redundancy, it is likely often to fulfill a specific role. E.g. the different isoforms might be important during stress response, in different tissues, developmental stages, etc. That said, even if the existence of different isoforms does not give an evolutionary advantage, if it does not cause a loss of fitness either, it may be kept and not necessary erased.

Aim of this work

In this work, I aimed to reveal new insights about the enzymes encoded by multiple genes in primary carbohydrate metabolism. While the biochemical basis of the primary carbohydrate metabolic reactions are relatively well described, even the basics can be sometimes questioned (e.g. whether the isoforms predicted from genome sequence information all catalyze the same reactions, which is not always absolutely correct). They may not have a catalytic role; some of them might have turned into a pseudogene or gained another (i.e. signaling) function. Even if distinct isoforms are responsible for the same metabolic step, it is possible to ask, what are their relative contributions and do they have distinct properties? Enzyme kinetic and substrate affinity data of individual members of most gene families are still lacking. It would not be feasible to analyze all the isoforms of all the enzymes of primary carbohydrate metabolism in the framework of this work, but based on our top-down approaches I selected a single gene family. The FBAs were selected and characterized in detail.

We established a hydroponic growth system, where plants were grown in liquid media and this enabled us to apply different controlled long-term, mild stress treatments. Plants were exposed to cold (15°C) or warm (25°C) temperatures, to 50 mM salt (NaCl) or to an increased osmoticum (5% PEG6000), as to nitrate, as phosphate deficiencies for 10 days. The mild conditions were set up so that the plants would be still able to develop and grow to a certainextent. The goal was to monitor them as they acclimated to the suboptimal environment, and to investigate it and how they rewire their metabolism in the changed conditions. The hydroponic system also allowed us to collect data from both the shoot and the root.

In Chapter 1, a comparative proteomic analysis was carried out. Together with other physiological results (leaf area, relative growth rate, fresh and dry weight) we characterized the stress responses of plants. The growth patterns and the proteomic data suggested that the adapted strategies of the plants were actually quite distinct being specific to the respective stress and also to the shoot and root tissues. I aimed to identify specific enzyme isoforms important in certain stress environment with proteomic experiments. Since major metabolic enzymes are abundant proteins this approach was feasible I was able to generate a list of

potential enzyme isoform that can play a role in the long-term stress response and acclimation. These candidates were further investigated individually.

Carbohydrates (starch and soluble sugars) were also measured in the same experiments (Chapter 2) to link the changes in the proteome and the level of carbohydrates. A mutant collection was also created as another top-down approach. Homozygous single gene knock-out mutants were created, each of which lacked an enzyme isoform of cytosolic sucrose metabolism or of the Calvin-Benson cycle. These mutants underwent a basic phenotyping and selected ones were also exposed to the stress treatments.

Both the cytosolic and plastidial isoforms of the fructose 1,6-bisphosphate aldolase (FBA) are considered to be crucial in the metabolism of the plants. FBA8, which is one the five cytosolic isoform, might be the key FBA enzyme in the cytosol. In the Chapter 3, I characterized the three plastidial isoforms (AtFBA1, AtFBA2, and AtFBA3) in-depth. The homozygous single knock-out mutants were isolated, crossed to create multiple mutants and further analyzed; enzyme activity, carbon assimilation, carbohydrate levels were measured in these mutants. These were complemented with phylogenetic and bioinformatic analysis and with experimental tissue localizations.

Reference

Aebersold, R., & Mann, M. (2003). Mass spectometry-based proteomics. *Nature*, 422(March), 198–207.

Agren, G. I., Wetterstedt, J. Å. M., & Billberger, M. F. K. (2012). Nutrient limitation on terrestrial plant growth - modeling the interaction between nitrogen and phosphorus. *New Phytologist*, 194, 953–960.

Albi, T., Ruiz, M. T., De Los Reyes, P., Valverde, F., & Romero, J. M. (2016). Characterization of the sucrose phosphate phosphatase (SPP) isoforms from *Arabidopsis thaliana* and role of the S6PPc domain in dimerization. *PLoS ONE*, 11(11), 1–19.

Bae, H., Herman, E., Bailey, B., Bae, H. J., & Sicher, R. (2005). Exogenous trehalose alters Arabidopsis transcripts involved in cell wall modification, abiotic stress, nitrogen metabolism, and plant defense. *Physiologia Plantarum*, 125(1), 114–126.

Baerenfaller, K., Massonnet, C., Walsh, S., Baginsky, S., Bühlmann, P., Hennig, L., … Gruissem, W. (2012). Systems-based analysis of Arabidopsis leaf growth reveals adaptation to water deficit. *Molecular Systems Biology*, 8(606), 606.

Baginsky, S. (2009). Plant proteomics: concepts, applications, and novel strategies for data interpretation. *Mass Spectrometry Reviews*, 28, 93–120.

Baroja-Fernández, E., Muñoz, F. J., Li, J., Bahaji, A., Almagro, G., Montero, M., … Pozueta-Romero, J. (2012). Sucrose synthase activity in the *sus1/sus2/sus3/sus4* Arabidopsis mutant is sufficient to support normal cellulose and starch production. *Proceedings of the National Academy of Sciences of the United States of America*, 109(1), 321–6.

Barratt, D. H. P., Derbyshire, P., Findlay, K., Pike, M., Wellner, N., Lunn, J., … Smith, A. M. (2009). Normal growth of Arabidopsis requires cytosolic invertase but not sucrose synthase. *Proceedings of the National Academy of Sciences of the United States of America*, 106(31), 13124–13129.

Cai, B., Li, Q., Xu, Y., Yang, L., Bi, H., & Ai, X. (2016). Genome-wide analysis of the fructose 1,6-bisphosphate aldolase (FBA) gene family and functional characterization of FBA7 in tomato. *Plant Physiology and Biochemistry*, 108, 251–265.

Calvin, M. (1962). The path of carbon in photosyntheis. *Angewandte Chemie*, I(February), 65–75.

Caspar, T., Huber, S. C., & Somerville, C. (1985). Alterations in growth, photosynthesis, and respiration in a starchless mutant of *Arabidopsis thaliana* (L.) deficient in chloroplast phosphoglucomutase activity. *Plant Physiol*, 79(1), 11–17.

Challinor, A. J., Watson, J., Lobell, D. B., Howden, S. M., Smith, D. R., & Chhetri, N. (2014). A meta-analysis of crop yield under climate change and adaptation. *Nature Climate Change*, 4, 287–291.

Chen, L.-Q., Qu, X.-Q., Hou, B.-H., Sosso, D., Osorio, S., Fernie, A. R., … Münch, E. (2012). Sucrose efflux mediated by SWEET proteins as a key step for phloem transport. *Science*, 335(6065), 207–211.

Chen, Y., Wang, X. M., Zhou, L., He, Y., Wang, D., Qi, Y. H., & Jiang, D. A. (2015). Rubisco activase is also a multiple responder to abiotic stresses in rice. *PLoS ONE*, 10(10), 1–16.

Claeyssen, E., & Rivoal, J. (2007, March). Isozymes of plant hexokinase: occurrence, properties and functions. *Phytochemistry*.

Curtis, T., & Halford, N. G. (2014). Food security: The challenge of increasing wheat yield and the importance of not compromising food safety. *Annals of Applied Biology*, 164(3), 354–372.

Dai, A. G. (2013). Increasing drought under global warming in observations and models. *Nature Climate Change*, 3(1), 52–58.

Ding, F., Wang, M., Zhang, S., Ai, X., Geiger, D. R., Servaites, J. C., … Heldt, H. W. (2016). Changes in SBPase activity influence photosynthetic capacity, growth, and tolerance to chilling stress in transgenic tomato plants. *Scientific Reports*, 6(August), 32741.

Dockter, C., Gruszka, D., Braumann, I., Druka, A., Druka, I., Franckowiak, J., … Hansson, M. (2014). Induced variations in brassinosteroid genes define barley height and sturdiness, and expand the Green Revolution genetic toolkit. *Plant Physiology*, 166(December), 1912–1927.

Egli, B., Kölling, K., Köhler, C., Zeeman, S. C., & Streb, S. (2010). Loss of cytosolic phosphoglucomutase compromises gametophyte development in Arabidopsis. *Plant Physiology*, 154(4), 1659–71.

Feiz, L., Williams-carrier, R., Wostrikoff, K., Belcher, S., Barkan, A., Stern, D.B., (2012). Ribulose-1 , 5-Bis-Phosphate Carboxylase / Oxygenase Accumulation Factor1 Is Required for Holoenzyme Assembly in Maize. *The Plant Cell*, 24, 3435–3446.

Frohlich, a., Gaupels, F., Sarioglu, H., Holzmeister, C., Spannagl, M., Durner, J., & Lindermayr, C. (2012). Looking deep inside: detection of low-abundance proteins in leaf extracts of Arabidopsis and phloem exudates of pumpkin. *Plant Physiology*, 159(3), 902–914.

Fujii, S., Hayashi, T., & Mizuno, K. (2010). Sucrose synthase is an integral component of the cellulose synthesis machinery. *Plant & Cell Physiology*, 51(2), 294–301.

Ghosh, D., & Xu, J. (2014). Abiotic stress responses in plant roots: a proteomics perspective. *Frontiers in Plant Science*, 5(JAN), 6.

Gilbert, N. (2009). Environment: the disappearing nutrient. *Nature*, 461(7265), 716–718.

Goyer, A. (2010). Thiamine in plants: aspects of its metabolism and functions. *Phytochemistry*, 71(14–15), 1615–1624.

Graciet, E., Lebreton, S., & Gontero, B. (2004). Emergence of new regulatory mechanisms in the Benson-Calvin pathway via protein-protein interactions: a glyceraldehyde-3-phosphate dehydrogenase/CP12/phosphoribulokinase complex. *Journal of Experimental Botany*, 55(400), 1245–54.

Guerreiro, A. C. L., Benevento, M., Lehmann, R., van Breukelen, B., Post, H., Giansanti, P., … Heck, A. J. R. (2014). Daily rhythms in the cyanobacterium synechococcus elongatus probed by high-resolution mass spectrometry-based proteomics reveals a small defined set of cyclic proteins. *Molecular & Cellular Proteomics*: MCP, 13(8), 2042–55.

Gupta, R., Wang, Y., Agrawal, G. K., Rakwal, R., Jo, I. H., Bang, K. H., & Kim, S. T. (2015). Time to dig deep into the plant proteome: a hunt for low-abundance proteins. *Frontiers in Plant Science*, 6(January), 22.

Jang, J. C., León, P., Zhou, L., & Sheen, J. (1997). Hexokinase as a sugar sensor in higher plants. *The Plant Cell*, 9(1), 5–19.

Janmohammadi, M., Zolla, L., & Rinalducci, S. (2015). Low temperature tolerance in plants: Changes at the protein level. *Phytochemistry*, 117, 76–89.

Jorrín-Novo, J. V., Pascual, J., Sánchez-Lucas, R., Romero-Rodríguez, M. C., Rodríguez-Ortega, M. J., Lenz, C., & Valledor, L. (2015). Fourteen years of plant proteomics reflected in

Proteomics: Moving from model species and 2DE-based approaches to orphan species and gel-free platforms. *Proteomics*, 15(5–6), 1089–1112.

Kempa, S., Krasensky, J., Dal Santo, S., Kopka, J., & Jonak, C. (2008). A central role of abscisic acid in stress-regulated carbohydrate metabolism. *PLoS ONE*, 3(12).

Kölling, K., Thalmann, M., Müller, A., Jenny, C., & Zeeman, S. C. (2015). Carbon partitioning in *Arabidopsis thaliana* is a dynamic process controlled by the plants metabolic status and its circadian clock. *Plant, Cell and Environment*, 38(10), 1965–1979.

Kosová, K., Vítámvás, P., Prásil, I. T., & Renaut, J. (2011). Plant proteome changes under abiotic stress - Contribution of proteomics studies to understanding plant stress response. *Journal of Proteomics*, 74(8), 1301–1322.

Krasensky, J., & Jonak, C. (2012). Drought, salt, and temperature stress-induced metabolic rearrangements and regulatory networks. *Journal of Experimental Botany*.

Kühn, C., & Grof, C. P. L. (2010). Sucrose transporters of higher plants. *Current Opinion in Plant Biology*, 13(3), 288–298.

Kunz, H. H., Häusler, R. E., Fettke, J., Herbst, K., Niewiadomski, P., Gierth, M., … Schneider, A. (2010). The role of plastidial glucose-6-phosphate/phosphate translocators in vegetative tissues of *Arabidopsis thaliana* mutants impaired in starch biosynthesis. *Plant Biology*, 12(SUPPL. 1), 115–128.

Li, J., Wu, L., Foster, R., & Ruan, Y. L. (2017). Molecular regulation of sucrose catabolism and sugar transport for development, defence and phloem function. *Journal of Integrative Plant Biology*, 59(5), 322–335.

Lim, H., Cho, M. H., Jeon, J. S., Bhoo, S. H., Kwon, Y. K., & Hahn, T. R. (2009). Altered expression of pyrophosphate: Fructose-6-phosphate 1-phosphotransferase affects the growth of transgenic Arabidopsis plants. *Molecules and Cells*, 27(6), 641–649.

Long, S. P., Marshall-Colon, A., & Zhu, X. G. (2015). Meeting the global food demand of the future by engineering crop photosynthesis and yield potential. *Cell*, 161(1), 56–66.

Lu, W., Tang, X., Huo, Y., Xu, R., Qi, S., Huang, J., … Wu, C. (2012). Identification and characterization of fructose 1,6-bisphosphate aldolase genes in Arabidopsis reveal a gene family with diverse responses to abiotic stresses. *Gene*, 503(1), 65–74.

Maeda, H., & Dudareva, N. (2012). The shikimate pathway and aromatic amino acid biosynthesis in plants. *Annu. Rev. Plant Biol*, 63, 73–105.

Masclaux-Daubresse, C., Daniel-Vedele, F., Dechorgnat, J., Chardon, F., Gaufichon, L., & Suzuki, A. (2010). Nitrogen uptake, assimilation and remobilization in plants: Challenges for sustainable and productive agriculture. *Annals of Botany*, 105(7), 1141–1157.

McCormick, A. J., & Kruger, N. J. (2015). Lack of fructose 2,6-bisphosphate compromises photosynthesis and growth in Arabidopsis in fluctuating environments. *Plant Journal*, 81(5), 670–683.

Michelet, L., Zaffagnini, M., Morisse, S., Sparla, F., Pérez-Pérez, M. E., Francia, F., … Lemaire, S. D. (2013). Redox regulation of the Calvin-Benson cycle: something old, something new. *Frontiers in Plant Science*, 4(November), 470.

Mininno, M., Brugière, S., Pautre, V., Gilgen, A., Ma, S., Ferro, M., … Ravanel, S. (2012). Characterization of chloroplastic fructose 1,6-bisphosphate aldolases as lysine-methylated proteins in plants. *The Journal of Biological Chemistry*, 287(25), 21034–44.

Muñoz-Bertomeu, J., Cascales-Miñana, B., Mulet, J. M., Baroja-Fernández, E., Pozueta-Romero, J., Kuhn, J. M., … Ros, R. (2009). Plastidial glyceraldehyde-3-phosphate

dehydrogenase deficiency leads to altered root development and affects the sugar and amino acid balance in Arabidopsis. *Plant Physiology*, 151(2), 541–558.

Mustroph, A., Sonnewald, U., & Biemelt, S. (2007). Characterisation of the ATP-dependent phosphofructokinase gene family from *Arabidopsis thaliana*. *FEBS Letters*, 581(13), 2401–2410.

Niittyla, T., Messerli, G., Trevisan, M., Chen, J., Smith, A. M., & Zeeman, S. C. (2004). A previously unknown maltose transporter essential for starch degradation in leaves. *Science*, 303(5654), 87–89.

Nishizawa, a., Yabuta, Y., & Shigeoka, S. (2008). Galactinol and raffinose constitute a novel function to protect plants from oxidative damage. *Plant Physiology*, 147(3), 1251–1263.

Nunes-Nesi, A., Fernie, A. R., & Stitt, M. (2010). Metabolic and signaling aspects underpinning the regulation of plant carbon nitrogen interactions. *Molecular Plant*, 3(6), 973–996.

Okazaki, Y., Shimojima, M., Sawada, Y., Toyooka, K., Narisawa, T., Mochida, K., … Saito, K. (2009). A chloroplastic UDP-glucose pyrophosphorylase from Arabidopsis is the committed enzyme for the first step of sulfolipid biosynthesis. *The Plant Cell*, 21(3), 892–909.

Panchy, N., Lehti-Shiu, M. D., & Shiu, S.-H. (2016). Evolution of gene duplication in plants. *Plant Physiology*, 171(4), 2294–2316.

Park, J.-I., Ishimizu, T., Suwabe, K., Sudo, K., Masuko, H., Hakozaki, H., … Watanabe, M. (2010). UDP-glucose pyrophosphorylase is rate limiting in vegetative and reproductive phases in *Arabidopsis thaliana*. *Plant & Cell Physiology*, 51(6), 981–96.

Portis, A. (2003). Rubisco activase - Rubisco's catalytic chaperone. *Photosynthesis Research*, 75(1), 11–27.

Raines, C. (2011). Increasing photosynthetic carbon assimilation in C3 plants to improve crop yield: current and future strategies. *Plant Physiology*, 155(January), 36–42.

Riggs, J. W., Cavales, P. C., Chapiro, S. M., & Callis, J. (2017). Identification and biochemical characterization of the fructokinase gene family in *Arabidopsis thaliana*. *BMC Plant Biol.*, 17(1), 83.

Rodziewicz, P., Swarcewicz, B., Chmielewska, K., Wojakowska, A., & Stobiecki, M. (2014). Influence of abiotic stresses on plant proteome and metabolome changes. *Acta Physiologiae Plantarum*, 36(1), 1–19.

Rojas-González, J. A., Soto-Súarez, M., García-Díaz, Á., Romero-Puertas, M. C., Sandalio, L. M., Mérida, Á., … Sahrawy, M. (2015). Disruption of both chloroplastic and cytosolic FBPase genes results in a dwarf phenotype and important starch and metabolite changes in *Arabidopsis thaliana*. *Journal of Experimental Botany*, 66(9), 2673–2689.

Rouached, H., Arpat, A. B., & Poirier, Y. (2010). Regulation of phosphate starvation responses in plants: Signaling players and cross-talks. *Molecular Plant*, 3(2), 288–299.

Ruan, Y. L., Jin, Y., Yang, Y. J., Li, G. J., & Boyer, J. S. (2010). Sugar input, metabolism, and signaling mediated by invertase: Roles in development, yield potential, and response to drought and heat. *Molecular Plant*, 3(6), 942–955.

Schmitz, J., Schöttler, M. A., Krueger, S., Geimer, S., Schneider, A., Kleine, T., … Häusler, R. E. (2012). Defects in leaf carbohydrate metabolism compromise acclimation to high light and lead to a high chlorophyll fluorescence phenotype in *Arabidopsis thaliana*. *BMC Plant Biology*, 12(1), 8.

Shinozaki, K.; Uemura, M.; Bailey-Serres, J.; Bray, E. A.; Weretilnyk, E. Responses to abiotic stress. In: Buchanan, B. B.; Gruissem, W.; Jones, R. L. (ed.) Biochemistry and molecular biology of plants. 2. ed. Oxford: Wiley Black Well, 2015. 1264p.

Simkin, A. J., Lopez-Calcagno, P. E., Davey, P. A., Headland, L. R., Lawson, T., Timm, S., … Raines, C. A. (2016). Simultaneous stimulation of the SBPase, FBP aldolase and the photorespiratory GDC-H protein increases CO2 assimilation, vegetative biomass and seed yield in Arabidopsis. *Plant Biotechnology Journal*, 1–12.

Simkin, A. J., McAusland, L., Headland, L. R., Lawson, T., & Raines, C. A. (2015). Multigene manipulation of photosynthetic carbon assimilation increases CO_2 fixation and biomass yield in tobacco. *Journal of Experimental Botany*, 66(13), 4075–90.

Stasolla, C., Katahira, R., Thorpe, T. a, & Ashihara, H. (2003). Purine and pyrimidine nucleotide metabolism in higher plants. *Journal of Plant Physiology*, 160(11), 1271–1295.

Stitt, M., & Krapp, a. (1999). The interaction between elevated carbon dioxide and nitrogen nutrition: the physiological and molecular background. *Plant, Cell and Environment*, 22, 553–621.

Stitt, M., Lunn, J., & Usadel, B. (2010). Arabidopsis and primary photosynthetic metabolism - More than the icing on the cake. *Plant Journal*, 61(6), 1067–1091.

Stitt, M., & Zeeman, S. C. (2012). Starch turnover: Pathways, regulation and role in growth. *Current Opinion in Plant Biology*, 15(3), 282–292.

Streb, S., & Zeeman, S. C. (2012). Starch metabolism in leaves. The Arabidopsis Book.

Sun, J., Zhang, J., Larue, C. T., & Huber, S. C. (2011). Decrease in leaf sucrose synthesis leads to increased leaf starch turnover and decreased RuBP regeneration-limited photosynthesis, but not Rubisco-limited photosynthesis in Arabidopsis null mutants of SPSA1. *Plant, Cell & Environment*, 34(4), 592–604.

Thalmann, M. R., Pazmino, D., Seung, D., Horrer, D., Nigro, A., Meier, T., … Santelia, D. (2016). Regulation of leaf starch degradation by abscisic acid is important for osmotic stress tolerance in plants. *The Plant Cell*, tpc.00143.2016.

Ventriglia, T., Kuhn, M. L., Ruiz, M. T., Ribeiro-Pedro, M., Valverde, F., Ballicora, M. A., … Romero, J. M. (2008). Two Arabidopsis ADP-glucose pyrophosphorylase large subunits (APL1 and APL2) are catalytic. *Plant Physiology*, 148(1), 65–76.

Volkert, K., Debast, S., Voll, L. M., Voll, H., Schießl, I., Hofmann, J., … Börnke, F. (2015). Loss of the two major leaf isoforms of sucrose-phosphate synthase in *Arabidopsis thaliana* limits sucrose synthesis and nocturnal starch degradation but does not alter carbon partitioning during photosynthesis. *Journal of Experimental Botany*, 66(3), 1042.

Walters, R. G., Ibrahim, D. G., Horton, P., & Kruger, N. J. (2004). A mutant of Arabidopsis lacking the triose-phosphate/phosphate translocator reveals metabolic regulation of starch breakdown in the light. *Plant Physiology*, 135(2), 891–906.

Yu, T. S., Lue, W. L., Wang, S. M., & Chen, J. (2000). Mutation of Arabidopsis plastid phosphoglucose isomerase affects leaf starch synthesis and floral initiation. *Plant Physiology*, 123(1), 319–26.

Zhu, X.-G., de Sturler, E., & Long, S. P. (2007). Optimizing the distribution of resources between enzymes of carbon metabolism can dramatically increase photosynthetic rate: a numerical simulation using an evolutionary algorithm. *Plant Physiology*, 145(2), 513–526.

Zhu, X.-G., Long, S. P., & Ort, D. R. (2010). Improving photosynthetic efficiency for greater yield. *Annual Review of Plant Biology*, 61(1), 235–261.

2) Comparative proteomic analysis of plant acclimation to six different long-term environmental changes

Dániel Á. Carrera[a], Sebastian Oddson[a], Jonas Grossmann[b], Christian Trachsel[b], Sebastian Streb[a1]

a) Institute for Agricultural Sciences, Plant Biochemistry, ETH Zürich, CH-8092 Zürich, Switzerland
b) Functional Genomics Center Zürich, ETH Zürich/University of Zürich, Zürich CH-8057, Switzerland

To whom correspondence should be addressed. Email: sstreb@ethz.ch

Phone: +41 44 632 36 16

Reference:

Manuscript submitted to Plant Cell and Physiology

Contribution:

The hydroponic growth system was established together with Sebastian Oddson, I optimized the abiotic stress treatment and he was responsible for the nutrient deficient. The mass spectrometry measurements were carried out by me and Sebastian Oddson with the assistance of Christian Trachsel. The raw data was evaluated by Jonas Grossmann and I did the further bioinformatic analysis.

Abstract

Plants are constantly challenged in their natural environment by a range of changing conditions. We investigated the acclimation processes and adaptive plant responses to various long-term mild changes and compared them directly within one experimental setup. *Arabidopsis thaliana* plants were grown in hydroponic culture for 10 days under controlled abiotic stress (15°C, 25°C, salt and osmotic) and in nutrient deficiency (nitrate and phosphate). Plant growth was monitored and proteomic experiments were performed. Resource allocation between tissues altered during the plants' response. The growth patterns and induced changes of the proteomes indicated that the underlying mechanism of the adaptation processes are highly specific to the respective environmental condition. Our results indicated differential regulation of response to salt and osmotic treatment, while the proteins in changed temperature regime showed an inverse, temperature-sensitive control. There was a high correlation of protein level between the nutrient deficient treatments, but the enriched pathways varied strongly. The proteomic analysis also revealed new insights about the regulation of proteins specific to the shoot and the root. Our investigation revealed unique strategies of plant acclimation to the different applied treatments on a physiological and proteome level, and these strategies are quite distinct in tissues below and above ground.

Keywords:

Long-term stress, abiotic stress, nutrient deficiency, proteomics, plant acclimation and adaptation

Introduction

Human nutrition relies almost entirely on agriculture and its productivity, but the sustainability of the agricultural system is doubtful. A conservative estimate projects that there will be approximately 9 billion inhabitants on Earth in 2050 (FAO, 2012). Based on this estimate, agricultural production will have to increase by 50 to 100% until 2050, but historical rates of yield growth for most crops are only half of what would be required to achieve this (Curtis and Halford, 2013). Increasing food production is technically very challenging (Raines, 2011; Dockter et. al 2014), and climate change further endangers the whole process. A mild scenario suggests a 2°C rise in global temperature, and the effects of global warming on food production will be only partially and temporary compensated by the ability of acclimation and adaptation of the existing crops (Challinor et. al, 2013). Increased temperature will be coupled with further stresses (i.e. drought, floods, increased salt concentration in soil, nutrient limitations, etc.), and by the end of the 21st century, many densely populated areas will be seriously arid regions (Dai, 2012).

Plants are inevitably exposed to the changing environmental conditions; hence, they have to cope with them in order to minimize the loss in their fitness. The acclimation and adaptation responses have been extensively investigated, but the underlying mechanisms are complex and still poorly understood. Increased knowledge about pathways and regulated proteins of the cellular machinery would facilitate efforts to optimize rational breeding.

Nutrient availability is one of the key factor that can substantially reduce plant growth and, as a result, yield. Liebig's law of the minimum states that the growth of plants is highly controlled by single nutrients, which are the least available (Liebig, 1840, 1855). Although it is a good estimate, there are other hypotheses that discuss the relation between nutrient availability and plant growth (Ågren et. al, 2012). Nitrogen (N) and phosphorus (P) are two essential macronutrients, and are often limiting factors in agriculture without the application fertilizers (Masclaux-Daubresse et. al, 2010; Ågren et. al, 2012).

Stress response in plants has been studied extensively in recent decades, illustrating an awareness for the importance of a better understanding of the underlying adaptive responses. Traditionally, whole plant responses were studied with transcriptomic approaches (Agarwal

et. al, 2014), as that method promises to deliver the most complete picture. However, based on transcriptional changes, it is not always possible to explain the current metabolic status of a biological system. Transcripts can be seen as snapshots, which are followed by protein changes, and therefore, a remodeling of the cellular machinery over time (Stitt et. al, 2010; Baerenfaller et. al, 2012; Guerreiro et. al, 2014). Proteomics allows quantification of the most abundant proteins in a biological sample. Thereby proteins involved in the main processes, which are usually also the most resource-demanding processes are well covered in contrast to low abundant transcription factors. Thus, proteomics is a powerful tool to investigate how plants adjust their metabolism and physiology in response to a recently altered environment. Proteomic experiments carried out in different stress conditions, tissues, organelles and plant species have been reviewed several times (Kosová et. al, 2011; Rodziewicz et. al, 2013; Ghosh and Xu, 2014; Jorrín-Novo et. al, 2015; Janmohammadi et. al, 2015). Research on early stress response to an unnaturally strong abiotic stressor is the main focus in the field of *Arabidopsis* research. However, such experiments may be unsuitable to investigate how plants rewire their cellular machinery and acclimate to long-term environmental changes (i.e. climate change). Further, the extrapolation of data obtained from different experiments can be biased and occasionally contradictory due to the different experimental, technical and statistical approaches. Thus, it remains challenging to compare responses to different environmental conditions and draw universal conclusions on stress responses (Dupae et. al, 2014) similarly to other 'omics' research areas (Michael Deyholos, 2010; Rest et. al, 2016).

The aim of our research was to examine a more realistic scenario of long-term acclimation processes of plants under mild environmental perturbations. We conducted a comparative analysis that involved several abiotic stresses and nutrient limitations in a well-defined experimental setup, which allowed us to analyze and compare them to each other directly. The acclimation process of *Arabidopsis thaliana* plants was monitored under moderately changed environmental conditions: temperature changes (±5°C), phosphate and nitrogen deficiency, elevated salt and higher osmotic pressure. All these different conditions were successfully established in a hydroponic system, and comparative analysis were carried out.

Materials and methods

Plant growth

Arabidopsis thaliana wild-type plants (Col-0) seeds were individually distributed on cut 0.5 ml tubes containing 0.65% phytoagar. They were grown hydroponically in Cramer's solution (Gibeaut et. al, 1997; Tocquin et. al, 2003) in control environment for eighteen days in a Percival AR95 growth chamber (CLF Plant Climatics) with 12-h photoperiod, 20°C and 60% relative humidity. Light intensity was uniform at 150 µmol quanta m^{-2} s^{-1}. The tubes were soaked in nutrient solution (pH was adjusted to 6), which contained the following macronutrients: 1.5 mM $Ca(NO_3)_2$, 1.25 mM KNO_3, 0.75 mM $Mg(SO_4)$, 0.5 mM KH_2PO_4, 1 mM $(NH_4)_2SO_4$, 72 µM $C_{10}H_{12}FeN_2NaO_8$ and 100 µM Na_2O_3Si and micronutrients: 50 µM KCl, 10 µM $MnSO_4$, 1.5 µM $CuSO_4$, 2 µM $ZnSO_4$, 50 µM H_3BO_3 and 0.075 µM $(NH_4)_6Mo_7O_{24}$. 18 days after germination, plants were exposed to different treatments: 50 mM NaCl or 5% PEG6000 dissolved in hydroponic solution, ±5°C in E-41L2 growth chamber (CLF Plant Climatics) and no phosphate and nitrate in the hydroponic solution. The plants were grown under changed conditions for additional 10 days.

Growth analysis

During a 12 days period (from 16 to 28 days after germination) rosettes were photographed to quantify the leaf area. Leaf area of plants were evaluated with ImageJ software. The growth of each plant was described with a polynomial (3rd order) model: $y = ax^3 + bx^2 + cx + d$. Relative growth rate (RGR) is defined as the relative increase in leaf area over time period (GR) and was calculated by taking the difference between the polynomial transformation of the leaf area at the end (G_n) and at the beginning of the timeframe (G_{n-1}) divided by G_{n-1}: $GR_n = (G_n - G_{n-1})/ G_{n-1}$ (Hendrik Poorter, 1989; M. Heinen, 1999; Paine et. al 2012; Ruts et. al, 2013).

Protein extraction and gel-free digestion for mass spectrometry analysis

Proteins were purified and digested using a modified filter-aided sample preparation (FASP) protocol (Wisniewksi et al. 2009), Microcon-30 kDa centrifugal filter with Ultracel-30 membrane was used (Merck Millipore). Whole rosettes were frozen in liquid N2 and grinded to powder and aliquoted. The hydroponic system allowed us to harvest the roots in a similar

way; they were cut off, quickly dried with tissue paper and finally frozen and grinded in liquid N_2. Proteins were extracted from aliquoted powder (20-50 µg) in SDS-lysis buffer (4% (w/v) SDS, 100 mM Tris/HCL pH 8.2) with 1:10 sample to buffer ratio and incubated 30 minutes at room temperature without DTT, which was added afterwards to a final 0.1 M and sonicated 12 minutes with Bioruptor sonificator (Diagenode), boiled 5 minutes at 95°C. Protein concentration was measured with Qubit (Invitrogen). 200 µl 8 M urea in 100 mM Tris/HCl pH 8.2 was mixed with 30 µl sample, and loaded on the filter by centrifugation at 14000 x g. Samples were washed once with 200 µl 8M Urea and centrifuged at 14000 x g. Thiol groups of proteins were blocked with 100 µl 0.05 M iodoacetamide for one minute at room temperature followed by removal of the chemicals by centrifugation at 14000 x g. SDS, Urea and other digestion incompatible chemicals were washed away with two times 200 µl of 0.5 M NaCl followed by centrifugation at 14000 x g. Proteins were digested with trypsin in a 1:100 ratio of trypsin to protein in 0.05 M Triethylammonium bicarbonate overnight on the filter. Peptides were harvested by centrifugation at 14000 x g collection tube and acidified with trifluoroacetic acid (TFA) to a final concentration of 0.5%.

Peptide purification for mass spectrometry analysis

The digested peptides were purified and desalted on C18 Solid Phase Extraction columns (Sep-Pak), which were attached to a QIAvac 24 Plus (QIAGEN) vacuum manifold. Columns were washed once with 1 ml 100 % methanol, once with 1 ml 60 % ACN, 0.1 % TFA and twice with 1 ml 3 % ACN, 0.1 % TFA solution. 600-1000 µl 3% acetonitrile (ACN) and 0.1% TFA solution was added to the peptides and loaded on the column. The column was washed 3 times with 1 ml 3 % ACN, 0.1 % TFA. Peptides were eluted with 200 µl 60 % ACN, 0.1 % TFA, lyophilized, and redissolved in 40 µl 3% ACN and 0.1% formic acid.

Mass spectrometry analysis

The protocol was established accordingly to Biner et. al (2015), 5-10 µL of peptide solution was analyzed on a Q-Exactive mass spectrometer (Thermo Scientific) coupled to an EASY-nLC1000 (Thermo Scientific). Instrument parameters followed the “sensitive” method published by Kelstrup et al. (2012) with slight modifications. Full scan MS spectra were acquired in profile mode from 300-1700 m/z with automatic gain control target of 3e6,

Orbitrap resolution of 70’000 (at 200 m/z), and maximum injection time of 120 ms. The 12 most intense multiply charged (z = +2 to +8) precursor ions from each full scan were selected for higher-energy collisional dissociation fragmentation. Precursor was accumulated with automatic gain control value of 5e4 and a maximum injection time of 120 ms and fragmented with a normalized collision energy of 28 (arbitrary unit). Generated fragment ions were scanned with Orbitrap resolution of 35’000 (at 200 m/z) from a fixed first mass of 120 m/z. The isolation window for precursor ions was set to 2.0 m/z and the underfill ratio was 2% (referring to an intensity of 8.3e3). Each fragmented precursor ion was set onto the dynamic exclusion list for 30 s. Peptide separation was achieved by RP-HPLC on C18 column (150 mm x 75 µm, 1.9 µm, C-18 AQ, 120 Å). Samples were separated with a linear gradient of 130 minutes from 3-25% solvent B (0.1% formic acid in ACN) in solvent A (0.1% formic acid in H_2O) with flow rate 250 nl/min.

Protein Identification and Protein Quantification using Progenesis QI for Proteomics

For every stress experiment and tissue, Progenesis experiments were set up separately. Raw mass spectrometer files were loaded into ProgenesisQI for Proteomics (v.4.0.4265.42984). The aligning reference was a combined pool of all respective samples. From each peptide ion a maximum of the top five tandem mass spectra were exported using charge deconvolution and deisotoping option and a maximum number of 200 peaks per MS/MS. The Mascot generic file (.mgf) was searched with Mascot Server v.2.4.1 (www.matrixscience.com) using the parameters 10ppm for precursor ion mass tolerance, 0.2 Da for fragment ion tolerance. Trypsin was used as the protein-cleaving enzyme, two missed cleavages were allowed. Carbamidomethylation of cysteine was specified as a fixed modification, and oxidation of methionine was selected as variable modifications.

Searched was a forward and reversed TAIR10 database concatenated to 260 known mass spectrometry contaminants in order to evaluate the false discovery rate using the target-decoy strategy (Kaell et al, 2008). The mascot result was loaded into Scaffold v4.1.1 using local FDR and protein cluster analysis. The spectrum report was loaded into ProgenesisQI for Proteomics. A between group analysis was used with a Control and Stress condition group (4-6 replicates). Normalization was kept with default settings. Quantification inlcuded proteins

identified with at least 2 features and one unique peptide. Proteins were grouped with Progenesis and quantified based on non-conflicting features.

Normalized abundance from all non-conflicting peptide ions of the same protein group were summed individually for each sample. The parametric test (two tailed t-test) on the transformed (hyperbolic arcsine transformation) normalized protein abundance was applied. Fold changes were calculated using the group means of the protein sums. The proteomics data have been deposited to the ProteomeXchange Consortium via the PRIDE (Vizcaíno et. al, 2016) partner repository with the dataset identifier PXD006797 (reviewer account details: Username: reviewer34305@ebi.ac.uk, Password: OopPQSdq).

Bioinformatic analysis

GO term enrichment analyses were based on TAIR 10 (May 2015) GO term association lists excluding associations based on GO evidence codes IEA (Inferred from Electronic Annotation) or RCA (Inferred from Reviewed Computational Analysis). GO categories overrepresented by genes with a significant high (±1.5) fold change in particular responses in a given condition were determined by a hypergeometric test against all proteins detected in that condition. Only GO categories represented by at least 5 genes in the background list were considered. The assignments and tests were performed in R (R Development Core Team, 2010). R was also used for the clustering analysis and correlation matrix with the ggplot2, gplots, reshape and gridExtra packages.

Results

Plant growth under changed environmental conditions

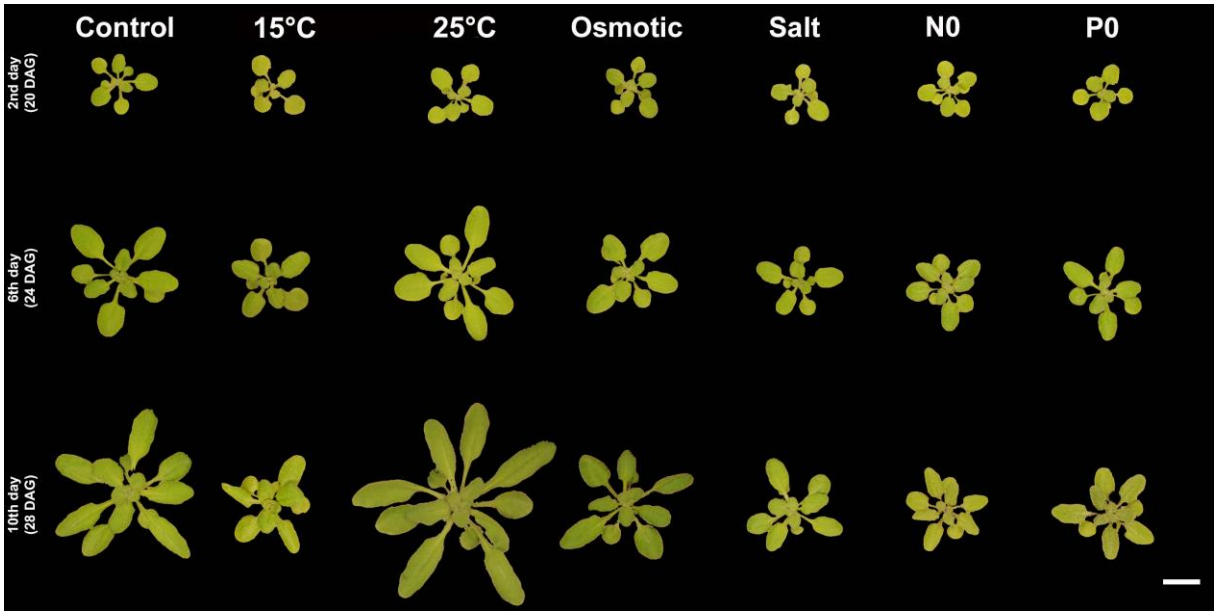

Figure 2-1. Plants grown in 6 environmental changed conditions for 10 days. Pictures were taken on the 2nd, 6th and 10th day of the treatment (20th, 24th and 28th day after germination (DAG) respectively). The scale bar corresponds to 1 cm.

We compared plant responses to a set of environmental perturbations. Treatments were chosen accordingly, in which plants were able to adjust their metabolism and sustain growth under unfavorable environmental conditions. Plants were grown for 18 days in hydroponics under standard full nutrient conditions at 20 °C and then subjected to different treatments (temperature (15°C and 25°C), mild salt (50 mM NaCl) or osmotic stress (5% PEG6000), phosphate (P0) or nitrogen deficiency (N0)) for additional 10 days.

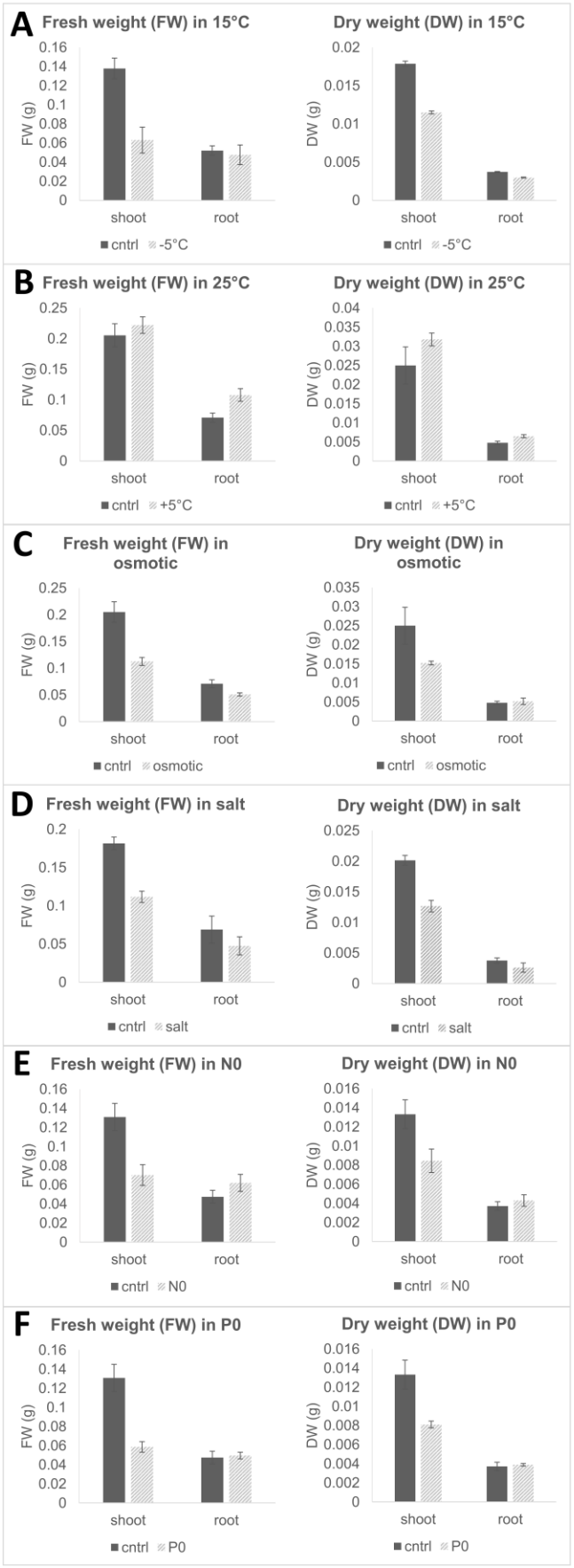

Figure 2-2. Weight of plants at the end of the 10 days treatment. Fresh weight (FW) is above, dry weight (DW) is below. **A)** 15°C treatment **B)** 25°C treatment **C)** osmotic treatment with 5% PEG6000 **D)** salt treatment with 50 mM NaCl **E)** nitrogen deficiency **F)** phosphate deficiency. Bars represent mean values and the error bars standard errors. A single bar represents 9 individual plants.

The applied environmental shifts affected growth, but the plants remained green and did not display chlorotic or dead tissues after 10 days (Fig. 1). Compared to the control plants, growth of plants exposed to 25°C appeared similar or slightly enhanced. However, in all other conditions plants showed a reduction in leaf area at the end of the 10d treatment (Fig. 1, 2 and 4). Fresh weight (FW) and dry weight (DW) were determined (Fig. 2); in 25°C FW and DW of the shoot was elevated while the other treatments had a negative effect on biomass production. We correlated FW and DW with the surface area of the plants and the correlation was high between all three parameters (Suppl. Fig. 1). Leaf area surface was chosen as a non-

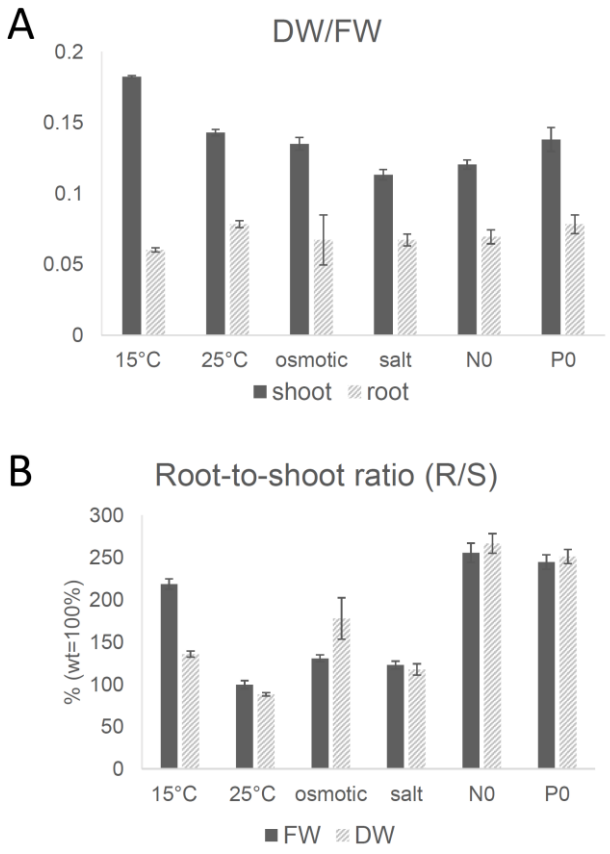

Figure 2-3. Ratio of biomass production between roots and shoots under changed conditions. A) Ratio of dry weight and fresh weight (DW/FW) of the shoot and root and **B)** ratio of the root and shoot (R/S) of the fresh (FW) and dry weight (DW) at the end of the 10 days treatment expressed in relative percentage to the control conditions. Bars represent mean values and the error bars standard errors.

destructive approximation of biomass production. The DW/FW ratio was approximately similar in all the conditions except of the 15°C, which showed a higher value in the shoot indicating a relatively lower water content in the leaves (Fig. 3a).

Growth of roots was measured as biomass at the end of the experiment. In contrast to the shoot, the growth of roots was relatively robust in all experiments. In nutrient limiting conditions (N0 and P0) roots biomass increased, whereas osmotic stress, salt stress and reduced temperature resulted in unchanged or slightly less biomass compared to the plants

in control environment. Under elevated temperatures (25°C) root biomass increased significantly by 50%. The root-to-shoot ratio (R/S) in the treatments was never below the ratio detected in the control (Fig. 3b). At 25°C, osmotic and salt treatments plants invested slightly more into root than shoot. Plants grown in N0, P0 and 15°C invested significantly more resources into the roots (Fig. 3b).

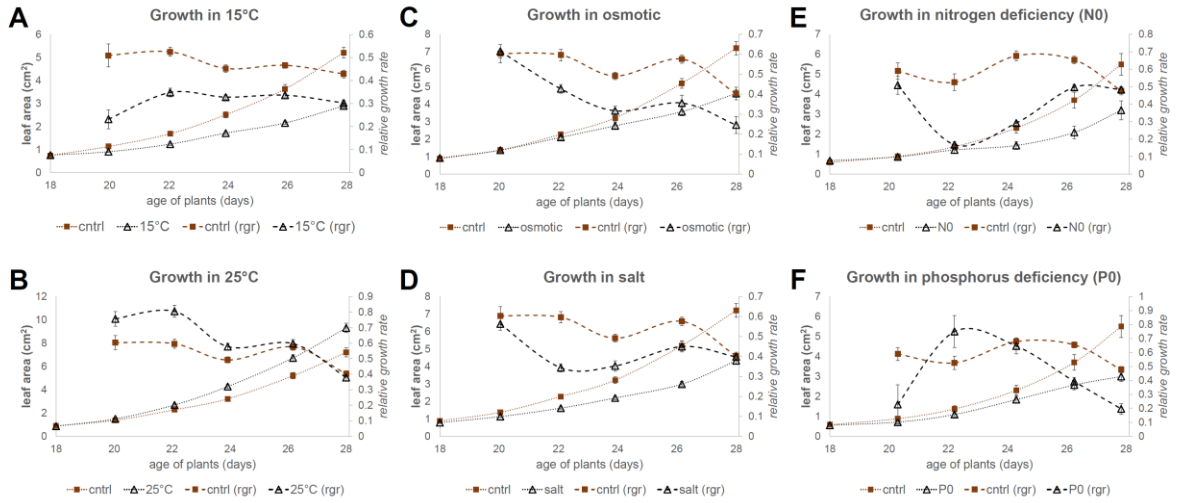

Figure 2-4. Leaf area and relative growth rate (RGR) measurements of plants grown in 6 environmental changed conditions for 10 days (18-28 DAG). On the left y-axis leaf area in cm^2, on the right y-axis the RGR is depicted. Each experiment was performed independently with internal control plants. A) 15°C treatment B) 25°C treatment C) osmotic treatment with 5% PEG6000 D) salt treatment with 50 mM NaCl E) nitrogen deficiency F) phosphorus deficiency. Bars represent mean values and the error bars standard errors. Each experiment included 10 to 18 individual plants.

The relative growth rate (RGR) curves showed distinct patterns for each applied treatment. RGR analysis revealed a sigmoid-like growth pattern in the control condition and abiotic stress, but this was broken under nutrient deficiency (Fig. 2e and 2f). In the warmer environment, plants grew faster than the control plants initially for the first 6 days and the RGRs converged towards the end of the experiment. Under mild salt and osmotic stresses, the plants maintained a control-level growth in the first two days before it declined. At 15°C, RGR dropped initially by more than 50% and recovered only partially. Nutrient deficiency resulted in different growth responses. In N0, growth was not affected the first 2d after the introduced perturbation, but growth was reduced at later time points. At the end of the treatment, N limited plants and control plants had a similar RGR. P limitation initially had a strong negative effect on growth but later seemed to promote plant growth in the middle of the treatment. At later time-points, growth compared to control plants was reduced again.

Induced proteomic alterations in plants grown under changed environmental conditions

Treatment	25°C			15°C			Osmotic		
Treshold	**all**	**p≤0.05**	**FC ±1.5**	**all**	**p≤0.05**	**FC ±1.5**	**all**	**p≤0.05**	**FC ±1.5**
Shoot	2406	551	68	2880	1087	114	2697	150	6
Root	2905	819	100	3256	484	75	3173	792	236

Treatment	Salt			N0			P0		
Treshold	**all**	**p≤0.05**	**FC ±1.5**	**all**	**p≤0.05**	**FC ±1.5**	**all**	**p≤0.05**	**FC ±1.5**
Shoot	2860	835	91	2827	917	227	2829	705	122
Root	3260	311	84	3483	1027	441	3485	1007	272

Table 2-1. Number of proteins identified in the environmental treatments in the shoot and the root. Every protein (all), proteins with significant expression (pV≤0.05) and proteins with significantly high expression (FC ±1.5)

Plant growth was compromised under the applied environmental changes excepts of plants at 25°C and the dynamics of the observed growth responses suggested different adaptation processes. Therefore, we aimed to elucidate the rewired cellular machinery of the newly adapted physiological state by a quantitative analysis of proteomes at the end of the treatments (10d).

Treatment	15°C			25°C			Osmotic		
Treshold	**all**	**FC ±1.5**	**overlap**	**all**	**FC ±1.5**	**overlap**	**all**	**FC ±1.5**	**overlap**
Shoot	1820	53	7 (9.6%)	1490	36	7 (10.8%)	1738	5	0 (0%)
Root		20			29			79	

Treatment	Salt			N0			P0		
Treshold	**all**	**FC ±1.5**	**overlap**	**all**	**FC ±1.5**	**overlap**	**all**	**FC ±1.5**	**overlap**
Shoot	1812	41	5 (7.9%)	1807	141	23 (7.5%)	1808	72	20 (11.4%)
Root		22			163			103	

Table 2-2. Overlap of proteome changes between roots and shoots. The overlap between proteins with a significant high (pV≤0.05, FC ±1.5) abundance change in every treatment. The subgroup of proteins was included, which were detected in the shoot and the root and the significance and fold change threshold (FC ±1.5) was applied on them.

Unfractionated single-tube method was used with root and shoot samples of every treatment. 2400 to 3500 proteins were detected in every sample with about 500 more proteins in roots than in shoots (Table 1). In comparison between control and treatment, 150 to 1087 changed quantitatively with a p-value ≤ 0.05 (*changing proteins*) and 6 to 441 of these changed with a fold change (FC) exceeding ±1.5 FC (*changing proteins with ±1.5 FC*) (Table 1). Nutrient deficiency tended to induce more pronounced changes in the proteome than the mild abiotic stresses, although the number of changing proteins was the highest in the 15°C treatment. Mild osmotic stress affected the shoot proteome least, even though the same treatment affected the root proteome strongly.

For all corresponding samples, around 40% of the detected proteins were found both in roots and shoots. Among these, only 10% changed with a ±1.5 FC in both tissues (Table 2), but the vast majority (84%) of these proteins changed their abundance in the same direction (Supplementary Fig. 2).

Responses on proteome level between treatments

To see, if different treatments have similar effects on proteome all the twelve experiments were clustered based on changing proteins (p≤ 0.05). Roots and shoots grouped together on distinct branches, suggesting that tissue specific proteomes differ more than the treatment induced changes (Fig. 5a). In roots, the altered nutrient conditions (N0 and P0) cluster together with osmotic stress, while the mild salt stress did not cluster closely with other treatments. Both temperature treatments grouped together. The grouping in the leaves differed. Salt and cold clustered together, as again N0 and P0 did, whereas heat and osmotic stress were apart from the others.

Correlation was calculated between two experiments with all possible pairwise combination based on proteins, which changed in both (Fig. 5b). Initially, we expected that the two nutrient

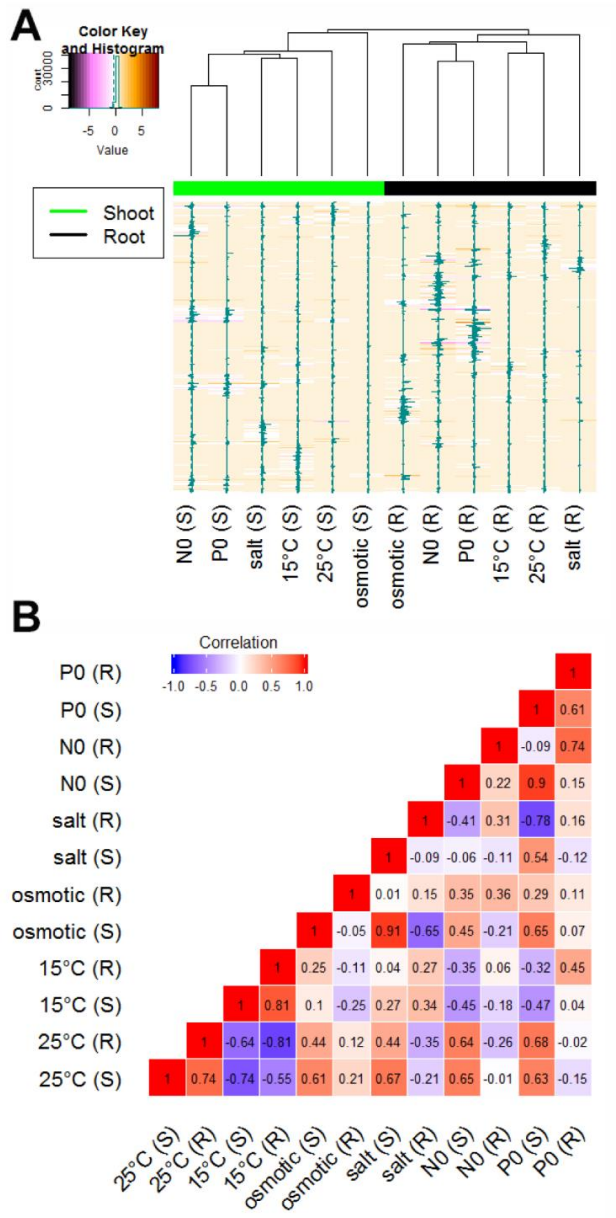

Figure 2-5. Leaf area and relative growth rate (RGR) measurements of plants grown in 6 environmental changed conditions for 10 days (18-28 DAG). On the left y-axis leaf area in cm^2, on the right y-axis the RGR is depicted. Each experiment was performed independently with internal control plants. A) 15°C treatment B) 25°C treatment C) osmotic treatment with 5% PEG6000 D) salt treatment with 50 mM NaCl E) nitrogen deficiency F) phosphorus deficiency. Bars represent mean values and the error bars standard errors. Each experiment included 10 to 18 individual plants.

limitations (Nguyen et. al, 2015) and the osmotic and salt treatments might induce similar responses. However, the correlation was mostly higher between tissues than treatment. The correlation was strong between the proteome changes of the shoot (R = 0.898) and the root (R = 0.736) in N0 and P0, but it was lower if we compared the shoot and root of the same treatment. The correlation between the shoot and the root of N0 was low (R = 0.222). However, in P0 it was higher (R = 0.611), it was still lower than the above-mentioned values. The vast majority of the changing proteins were up- or downregulated in the same direction (Fig. 6e and 6f). The mild osmotic and salt stresses showed a distinct tendency; changes in the

shoot proteome under osmotic stress correlated highly positive (R = 0.909) with the shoot proteome of the salt treatment. In contrast, almost no correlation was detected between roots of the plants exposed to salt and osmotic treatments (Fig. 6c and 6d).

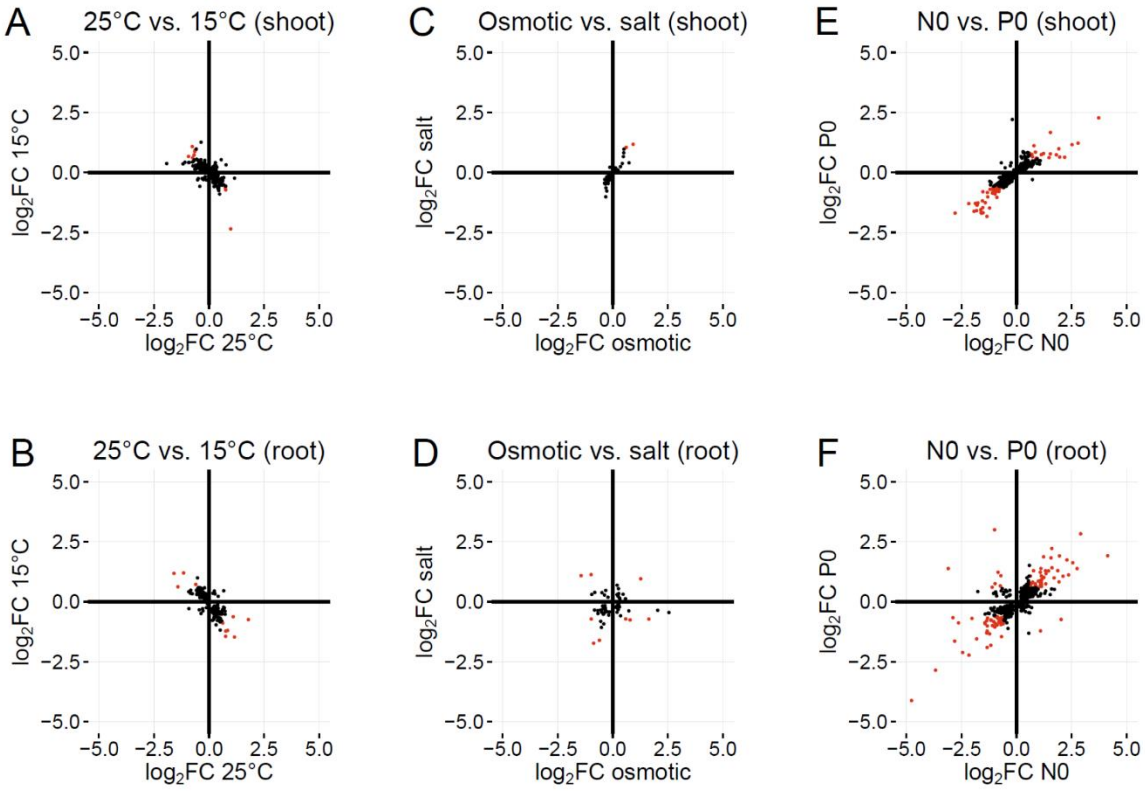

Figure 2-6. Fig. 5 Cluster and correlation analysis of proteomics changes Heatmap and correlation matrix of each tissue from every experiment based on significant changing proteins ($p<0.05$) in the shoot (S) and root (R) separately. **A)** Heatmap and clustering of every treatment, shoot (S) and root (R) separately. The coloring corresponds to the fold change value of the individual proteins: red represents a strong increase, black represents a strong decrease in protein abundance. The blue trace and its distance from the center in each column also represents the fold change in the protein amount. **B)** Pearson Correlation between the proteome changes of each tissue from every experiment. Pairwise Pearson correlation coefficient was calculated between all experiments.

The proteins which were found to be significantly changed in both (15°C and 25°C) temperature treatments revealed strong negative correlation (Fig. 5b); it was high between the shoot (R = -0.735) and the root (R = -0.811). This strong negative correlation was reflected in the opposite fold change of individual proteins (Fig. 6a and 6b). This became even more pronounced if only proteins with ±1.5 fold change were included (Fig. 7 and Supplementary

Table 1). If they were upregulated in 15°C, they were downregulated in 25°C and *vice versa* irrespective of the tissue.

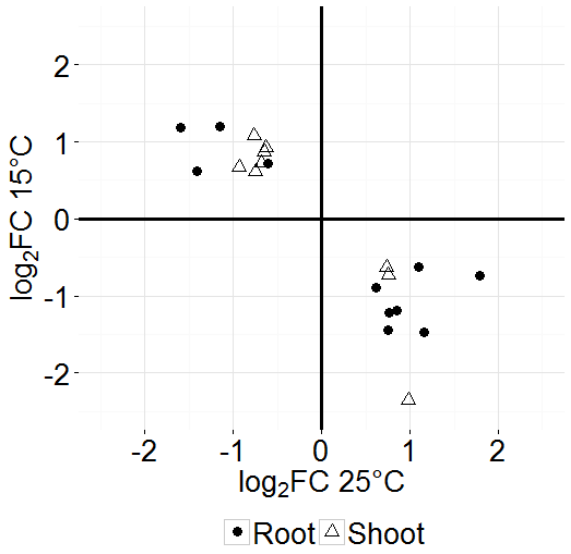

Figure 2-7. Antagonistic regulation of proteins under changed temperature conditions. Changing proteins with a log_2FC ± 0.58 (±1.5 FC) detected in the 15°C and 25°C treatment. Shoot and the root were combined. Fold change of protein is the ratio of its normalized abundance in the treatment divided by its normalized abundance in the control.

Commonly changed proteins under different growth conditions

We separated treatments according to tissues and tested whether any significantly changed protein with ±1.5 FC could be observed in several different treatments. Most proteins (78% - shoot, 79% - root) seemed to respond only to single conditions (Fig. 8). However, a number of proteins responded to several treatments in roots and shoots (Table 3 and 4).

In roots, 29 proteins (Table 3) changed significantly in three or more treatments. One of them was an N-methyltransferase (NMT1, At3g18000), which had a significant fold change in every root experiment except of the osmotic stress. In the shoot, similar to roots, there was also only a small fraction of significant changed proteins (30), which were found in three or more treatment (Table 4). One of them was again the NMT1, it was upregulated in salt and 15°C and downregulated in N0 and P0.This protein changed virtually under all changed conditions except of the osmotic stress. These changes were not only stress specific, but for instance in nutrient deficiency it showed opposite protein levels indicating different roles in different tissues.

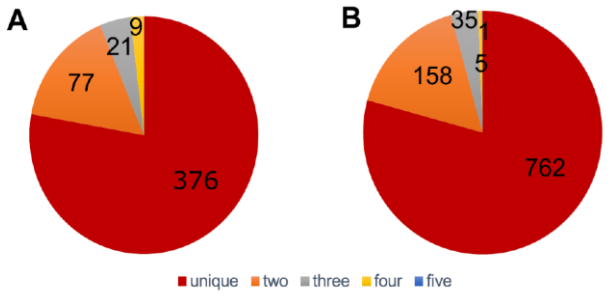

Figure 2-8. Proteins specific to one or multiple treatments. Number of changing proteins with ±1.5 FC detected in one or multiple treatment. **A)** in the shoot and **B)** in the root.

AGI	stress-related (Ref.)	15°C	25°C	salt	osmotic	N0	P0
AT1G12780		-1.18	*0.51*	*-0.57*		-1.09	-1.00
AT1G13080	Gao et. al, 2008	-0.89	0.62		0.88		
AT1G33590			0.86			-0.83	-0.71
AT1G52050			*-0.43*	-0.76	0.79	0.84	
AT1G56680		*0.35*	-0.84	-1.73	-0.87		*0.47*
AT1G65970	Kumar et. al, 2015	-1.22	0.76		-0.89	-2.27	
AT1G70850			0.89			0.72	0.79
AT1G73260	Li et. al, 2008	-0.63	1.10			-1.16	-0.76
AT1G78830		*-0.39*	0.72			-0.84	1.23
AT1G80240			*0.33*	-0.72	-0.98	-0.60	*0.31*
AT2G01520		-0.74	1.79			1.13	0.81
AT2G41100	Sistrunk et. al, 1994	0.62		-1.61	-0.61		
AT2G43920		3.42				-1.00	3.00
AT3G01290	Qi and Katagiri, 2012	-0.68	*0.48*			1.11	1.39
AT3G03640		0.67			-0.67		0.63
AT3G05950		-1.47	1.16	*-0.36*	2.04		
AT3G06850		-0.60		*-0.52*	*-0.43*	-1.32	-0.68
AT3G16390	Kissen and Bones, 2009	1.18	-1.60		*0.47*	1.23	1.87
AT3G16430	Yamada et. al, 2011		0.92	-0.67		-0.66	*-0.36*
AT3G18000	Zhang et. al, 2010	1.20	-1.16	1.50		1.08	1.23
AT3G49120	Mammarella et. al, 2014		1.07		0.59	-0.77	
AT3G59480			0.80	1.60		-2.16	-2.23
AT4G25250		*-0.29*	-0.92	1.09	-1.44		
AT4G25340			-0.59		0.63	-1.74	
AT4G32460		0.62	-1.41	0.76			
AT4G37410			0.83	-0.63			-0.81
AT4G39800	Ahmad et. al, 2015	0.75				2.11	1.06
AT5G15970	Gorsuch et. al, 2010	1.09		0.96	1.27		
AT5G38940			0.68	-1.47			-0.73

Table 2-3. Proteins detected in three and more treatments in the root. Proteins with a significant high FC ($p \leq 0.05$, $\log_2 FC \pm 0.58$ (±1.5)). FC in italics are below the threshold of expression. Stress-relatedness was defined based on the TAIR database

AGI	stress-related (Ref.)	15°C	25°C	salt	osmotic	N0	P0
AT1G02930	Tolin et. al, 2012	0.72		0.96		1.92	0.99
AT1G12770		0.68				-1.59	-1.70
AT1G15500		*0.25*	-0.59	*-0.37*		-1.32	-0.84
AT1G23130		-0.82		-0.70		0.80	
AT1G45201		*-0.37*	0.61	*0.57*		0.73	0.65
AT1G48570		0.90				-1.80	-1.37
AT1G54100	Li-Beisson et. al, 2013		*0.43*	1.04	0.61	0.82	
AT2G22400		1.02				-0.82	-0.78
AT2G33380	Blée et. al, 2014		1.24	1.99		1.48	0.62
AT2G39800	Székely et. al, 2008			1.17	0.92	-0.69	0.40
AT3G06980	Li et. al, 2008	*0.42*	-0.91			-1.55	-1.19
AT3G18000	Zhang et. al, 2010	0.87		0.94		-1.75	-1.27
AT3G18680		*0.44*	-0.75	*-0.51*		-1.87	-1.29
AT3G19710	Less and Galili, 2008		0.98			1.13	0.74
AT3G28220		1.01		1.04		*0.30*	0.87
AT3G44750	Han et. al, 2016	0.67	-0.93			-3.21	
AT3G47450	Xie et. al, 2013			-0.92		-1.34	-1.83
AT3G53460	Kupsch et. al, 2012	0.61	-0.75	-0.55		-1.20	-0.71
AT4G02990	Robles et. al, 2012	0.64				-1.60	-1.68
AT4G11960	Lehtimäki et. al, 2010	-2.35	0.98	0.97	*0.51*	0.96	
AT4G14090	Pourcel et. al, 2010	1.26	-0.36	1.41		2.80	1.22
AT4G15530			0.63			1.23	0.79
AT4G22485			-0.78	0.60		0.93	*0.37*
AT4G22880	Bharti et. al, 2015			1.12		2.19	0.63
AT4G36390		0.87	-0.65			-1.31	-1.02
AT5G08610		1.08	-0.77	*-0.39*		-1.62	-1.55
AT5G13930	An et. al, 2016	0.73	-0.68			1.81	0.73
AT5G22580		-0.72	0.76	-0.73			
AT5G23900			-0.98			-1.42	-1.26
AT5G54180		0.71				-0.80	-0.80

Table 2-4. Proteins detected in three and more treatments in the shoot. Proteins with a significant high FC ($p \leq 0.05$, $\log_2 FC \pm 0.58$ (±1.5)). FC in italics are below the threshold of expression. Stress-relatedness was defined based on the TAIR database

Gene Ontology (GOterm) enrichment and analysis of single proteins with the highest significant fold change under changed temperature

To detect processes that might be affected by the adaptation to the applied mild stresses, we performed a GO enrichment analysis on the changing proteins with ±1.5 FC. In response to the 15°C treatment, `cold stress` related GOterms were enriched: in shoots `acclimation to the cold` (GO:0009631), and in roots the `response to cold` (GO:0009409). Several transport GOterms were enriched with the highest significance level (GO:0006810 – `transport`, GO:0015250 - `water channel activity`) and the proteins contained in these categories were all downregulated in shoot and root. Especially in the shoot a strong reduction of aquaporins (Supplementary Table 2) was observed. There might be a link between the water transport and the induced response to water deprivation in both tissues (GO:0009414 - `response to water deprivation`). Besides the transport processes, RNA-metabolic pathways were enriched in the shoot and the root (GO:0004004 - `ATP-dependent RNA helicase activity`, GO:0008168 - `methyltransferase activity`, GO:0010501 - `RNA secondary structure unwinding`).

In the 15°C treatment, photosynthetic light reaction proteins were reduced in the shoot. Two of the proteins with the biggest decrease in protein amount was were another a photosynthetic enzyme, a ribulose bisphosphate carboxylase a putative large chain protein of the ribulose-1,5-bisphosphate carboxylase/oxygenase (At2g07732) and a thylakoid transmembrane protein (PGRL1B, At4g11960). The PGRL1B belonged to the abovementioned group of proteins, which were detected with a significantly high fold change in more than three treatments, but everywhere else, it was upregulated. In the root the top upregulated proteins are mainly involved in cold and other stress responses as well: KIN1 (At5g15960) is a cold- and ABA-inducible protein, RNA HELICASE 25 (At5g08620) controls gene expression during cold, salt and drought stress, and the COLD REGULATED 78 (At5g52310), as its name shows, is regulated by lower temperature. A protein (HARMLESS TO OZONE LAYER 2, AT2G43920) described to a lesser extent was upregulated the most, which was also one of the commonly changed protein under several treatments. Similarly, the two proteins with the highest decrease in protein abundance (At1g77520 and At3g05950) are not well characterized either.

The 25°C treatment induced different responses in the shoot and the root `Heat response` (GO:0009408), `response to hydrogen peroxide` (GO:0009408) and `response to virus` (GO:0009615) were enriched in both tissues. In the shoot, proteins of `ribosome` (GO:0005840) and participating in `translation` (GO:0006412) had a lower protein level, while in the root no significant enrichment of these terms was detected. In the warmer environment, flavonoid biosynthesis was downregulated in the shoot (GO:0009813).

The warmer environment induced fewer changes in the proteome of the shoot, it had the lowest number of changing proteins with ±1.5 FC after the osmotic treatment. There was no clear pattern in changes of protein abundance of stress-related proteins. One heat shock protein (HSP70, At3g12580), had an elevated fold change in the shoot and in the root, but two flavonoid proteins (At5g13930, At5g08640) were decreased. The top upregulated protein in the shoot is a cytosolic beta-amylase (BAM5, At4g15210), which was shown previously to to be sugar induced (Mita et. al, 1995) and responding in heat and salt stress (Monroe et. al, 2014) and it was upregulated in our salt treatment as well. The top upregulated protein in the root is a HOP3 (At4g12400), which participates in heat acclimation and it is a potential interaction partner of chaperone proteins, i.e. the abovementioned HSP70 (Fellerer et. al, 2011).

Gene Ontology (GOterm) enrichment and analysis of single proteins with the highest significant fold change under higher salt and osmotic environment

The elevated salt condition induced response processes in the shoot and the root (GO:0006952 - `defense response, GO:0009611` - `response to wounding`, GO:0009753 - `response to jasmonic acid`, GO:0009620 - `response to fungus`), but they reacted in different directions; together with other stress-related terms they were mainly downregulated in the root. The shoot response included proteins, which belonged to the enriched terms of water deprivation (GO:0009414 - `response to water deprivation` and GO:0009269 - `response to desiccation`). Similar GOterms were enriched as in the 15°C treatment, three aquaporins were detected in both experiments, but less than in 15°C. However, their protein abundance was increased in the 50mM NaCl environment. Salt stress groups were enriched in the shoot (GO:0042538 - hyperosmotic salinity response, GO:0009651 - response to salt stress).

The photosystem might have been positively affected in salt stress: two light harvesting complex (LHC) proteins were upregulated (At2g05100, At3g27690) together with the previously mentioned thylakoid transmembrane PGRL1B, while the protein level of two CP12 enzymes were decreased. This was accompanied with the increased content of two VEGETATIVE STORAGE PROTEIN (VSP) isoforms: VSP1 (At5g24780) and VSP2 (At5g24770). The VSPs are acid phosphatases, which mobilize nutrient sources (abundance of VSP2 was decreased in P0), but they play also an active role against herbivores in biotic stress responses (Liu et. al, 2005). CALEOSIN 3 (RD20, At2g33380) was highly upregulated in salt stress. It is involved in the stress responses of the plants (Blée et. al, 2014and had a significantly high fold change in several other treatments (Table 4).

The long-term osmotic treatment showed a unique response and acclimation process. Due to the very low number (6) of changing proteins with ±1.5 FC in the shoot, we focused on the root only. The GOterm with the highest significance level was the `plastoglobule` (GO:0010287), 9 proteins were increased in this cellular compartment. The expected stress-related GOterms as `response to abscisic acid` (GO:0009737), `response to osmotic stress` (GO:0006970), `response to hypoxia` (GO:0001666) were upregulated and several cold response proteins were upregulated as well. Proteins related to thylakoid membranes (GO:0009579) were enriched in the osmotic stress, increased their protein concentration was increased significantly

RNA-, DNA- and protein metabolism was negatively affected, and a big part of the DNA-metabolic proteins consisted of chromatin and histone proteins. Cell wall metabolism was enhanced, the UDP-XYL SYNTHASE 6 (UXS6, At2g28760) was the most upregulated protein in the root. UDP-xylose is used in the synthesis of major plant cell wall polysaccharides (Kuang et. al, 2016), while other cell wall enzymes were highly downregulated: i.e. FASCICLIN-LIKE ARABINOGALACTAN PROTEIN 11 (FLA11, At5g03170). Next to the cell wall and histone proteins, response proteins were expressed too. The THIOGLUCOSIDE GLUCOHYDROLASE 1 (TGG1, At5g26000) was highly upregulated, it is considered to play a role mainly in herbivore resistance by producing toxic compounds (Badenes-Perez et. al, 2012).

Gene Ontology (GOterm) enrichment and analysis of single proteins with the highest significant fold change under changed nutrient availability

When nitrogen (N0) was omitted, translation and RNA-metabolism were suppressed. Among the enriched terms in the shoot, the downregulated pathways with the highest significance belonged to these processes: 32 proteins related to `translation` (GO:0006412), 14 proteins to `RNA binding` (GO:0003723) and 25 proteins to `cytosolic ribosome` (GO:0022626). In the root, similar tendencies were detected, but DNA-metabolism was also highly affected. 97 proteins of `nucleus` (GO:0005634) were downregulated and among the enriched pathways with the highest significance are the chromatin structure terms (GO:0003682 - `chromatin binding`, GO:0042393 - `histone binding`, etc.). GOterms covering the `cellular response to nitrogen starvation` (GO:0006995) and `to nitrate` (GO:0010167) and `nitrate transmembrane transporter activity` (GO:0015112) was enriched significantly, while proteins of nitrate assimilation were downregulated (GO:0042128).

Among the most increased proteins were anthocyanin metabolism (At4g14090, At5g54060) and stress response genes (ERD1, At5g54060; CPK32, At3g57530). Several nitrate transporter (NRT2, At1g08090; NRT2.5, At1g12940; WR3, At5g50200) were upregulated together with ammonium transporters (AMT1;1, At4g13510; AMT1;3, At3g24300) in the root (AMT1 in the shoot too). The level of glutamate-ammonia ligases (GLN1;1, At5g37600; GLN1;4, At5g16570; GLN1;5, At1g48470), which play a role in glutamine synthesis, were elevated too. While the glutamine synthesis was enhanced, the catabolism of glutamine was downregulated. Glutamate synthase (GLT1, At5g53460) and glutamate dehydrogenases (GDH1, At5g18170; GDH2, At5g07440) showed a decreased protein abundance compared to the control. Glutamate synthase, which was enhanced, produces glutamate out of glutamine, which can be a substrate for glutamate dehydrogenase, which was downregulated.

Like N0, the phosphate deficiency decreased the level of RNA-metabolic and translational proteins in the shoot, while they were increased in roots. The defense and response pathways (GO:0050832 - `defense response to fungus`, GO:0009753 - `response to jasmonic acid`, etc.) were enriched in leaves with high significance. This included the `cellular response to phosphate starvation` (GO:0016036) in both tissues. Stress and response terms were

upregulated (i.e. GO:0009737 - `response to abscisic acid`, GO:0051707 - `response to other organism`) or downregulated (i.e. GO:0009409 - `response to cold`, GO:0009646 - `response to absence of light`). The term with the highest significance value was the `oxygen binding` (GO:0019825), which covered several cytochromes (CYP706A1, At4g22690; CYP71B7, AT1G13110; CYP76C7, At3g61040; CYP81F4, At4g37410) and a hemoglobin (HB1, At2g16060).

Some of the top downregulated proteins had a helicase, ribosomal or unknown function. As in N0, in the shoot of P0 the DNA-, RNA- and protein metabolism was strongly downregulated. The plants were actively responding the phosphate starvation; there were two sulfolipid biosynthetic proteins (SULFOQUINOVOSYLDIACYLGLYCEROL 1 (SQD1), At4g33030; SULFOQUINOVOSYLDIACYLGLYCEROL 2 (SQD2), At5g01220), which were highly upregulated in the shoot and the root. Co-expression showed a possible interaction (data not shown) with GLYCEROPHOSPHODIESTER PHOSPHODIESTERASE (GDPD1, At3g02040), its protein content increased in both tissues, and it had an extremely high FC ($log_2FC= 7.61$) in the root and they are important factors in maintenance of the cellular homoeostasis in phosphate deficiency (Wang et. al, 2007; Cheng et. al, 2011). Like the nitrate transporters in the N0 root, phosphate transporters (ATPT2, At2g38940; PHT1;1, At5g43350; APT1, At5g43370) were highly upregulated in the root during phosphate starvation.

Discussion

Plant responses to mild environmental perturbations

Arabidopsis thaliana plants were exposed to mildly altered environment for 10 days and the applied treatments provided us new insights about the acclimation and adaptation of plants to long-term changes. In the field of stress proteomics, where experiments are categorized (Kosová et. al, 2011; Zhang et. al, 2012; Gosh and Xu, 2014; Janmohammadi et. al, 2015), approximately one third adressed long-term stresses and these stresses were harsh. For instance, among the listed cold stress experiments (Janmohammadi et. al, 2015) in only 1 out 22 were the plants exposed to a temperature above 10°C. In our study, however, the 15°C environment already induced significant changes both in the physiology and proteome of the plants. It might be realistic that plants in their natural environment are not only exposed to severe and sudden stresses, but also to prolonged, milder impacts. Our setup allowed us to

investigate each response individually, and compare them directly. During the experiments under changed environment all plants preserved their physiological integrity illustrated by the fact that they were able to grow continuously throughout the experiments. No signs of irreversible tissue damage were observed. Transcripts usually respond fast and thus are excellent for investigation the plants' immediate sensing and response to altered conditions. Therefore, transcription changes could be interpreted as a plan and potential plasticity of plant acclimation. However, proteins are the integrated result of the transcript levels over time, they do not really follow a diurnal abundance fluctuation even if transcripts do (Baerenfaller et. al, 2012; Guerreiro et. al, 2014). Proteins rather describe and represent the newly established biological machinery over a longer time period. On the level of growth (RGR, FW and DW) and proteome, our experiments showed distinct patterns, indicating different dynamic adjustment. The resource allocation of plants culminates in biomass produced as roots and shoots. Environmental changes had a more profound effect on shoot biomass than root (Fig. 2 and 3). Except for the 25°C treatment, shoot growth was reduced by approximately 50%, whereas root biomass was mainly preserved or even increased. This observation is a common response of plants in agriculture (Richard-Molard et. al, 2008; Wang et. al, 2009). The root to shoot ratio was in all treatments higher than in the controls, indicating a preferential investment into root biomass.

Different dynamic growth pattern during the acclimation of plants to different environmental perturbations

Although shoot biomass at the end of the treatments was similar for some treatments, they often resulted from different temporal growth patterns. The RGR showed unique patterns for each of the applied conditions. In 15 °C, the shoot growth was suppressed constantly from the first day on. The initial drop in RGR is not surprising considering that enzymatic reactions are highly temperature sensitive. As a rule of thumb, a reduction of 10 °C halves the enzyme reaction rate. Obviously, this is a rough estimate and biochemical processes at a whole plant level are affected by many other parameters. Nevertheless, the fast drop in growth under reduced temperature suggests that some catalytic reactions were limiting. The RGR increased later, which might reflect the adaptation and increased synthesis of limiting enzymes.

However, the cold treated plants never reached the control RGR, implying that the rate limiting steps (enzymes) cannot be fully compensated for. In contrast, increasing the temperature by +5 °C had a positive impact on plant biomass production. The RGR showed that this growth promotion was largely dependent on the accelerated growth rate at the beginning of the treatment, whereas the RGR decreased to control levels later. This observation is again in agreement with an increased enzymatic reaction rate under increased temperature, if we assume rather constant enzyme amounts at the beginning of the treatment. Over the time of the treatment, plants likely optimize their enzyme quantity. This is in agreement with our proteomics results. For example, photosynthesis related proteins, which changed significantly decreased in 25 °C and increased in the 15 °C treatment, (Supplementary Table S5 and S6). Together with other results (increased RGR, downregulation of anthocyanin proteins, etc.) this implies that warmer environment was not necessarily a stress but rather a positive stimulus.

Other acclimation patterns were observed for both osmotic stresses (PEG and salt). At the beginning of the treatment, no reduction of growth rate was observed in the shoots and growth was only negatively affected later during the treatment. In contrast to the temperature treatments, the osmotic stresses were applied to the roots and might have consequences later on the shoots. This effect could be due to the different time the sodium and chloride ions or PEG molecules require to diffuse, be transported and accumulated in the shoots. While the ions can reach other tissues rapidly, the large PEG molecules might not even be able to overcome cellular obstacles or they do it slowly (Abraham Blum, 2008). Alternatively, the treatments could first affect root metabolism, which is sensed and transmitted to the shoots later and this would change resource allocation between shoots and roots. For the salt treatment, it is likely a combination of the two above-mentioned effects. However, in a more osmotic environment, it is more likely that the effect on shoot growth is a secondary effect on altered root metabolism. This is also substantiated by the observation that the shoot proteome in the PEG treatment was largely unaffected, whereas the salt treatment induced substantial changes in the shoot proteome. Interestingly, the RGR of the salt treated plants approached the one of the control plants at the end of the experiment, suggesting an efficient compensation response.

The two nutrient limiting conditions differed in their effect on RGR. In N0, the RGR remained the same as in control plants at the beginning, likely because nitrogen was not limiting during the first days, but this was followed by a vast drop in growth, probably due to depleted free inorganic nitrogen sources. The RGR recovered over time until it converged again towards the control levels after 10d, suggesting a gradual adaptation. This process had to rely on salvage and reuse of internal available nitrogen sources (e.g. proteins). The RGR response on phosphate limitation was somehow counterintuitive as it first dropped below control level and recovered for 4 days to control level with a decline at the end of the treatment. As the phosphate supply was omitted, it must have been sensed immediately by the plants and initiated a successful temporal growth stop in the shoots. That might be explained by relatively high internal phosphate storage pools in the vacuole (Liu et. al, 2016), which first had to be made accessible.

The analysis of the rewired proteomic machinery revealed crucial differences of the plants' acclimation processes

The number of significantly changed proteins with ±1.5 FC was higher in the nutrient deficient treatments. That suggests that they might have induced a deeper change in the plant proteome, although the growth measurements (FW, DW, RGR) did not necessary reflect that. However, if the number of significant changing proteins is used as an indicator for the complexity of proteome remodeling, the 15°C treatment in the shoot induced the greatest perturbation in the proteome. Among the proteins with the highest significant fold change in 15°C, stress-related proteins were overrepresented, which was quite unique compared to the other mild abiotic treatments, implying also that 5°C decrease can already have a strong effect on the plants.

Interestingly, while the osmotic treatment promoted strong changes of the proteome in the root, the shoot seemed almost unaffected. Similar phenomena were observed in comparative proteomic analysis of roots and shoots of drought-stressed soybean seedlings (Mohammadi et. al, 2012). The uptake of the long PEG6000 molecules is very slow and mostly concentrated in the roots, especially if root damage is avoided and the concentration is not high (Abraham Blum, 2008). The relatively unchanged proteome in the shoots suggest that their growth

retardation is mostly an indirect effect of changed metabolism in the roots, resulting in resource allocation towards the roots. It raises the question, whether stresses are local or systemic, whether the stress was communicated throughout the plant or the observed shoot phenotype could have been a secondary effect. Here, 4 out of 6 treatments (salt, PEG and nutrients) were applied to the roots through changes in the media, and as expected, they had an effect on the whole plant. In the case of PEG treatment, the stress response on proteome level remained local. This illustrates that observed phenotypes in one tissue are not necessarily easy to explain with measured factors (e.g. transcript, protein abundances) in the same tissue. Obviously, it is important to treat multicellular organism as a system to conclude about cause and effect. Although our experimental setup did not allow us to apply a tissue specific temperature treatment, plants in nature are exposed to different temperatures below and above ground and this should be considered in future experiments. The response processes between the shoot and root were different in every treatment; indicating highly tissue specific adaptation mechanism. To our knowledge, only a few experiments were performed, where the impact of the treatment on the proteome of both organs was analyzed. It was investigated in rice, soybean, barley, cotton (Lee et. al, 2010; Sobhanian et. al, 2010; Moller et. al, 2011; Mohammadi et. al, 2012; Chen et. al, 2016) and no major overlap of the changing proteins was detected and reported between the two organs. There was a relatively small overlapping fraction of changing proteins in both tissue, which often changed similar. This implies regulatory processes or certain pathways, which have a system-wide function.

The clustering and correlation analysis verified the tissue specificity and the mildness of the treatments. Responses to nutrient deficiencies (N0, P0) overlapped to a certain level on the proteomic level, they clustered always together and showed a high correlation. N and P metabolism is linked, the N:P ratio (supply, demand, etc.) is an important factor of growth (co-limitation) (Ågren et. al, 2012; Menge et. al, 2012). Nutrient limitations can induce either similar or opposite responses (Nguyen et. al, 2015), but in our experimental setup the changes in abundance of proteins, which were detected in both nutrient treatments, were similar. However, plants exposed to N0 and P0showed a different growth response.

In contrast to our starting hypothesis, the response to salt and osmotic treatment were quite different on the proteome level, especially in the root. Often, both are considered to have a

similar effect on plants and are at least discussed together (Jian-Kang Zhu, 2002; Fujita et. al, 2006; Zhang et. al, 2006; Golldack et. al, 2014), but there is some evidence at the transcriptomic level that already suggested differently (Kreps et. al, 2002; Patade et. al, 2012). Due to the low number of changed proteins in the osmotic stress the overlap between the two treatments was also low. Only two proteins changed with ±1.5 FC in both treatments. However, both proteins (At2g39800 and At1g54100) were characterized previously as stress-responsive proteins. They are induced by several external stimuli, which include water deprivation and elevated salt level (Székely et. al, 2008, Li-Beisson et. al, 2013).

The observed high correlation between salt and PEG treatment in the shoots (Fig. 6c) suggest the same tendencies of adaptation with a more accentuated response in the salt treatment. This could be caused by a harsher environmental challenge for the plant under salt conditions. However, this is not supported by the observed biomass production. It is more likely that the salt treatments evoke a multilevel response including simultaneous ion toxicity and water deprivation, whereas PEG induced responses to water deprivation only. In the shoots, the PEG treatment affected the proteome only slightly, but the root proteome was seriously affected. There were many proteins with much higher fold changes in both treatments that enabled us to draw a conclusion about the differences of the plant's response in the two experiments (Fig. 6d). Contrary to the long PEG molecules, which are likely not taken up by the plants, the excess salt ions might have a direct effect on the ionic homeostasis of cells across the whole plant. In osmotic stress induced by PEG, the changed osmotic inhibits the plants to uptake water and nutrient from the surroundings of the roots (Albert et. al, 2012). This is supported by the proteomics clustering analysis (Fig. 5a) where, in the case of the root, the osmotic treatment grouped together with the nutrient deficiencies.

As a response to the excess salt, the photosynthetic apparatus might have been even positively affected and this observation coincides with earlier proteomic findings in other plant species, mainly in the salt tolerant mangrove (Zhu et. al, 2012; Wang et. al, 2014). Two LHC proteins together with the thylakoid transmembrane PGRL1B protein had increased protein level, while the concentration of two CP12 enzymes decreased. The downregulation of the latter might reduce complex formation and subsequently increase the activity of two Calvin-Benson cycle enzymes (GAPDH and PRK) (López-Calcagno et. al, 2014).

The data revealed an unexpected group of proteins related to thylakoid membranes which was enriched upon the osmotic treatment. Although, these proteins should not be detected in the root in theory, most of them were expressed in most of the root experiments and this was confirmed by gene expression data (Suppl. Fig. 4) illustrating the occasional deceptive naming convention of GOterms. The PEG-treatment might have also affected the cell wall in the roots. Roots are considered the primary site of sensing drought and osmotic stress, and PEG-induced osmotic stress changes the properties of the cell wall in the root, especially the porosity (Sharp et. al, 2004; Yang et. al, 2013). UDP-xylose synthase 6, the protein with the highest fold change, is involved in xylan synthesis a major plant cell wall polysaccharide (Kuang et. al, 2016), while the abundance of other cell wall related enzymes were decreased.

Plants can sense temperature. Several pathways and proteins abundances are known to be affected and regulated by temperature changes (Patel and Franklin, 2009). However, most of them are described as either cold or heat dependent. We observed around 100 changing proteins with ±1.5 FC in each condition and tissue, and the majority was tissue and condition dependent. However, a subset of 20 proteins showed an inverse pattern between both temperature regimens. Further, including all significantly changing proteins into the analysis resulted in a high negative correlation between abundance and temperature. We tested if the observed correlation was linked to growth rather than temperature. 17 out of the 20 proteins were found with significant fold change in other treatments as well, and the change in abundance was growth-independent (Suppl. Table 3) suggesting that these 20 proteins are temperature dependent. Thereby, they are promising to be studied in more detail over a finer temperature gradient with a bigger range.

Is there a core stress response in plants?

The majority of the proteins with changed abundancies were rather specific for the treatment and only observed one or two times (94% in the shoot and 95% in the root). That could be interpreted as every change in the environment triggers specific responses even if two treatments are considered to be of similar nature. The underlying reason might be found in our experimental setup, where plants operate under tolerable changed conditions without experiencing fatal stresses. The later would probably result in chlorosis, necrotic tissues or

abscission which than would result in similar responses. On the other hand, there were still several key proteins (Table 3 and 4), which changed in three or more treatments. A cold stress might induces water deficit. Similarly, phosphate and nitrate limitations are cross-linked (Ågren et. al, 2012), drought changes not only the osmotic, but the ionic status of the cell. Further, upon environmental stresses reactive oxygen species, which are chemically highly reactive and harmful molecules, are always generated. The highly specific response to treatments at the proteome level do not exclude common response-characteristics between the treatments at earlier time points.

The protein NMT1 (At3g18000) came the closest to the definition to a “masterregulator”, as it was detected with significantly high fold change in 9 out 12 treatments, both in shoots and roots, but it showed no significant regulation in osmotic stress, although in different experimental setup in earlier findings it was shown to be also part of the response to osmotic stress (Zhang et. al, 2010). NMT1 is involved in phospholipid metabolism and catalyzes key methylation steps in choline biosynthesis (BeGora et. al, 2010; Eastmond et. al, 2010). The gene expression of NMT1 follows a similar stress-responsive pattern, and might be a good marker of lipid metabolism in stress (Supplementary Fig. S3). The overall large response of NMT1 levels in environmental changed conditions makes it a good target for more specific experiments to elucidate the exact role of this enzyme.

The GOterm analysis revealed the expected defense, response and acclimation processes. Further, an activation of DNA-, RNA- and protein metabolic processes was observed in most of the experiments. There was an upregulation in 15 °C of these processes, especially in the shoot, indicating more active transcription and translation. The salt treatment affected less of these major metabolic pathways, the protein synthesis machinery, which might have been intensified earlier, may have been stopped until the end of the 10th day. The downregulation of the few proteins in 25 °C rather suggest that the plants were not necessary stressed or the acclimation process was completed already. In other experiments (osmotic, N0, P0) the abundance of proteins, which belonged to translation, ribosome biogenesis, RNA-binding, helicase activity, etc., were decreased, which can be the result of the unavailability of the necessary building blocks. There were several changes in the proteome, which could be linked

to physiological processes. The lower water content in the shoot of the cold treated plants can be a result or consequence of downregulation of aquaporins.

Transporter activity, which is responsible for the transfer of the necessary nutrient, increased in the N0 and P0 environments, as it was previously shown (Lezhneva et. al, 2014; Ayadi et. al, 2015), however, nitrate assimilation was decreased in N0. The unavailability of nitrate was sensed by the plants, they did not invest into the whole assimilation machinery, but rather directed their resources into the synthesis of the nutrient transporters to increase nutrient uptake. Like the ammonium and nitrate transporters in N0, the phosphate transporter level was increased in the roots of plants exposed to phosphate starvation. SQD proteins are key enzymes involved in sulfolipid biosynthesis, crucial for photosynthetic membranes (Yu et. al, 2002) were extremely elevated in both tissues. Together with the increased amount of glycerophosphodiester phosphodiesterase (GDPD1, At3g02040) they maintain the phosphate homeostasis during phosphate starvation (Cheng et. al, 2011). Together with the abundant transporters these proteins probably contribute to the rapid incorporation and metabolism of phosphate, if any source becomes available. While the phosphorus is limited, the plants also enhance alternate pathways; the phosphoenolpyruvate carboxylase (PEPC, At1g53310), which had an increased protein level in the shoot and root of the plants exposed to phosphate starvation, provides a metabolic bypass for the cytosolic pyruvate kinase together with malate dehydrogenase and NAD-malic enzyme, which are ADP-limited to facilitate the supply of pyruvate (Gregory et. al, 2009; Plaxton and Tran, 2011). Further, phosphatases were upregulated for acquisition of phosphate from intra- and/or extracellular sources. In the root, the protein abundances of purple acid phosphatases (PAPs) were increased and the PAP17 (At3g17790), which had the highest fold change, had been previously shown to be strongly induced upon phosphate starvation (del Pozo et. al, 1999). The upregulation of this array of different proteins shows the complex response of the plants induced by phosphate starvation and their adjustment to the nutrient limiting environment. While metabolism is adjusted to be prepared for the rapid intake and incorporation of phosphate, simultaneously every available phosphorus, which can be temporary dispensable (vacuole, phospholipids, sulfolipids, etc.), is mobilized.

Future perspectives

Plants have adapted to cope with environmental changes, and these adaptations seem to be specific based on biomass allocation, growth strategy and proteome changes. Environment perturbations usually occur simultaneously and plants are often exposed to combination of stresses in the field. Transcriptomic data already revealed that the combination of different treatment induced response processes that could have not been predicted from the single stress experiment (Rasmussen et. al, 2013, Barah et. al, 2015). Some proteomic experiments were already carried out recently in maize and soybean with the application of a short-term strong heat and drought stress together (Das et. al, 2016; Zhao et. al, 2016), but we still lack a deep understanding on the mechanism of plant response to a combination of different stress. These investigations should be performed with a combination of "omics" methods to allow the building of predictive scenarios how plants adopt to environmental changes.

Acknowledgements

We thank our gardener, Andrea Ruckle, for supporting us with plant growth. We thank Samuel C. Zeeman for project discussion and inputs. We thank Johannes Fütterer for statistical support.

References

Agarwal, P., Parida, S.K., Mahto, A., Das, S., Mathew, I.E., Malik, N., et al., (2014). Expanding frontiers in plant transcriptomics in aid of functional genomics and molecular breeding. *Biotechnol. J.* 9, 1480–1492.

Agren, G.I., Wetterstedt, J.Å.M., Billberger, M.F.K., (2012). Nutrient limitation on terrestrial plant growth - modeling the interaction between nitrogen and phosphorus. *New Phytol.* 194, 953–960.

Ahmad, A., Niwa, Y., Goto, S., Kobayashi, K., Shimizu, M., Ito, S., et al., (2015). Genome-wide screening of salt tolerant genes by activation-tagging using dedifferentiated calli of Arabidopsis and its application to finding gene for Myo-inositol-1-P-Synthase. *PLoS One* 10, 1–22.

Alexandratos, N., Bruinsma, J., (2012). WORLD AGRICULTURE TOWARDS 2030 / 2050 The 2012 Revision. *FAO*

Albert, B., Le Cahérec, F., Niogret, M.F., Faes, P., Avice, J.C., Leport, L., et al., (2012). Nitrogen availability impacts oilseed rape (*Brassica napus* L.) plant water status and proline production efficiency under water-limited conditions. *Planta* 236, 659–676.

An, Y., Feng, X., Liu, L., Xiong, L., Wang, L., (2016). ALA-Induced Flavonols Accumulation in Guard Cells Is Involved in Scavenging H_2O_2 and Inhibiting Stomatal Closure in Arabidopsis Cotyledons. *Front. Plant Sci.* 7, 1713.

Ayadi, A., David, P., Arrighi, J.-F., Chiarenza, S., Thibaud, M.-C., Nussaume, L., et al., (2015). Reducing the genetic redundancy of Arabidopsis PHOSPHATE TRANSPORTER1 transporters to study phosphate uptake and signaling. *Plant Physiol.* 167, 1511–26.

Badenes-Perez, F.R., Reichelt, M., Gershenzon, J., Heckel, D.G., (2013). Interaction of glucosinolate content of *Arabidopsis thaliana* mutant lines and feeding and oviposition by generalist and specialist lepidopterans. *Phytochemistry* 86, 36–43.

Baerenfaller, K., Massonnet, C., Walsh, S., Baginsky, S., Bühlmann, P., Hennig, L., et al., (2012). Systems-based analysis of Arabidopsis leaf growth reveals adaptation to water deficit. *Mol. Syst. Biol.* 8, 606.

Barah, P., B N, M.N., Jayavelu, N.D., Sowdhamini, R., Shameer, K., Bones, A.M., (2015). Transcriptional regulatory networks in *Arabidopsis thaliana* during single and combined stresses. *Nucleic Acids Res.* 44, 3147–64.

BeGora, M.D., Macleod, M.J.R., McCarry, B.E., Summers, P.S., Weretilnyk, E.A., (2010). Identification of phosphomethylethanolamine N-methyltransferase from Arabidopsis and its role in choline and phospholipid metabolism. *J. Biol. Chem.* 285, 29147–29155.

Bharti, P., Mahajan, M., Vishwakarma, A.K., Bhardwaj, J., Yadav, S.K., (2015). AtROS1 overexpression provides evidence for epigenetic regulation of genes encoding enzymes of flavonoid biosynthesis and antioxidant pathways during salt stress in transgenic tobacco. *J. Exp. Bot.* 66, 5959–5969.

Blée, E., Boachon, B., Burcklen, M., Le Guédard, M., Hanano, A., Heintz, D., et al., (2014). The reductase activity of the Arabidopsis caleosin RESPONSIVE TO DESSICATION20 mediates gibberellin-dependent flowering time, abscisic acid sensitivity, and tolerance to oxidative stress. *Plant Physiol.* 166, 109–24.

Blum, A.,(2008). Use of PEG to induce and control plant water deficit in experimental hydroponics' culture. *Plantstress.com* http://www.plantstress.com/methods/peg.htm

Challinor, A.J., Watson, J., Lobell, D.B., Howden, S.M., Smith, D.R., Chhetri, N., (2014). A meta-analysis of crop yield under climate change and adaptation. *Nat. Clim. Chang.* 4, 287–291.

Chen, T., Zhang, L., Shang, H., Liu, S., Peng, J., Gong, W., et al., (2016). ITRAQ-based quantitative proteomic analysis of cotton roots and leaves reveals pathways associated with salt stress. *PLoS One* 11, 1–15.

Cheng, Y., Zhou, W., El Sheery, N.I., Peters, C., Li, M., Wang, X., et al., (2011). Characterization of the Arabidopsis glycerophosphodiester phosphodiesterase (GDPD) family reveals a role of the plastid-localized AtGDPD1 in maintaining cellular phosphate homeostasis under phosphate starvation. *Plant J.* 66, 781–795.

Curtis, T., Halford, N.G., (2014). Food security: The challenge of increasing wheat yield and the importance of not compromising food safety. *Ann. Appl. Biol.* 164, 354–372.

Dai, A.G., (2013). Increasing drought under global warming in observations and models. *Nat. Clim. Chang.* 3, 52–58.

Das, A., Eldakak, M., Paudel, B., Kim, D.W., Hemmati, H., Basu, C., et al., (2016). Leaf proteome analysis reveals prospective drought and heat stress response mechanisms in soybean. *Biomed Res. Int.* 2016.

Del Pozo, J.C., Allona, I., Rubio, V., Leyva, A., De La Peña, A., Aragoncillo, C., et al., (1999). A type 5 acid phosphatase gene from *Arabidopsis thaliana* is induced by phosphate starvation and by some other types of phosphate mobilising/oxidative stress conditions. *Plant J.* 19, 579–589.

Deyholos, M.K., (2010). Making the most of drought and salinity transcriptomics. *Plant, Cell Environ.* 33, 648–654.

Dockter, C., Gruszka, D., Braumann, I., Druka, A., Druka, I., Franckowiak, J., et al., (2014). Induced variations in brassinosteroid genes define barley height and sturdiness, and expand the green revolution genetic toolkit. *Plant Physiol* 166, 1912–1927.

Dupae, J., Bohler, S., Noben, J.-P., Carpentier, S., Vangronsveld, J., Cuypers, A., (2014). Problems inherent to a meta-analysis of proteomics data: a case study on the plants' response to Cd in different cultivation conditions. *J. Proteomics* 108, 30–54.

Eastmond, P.J., Quettier, A.-L., Kroon, J.T.M., Craddock, C., Adams, N., Slabas, A.R., (2010). PHOSPHATIDIC ACID PHOSPHOHYDROLASE1 and 2 regulate phospholipid synthesis at the endoplasmic reticulum in Arabidopsis. *Plant Cell* 22, 2796–2811.

Fellerer, C., Schweiger, R., Schöngruber, K., Soll, J., Schwenkert, S., (2011). Cytosolic HSP90 cochaperones HOP and FKBP interact with freshly synthesized chloroplast preproteins of Arabidopsis. *Mol. Plant* 4, 1133–1145.

Fujita, M., Fujita, Y., Noutoshi, Y., Takahashi, F., Narusaka, Y., Yamaguchi-Shinozaki, K., et al., (2006). Crosstalk between abiotic and biotic stress responses: a current view from the points of convergence in the stress signaling networks. *Curr. Opin. Plant Biol.* 9, 436–442.

Gao, H., Brandizzi, F., Benning, C., Larkin, R.M., (2008). A membrane-tethered transcription factor defines a branch of the heat stress response in *Arabidopsis thaliana*. *Proc. Natl. Acad. Sci. U. S. A.* 105, 16398–16403.

Ghosh, D., Xu, J., (2014). Abiotic stress responses in plant roots: a proteomics perspective. *Front. Plant Sci.* 5, 6.

Gibeaut, D.M., Hulett, J., Cramer, G.R., Seemann, J.R., (1997). Maximal biomass of *Arabidopsis thaliana* using a simple, low-maintenance hydroponic method and favorable environmental conditions. *Plant Physiol.* 115, 317–9.

Golldack, D., Li, C., Mohan, H., Probst, N., (2014). Tolerance to drought and salt stress in plants: Unraveling the signaling networks. *Front. Plant Sci.* 5, 151.

Gorsuch, P.A., Sargeant, A.W., Penfield, S.D., Quick, W.P., Atkin, O.K., (2010). Systemic low temperature signaling in Arabidopsis. *Plant Cell Physiol.* 51, 1488–1498.

Gregory, A.L., Hurley, B.A., Tran, H.T., Valentine, A.J., She, Y.-M., Knowles, V.L., et al., (2009). *In vivo* regulatory phosphorylation of the phosphoenolpyruvate carboxylase AtPPC1 in phosphate-starved *Arabidopsis thaliana*. *Biochem. J.* 420, 57–65.

Guerreiro, A.C.L., Benevento, M., Lehmann, R., van Breukelen, B., Post, H., Giansanti, P., et al., (2014). Daily rhythms in the cyanobacterium *Synechococcus elongatus* probed by high-resolution mass spectrometry-based proteomics reveals a small defined set of cyclic proteins. *Mol. Cell. Proteomics* 13, 2042–55.

Han, Z., Yu, H., Zhao, Z., Hunter, D., Luo, X., Duan, J., et al., (2016). AtHD2D gene plays a role in plant growth, development, and response to abiotic stresses in *Arabidopsis thaliana*. *Front. Plant Sci.* 7, 310.

Heinen, M., (1999). Analytical growth equations and their Genstat 5 equivalents. *Netherlands J. Agric. Sci.* 47, 67–89.

Janmohammadi, M., Zolla, L., Rinalducci, S., (2015). Low temperature tolerance in plants: Changes at the protein level. *Phytochemistry* 117, 76–89.

Jorrín-Novo, J. V., Pascual, J., Sánchez-Lucas, R., Romero-Rodríguez, M.C., Rodríguez-Ortega, M.J., Lenz, C., et al., (2015). Fourteen years of plant proteomics reflected in Proteomics: Moving from model species and 2DE-based approaches to orphan species and gel-free platforms. *Proteomics* 15, 1089–1112.

Käll, L., Storey, J.D., MacCoss, M.J., Noble, W.S., (2008). Assigning significance to peptides identified by tandem mass spectrometry using decoy databases. *J. Proteome Res.* 7, 29–34.

Kelstrup, C.D., Young, C., Lavallee, R., Nielsen, M.L., Olsen, J. V., (2012). Optimized fast and sensitive acquisition methods for shotgun proteomics on a quadrupole orbitrap mass spectrometer. *J. Proteome Res.* 11, 3487–3497.

Kissen, R., Bones, A.M., (2009). Nitrile-specifier proteins involved in glucosinolate hydrolysis in *Arabidopsis thaliana*. *J. Biol. Chem.* 284, 12057–12070.

Kosová, K., Vítámvás, P., Prásil, I.T., Renaut, J., (2011). Plant proteome changes under abiotic stress - Contribution of proteomics studies to understanding plant stress response. *J. Proteomics* 74, 1301–1322.

Kreps, J.A., Wu, Y., Chang, H., Zhu, T., Wang, X., Harper, J.F., et al., (2002). Transcriptome changes for Arabidopsis in response to salt, osmotic, and cold stress. *Plant Physiol.* 130, 2129–2141.

Kuang, B., Zhao, X., Zhou, C., Zeng, W., Ren, J., Ebert, B., et al., (2016). Role of UDP-glucuronic acid decarboxylase in xylan biosynthesis in Arabidopsis. *Mol. Plant* 9, 1119–1131.

Kumar, D., Datta, R., Hazra, S., Sultana, A., Mukhopadhyay, R., Chattopadhyay, S., (2015). Transcriptomic profiling of *Arabidopsis thaliana* mutant pad2.1 in response to combined cold and osmotic stress. *PLoS One* 10(3).

Kupsch, C., Ruwe, H., Gusewski, S., Tillich, M., Small, I., Schmitz-Linneweber, C., (2012). Arabidopsis chloroplast RNA binding proteins CP31A and CP29A associate with large transcript pools and confer cold stress tolerance by influencing multiple chloroplast RNA processing steps. *Plant Cell* 24, 4266–4280.

Lee, K., Kang, and H., (2016). Emerging roles of RNA-binding proteins in plant growth, development, and stress responses. *Mol. Cells* 39, 179–185.

Lee, K., Bae, D.W., Kim, S.H., Han, H.J., Liu, X., Park, H.C., et al., (2010). Comparative proteomic analysis of the short-term responses of rice roots and leaves to cadmium. *J. Plant Physiol.* 167, 161–168.

Lehtimäki, N., Lintala, M., Allahverdiyeva, Y., Aro, E.M., Mulo, P., (2010). Drought stress-induced upregulation of components involved in ferredoxin-dependent cyclic electron transfer. *J. Plant Physiol.* 167, 1018–1022.

Less, H., Galili, G., (2008). Principal transcriptional programs regulating plant amino acid metabolism in response to abiotic stresses. *Plant Physiol.* 147, 316–330.

Lezhneva, L., Kiba, T., Feria-Bourrellier, A.B., Lafouge, F., Boutet-Mercey, S., Zoufan, P., et al., (2014). The Arabidopsis nitrate transporter NRT2.5 plays a role in nitrate acquisition and remobilization in nitrogen-starved plants. *Plant J.* 80, 230–241.

Li, D., Liu, H., Zhang, H., Wang, X., Song, F., (2008). OsBIRH1, a DEAD-box RNA helicase with functions in modulating defence responses against pathogen infection and oxidative stress. *J. Exp. Bot.* 59, 2133–2146.

Li, J., Brader, G., Palva, E.T., (2008). Kunitz trypsin inhibitor: An antagonist of cell death triggered by phytopathogens and fumonisin B1 in Arabidopsis. *Mol. Plant* 1, 482–495.

Li-Beisson, Y., Shorrosh, B., Beisson, F., Andersson, M.X., Arondel, V., Bates, P.D., et al., (2013). Acyl-Lipid Metabolism. *Arab. B.* 11, e0161.

Liebig J. 1840. Die organische Chemie in ihrer Anwendung auf Agrikultur und Physiologie. *Friedrich Vieweg und Sohn Publ. Co*.

Liebig J. 1855. Die Grundsätze der Agrikultur-Chemie mit Rücksicht auf die in England angestellten Untersuchungen, *1st and 2nd edn. Braunschweig, Germany: Friedrich Vieweg und Sohn Publ Co.*

Liu, T.-Y., Huang, T.-K., Yang, S.-Y., Hong, Y.-T., Huang, S.-M., Wang, F.-N., et al., (2016). Identification of plant vacuolar transporters mediating phosphate storage. *Nat. Commun.* 7, 11095.

Liu, Y., (2005). Arabidopsis vegetative storage protein is an anti-insect acid phosphatase. *Plant Physiol.* 139, 1545–1556.

López-Calcagno, P.E., Howard, T.P., Raines, C. a, (2014). The CP12 protein family: a thioredoxin-mediated metabolic switch? *Front. Plant Sci.* 5, 9.

Mammarella, N.D., Cheng, Z., Fu, Z.Q., Daudi, A., Bolwell, G.P., Dong, X., et al., (2015). Apoplastic peroxidases are required for salicylic acid-mediated defense against *Pseudomonas syringae*. *Phytochemistry* 112, 110–121.

Masclaux-Daubresse, C., Daniel-Vedele, F., Dechorgnat, J., Chardon, F., Gaufichon, L., Suzuki, A., (2010). Nitrogen uptake, assimilation and remobilization in plants: Challenges for sustainable and productive agriculture. *Ann. Bot.* 105, 1141–1157.

Menge, D.N.L., Hedin, L.O., Pacala, S.W., (2012). Nitrogen and phosphorus limitation over long-term ecosystem development in terrestrial ecosystems. *PLoS One* 7(8).

Mita, S., Suzukifujii, K., Nakamura, K., (1995). Sugar inducible expression of a gene for beta-amylase in *Arabidopsis thaliana*. *Plant Physiol* 107, 895–904.

Mohammadi, P.P., Moieni, A., Hiraga, S., Komatsu, S., (2012). Organ-specific proteomic analysis of drought-stressed soybean seedlings. *J. Proteomics* 75, 1906–1923.

Moller, A.L.B., Pedas, P., Andersen, B., Svensson, B., Schjoerring, J.K., Finnie, C., (2011). Responses of barley root and shoot proteomes to long-term nitrogen deficiency, short-term nitrogen starvation and ammonium. *Plant, Cell Environ.* 34, 2024–2037.

Monroe, J.D., Storm, A.R., Badley, E.M., Lehman, M.D., Platt, S.M., Saunders, L.K., et al., (2014). beta-amylase1 and beta-amylase3 are plastidic starch hydrolases in Arabidopsis that seem to be adapted for different thermal, pH, and stress Conditions. *Plant Physiol.* 166, 1748–1763.

Nguyen, G.N., Rothstein, S.J., Spangenberg, G., Kant, S., (2015). Role of microRNAs involved in plant response to nitrogen and phosphorous limiting conditions. *Front. Plant Sci.* 6, 1–15.

Paine, C.E.T., Marthews, T.R., Vogt, D.R., Purves, D., Rees, M., Hector, A., et al., (2012). How to fit nonlinear plant growth models and calculate growth rates: An update for ecologists. *Methods Ecol. Evol.* 3, 245–256.

Patade, V.Y., Bhargava, S., Suprasanna, P., (2012). Transcript expression profiling of stress responsive genes in response to short-term salt or PEG stress in sugarcane leaves. *Mol. Biol. Rep.* 39, 3311–3318.

Patel, D., Franklin, K.A., (2009). Temperature-regulation of plant architecture. *Plant Signal. Behav.* 4, 577–9.

Plaxton, W.C., Tran, H.T., (2011). Metabolic Adaptations of Phosphate-Starved Plants. *Plant Physiol.* 156, 1006–1015.

Poorter, H., (1989). Plant growth analysis: towards a synthesis of the classical and the functional approach. *Physiol. Plant.* 75, 237–244.

Pourcel, L., Irani, N.G., Lu, Y., Riedl, K., Schwartz, S., Grotewold, E., (2010). The formation of anthocyanic vacuolar inclusions in *Arabidopsis thaliana* and implications for the sequestration of anthocyanin pigments. *Mol. Plant* 3, 78–90.

Qi, Y., Katagiri, F., (2012). Membrane microdomain may be a platform for immune signaling. *Plant Signal Behav* 7, 454–456.

Raines, C.A., (2011). Increasing photosynthetic carbon assimilation in C3 plants to improve crop yield: current and future strategies. *Plant Physiol.* 155, 36–42.

Rasmussen, S., Barah, P., Suarez-Rodriguez, M.C., Bressendorff, S., Friis, P., Costantino, P., et al., (2013). Transcriptome responses to combinations of stresses in Arabidopsis. *Plant Physiol.* 161, 1783–94.

Rest, J.S., Wilkins, O., Yuan, W., Purugganan, M.D., Gurevitch, J., (2016). Meta-analysis and meta-regression of transcriptomic responses to water stress in Arabidopsis. *Plant J* 85, 548–560.

Richard-Molard, C., Krapp, A., Brun, F., Ney, B., Daniel-Vedele, F., Chaillou, S., (2008). Plant response to nitrate starvation is determined by N storage capacity matched by nitrate uptake capacity in two Arabidopsis genotypes. *J. Exp. Bot.* 59, 779–791.

Robles, P., Micol, J.L., Quesada, V., (2012). Arabidopsis MDA1, a nuclear-encoded protein, functions in chloroplast development and abiotic stress responses. *PLoS One* 7.

Rodziewicz, P., Swarcewicz, B., Chmielewska, K., Wojakowska, A., Stobiecki, M., (2014). Influence of abiotic stresses on plant proteome and metabolome changes. *Acta Physiol. Plant.* 36, 1–19.

Ruts, T., Matsubara, S., Walter, A., (2013). Synchronous high-resolution phenotyping of leaf and root growth in *Nicotiana tabacum* over 24-h periods with GROWMAP-plant. *Plant Methods* 9, 2.

Sharp, R.E., Poroyko, V., Hejlek, L.G., Spollen, W.G., Springer, G.K., Bohnert, H.J., et al., (2004). Root growth maintenance during water deficits: Physiology to functional genomics. *J. Exp. Bot.* 55, 2343–2351.

Sistrunk, M.L., Antosiewicz, D.M., Purugganan, M.M., Braam, J., (1994). Arabidopsis TCH3 encodes a novel Ca^{2+} binding protein and shows environmentally induced and tissues-specific regulation. *Plant Cell* 6, 1553–1565.

Sobhanian, H., Razavizadeh, R., Nanjo, Y., Ehsanpour, A.A., Jazii, F.R., Motamed, N., et al., (2010). Proteome analysis of soybean leaves, hypocotyls and roots under salt stress. *Proteome Sci.* 8, 19.

Stitt, M., Lunn, J., Usadel, B., (2010). Arabidopsis and primary photosynthetic metabolism - More than the icing on the cake. *Plant J.* 61, 1067–1091.

Székely, G., Ábrahám, E., Cséplo, Á., Rigó, G., Zsigmond, L., Csiszár, J., et al., (2008). Duplicated P5CS genes of Arabidopsis play distinct roles in stress regulation and developmental control of proline biosynthesis. *Plant J.* 53, 11–28.

Timabud, T., Yin, X., Pongdontri, P., Komatsu, S., (2016). Gel-free/label-free proteomic analysis of developing rice grains under heat stress. *J. Proteomics* 133, 1–19.

Tocquin, P., Corbesier, L., Havelange, A., Pieltain, A., Kurtem, E., Bernier, G., et al., (2003). A novel high efficiency, low maintenance, hydroponic system for synchronous growth and flowering of *Arabidopsis thaliana*. *BMC Plant Biol.* 3, 2.

Tolin, S., Arrigoni, G., Trentin, A.R., Veljovic-Jovanovic, S., Pivato, M., Zechman, B., et al., (2013). Biochemical and quantitative proteomics investigations in Arabidopsis *ggt1* mutant leaves reveal a role for the gamma-glutamyl cycle in plant's adaptation to environment. *Proteomics* 13, 2031–2045.

Vizcaíno, J.A., Deutsch, E.W., Wang, R., Csordas, A., Reisinger, F., Ríos, D., et al., (2014). ProteomeXchange provides globally coordinated proteomics data submission and dissemination. *Nat. Biotechnol.* 32, 223–226.

Wang, C., Ying, S., Huang, H., Li, K., Wu, P., Shou, H., (2009). Involvement of OsSPX1 in phosphate homeostasis in rice. *Plant J.* 57, 895–904.

Wang, L., Liu, X., Liang, M., Tan, F., Liang, W., Chen, Y., et al., (2014). Proteomic analysis of salt-responsive proteins in the leaves of mangrove *Kandelia candel* during short-term stress. *PLoS One* 9.

Wang, Y., Secco, D., Poirier, Y., (2008). Characterization of the PHO1 gene family and the responses to phosphate deficiency of *Physcomitrella patens*. *Plant Physiol.* 146, 646–656.

Wisniewski, J.R., Zougman, A., Nagaraj, N., Mann, M., (2009). Universal sample preparation method for proteome analysis. *Nat Methods* 6, 359–362.

Xie, Y., Mao, Y., Lai, D., Zhang, W., Zheng, T., Shen, W., (2013). Roles of NIA/NR/NOA1-dependent nitric oxide production and HY1 expression in the modulation of Arabidopsis salt tolerance. *J. Exp. Bot.* 64, 3045–3060.

Yamada, K., Kanai, M., Osakabe, Y., Ohiraki, H., Shinozaki, K., Yamaguchi-Shinozaki, K., (2011). Monosaccharide absorption activity of Arabidopsis roots depends on expression profiles of transporter genes under high salinity conditions. *J. Biol. Chem.* 286, 43577–43586.

Yang, Z.B., Eticha, D., Führs, H., Heintz, D., Ayoub, D., Van Dorsselaer, A., et al., (2013). Proteomic and phosphoproteomic analysis of polyethylene glycol-induced osmotic stress in root tips of common bean (*Phaseolus vulgaris* L.). *J. Exp. Bot.* 64, 5569–5586.

Yu, B., Xu, C., Benning, C., (2002). Arabidopsis disrupted in SQD2 encoding sulfolipid synthase is impaired in phosphate-limited growth. *Proc. Natl. Acad. Sci. U. S. A.* 99, 5732–5737.

Zhang, H., Han, B., Wang, T., Chen, S., Li, H., Zhang, Y., et al., (2012). Mechanisms of plant salt response: Insights from proteomics. *J. Proteome Res.* 11, 49–67.

Zhang, J., Jia, W., Yang, J., Ismail, A.M., (2006). Role of ABA in integrating plant responses to drought and salt stresses. *F. Crop. Res.* 97, 111–119.

Zhang, H., Murzello, C., Sun, Y., Kim, M.-S., Xie, X., Jeter, R.M., et al., (2010). Choline and osmotic-stress tolerance induced in Arabidopsis by the soil microbe *Bacillus subtilis* (GB03). *Mol. Plant. Microbe. Interact*. 23, 1097–104.

Zhao, F., Zhang, D., Zhao, Y., Wang, W., Yang, H., Tai, F., et al., (2016). The difference of physiological and proteomic changes in maize leaves adaptation to drought, heat, and combined both stresses. *Front. Plant Sci.* 7, 1471.

Zhu, J.-K., (2002). Salt and drought stress signal transduction in plants. *Annu. Rev. Plant Biol.* 40, 349–379.

Zhu, Z., Chen, J., Zheng, H.L., (2012). Physiological and proteomic characterization of salt tolerance in a mangrove plant, *Bruguiera gymnorrhiza* (L.) Lam. *Tree Physiol.* 32, 1378–1388.

Supplementary information

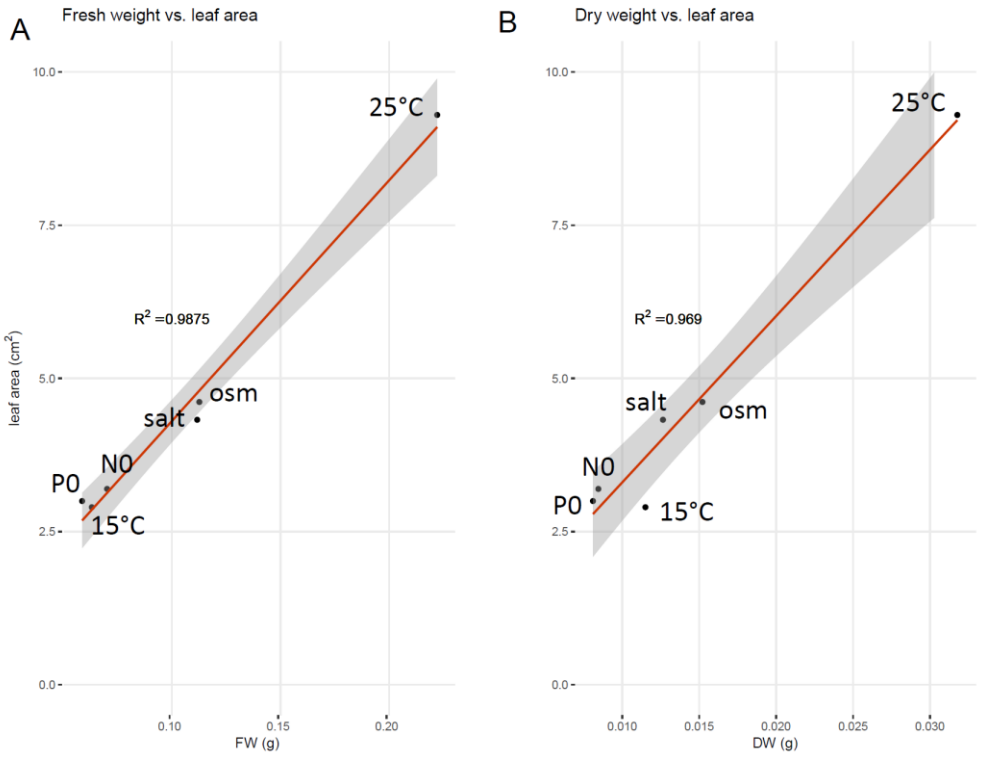

Supplementary Figure 2-1. Correlation between weight and leaf area of plants at the end of the 10-days treatments includes all the six (±5°C, salt, osmotic, nitrate and phosphate deficiency). **A)** Correlation between fresh weight and leaf area **B)** correlation between dry weight and leaf area.

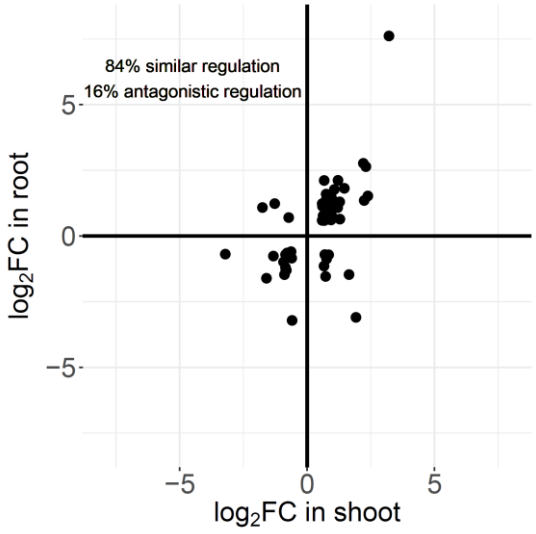

Supplementary Figure 2-2. Proteins both in the shoot and the root with a significantly high (p≤0.05) fold change (log_2FC ± 0.58 (±1.5 FC)). All 6 experiments were combined. Fold change of the proteins is the ratio of the normalized abundance in the treatment divided by the normalized abundance in the control

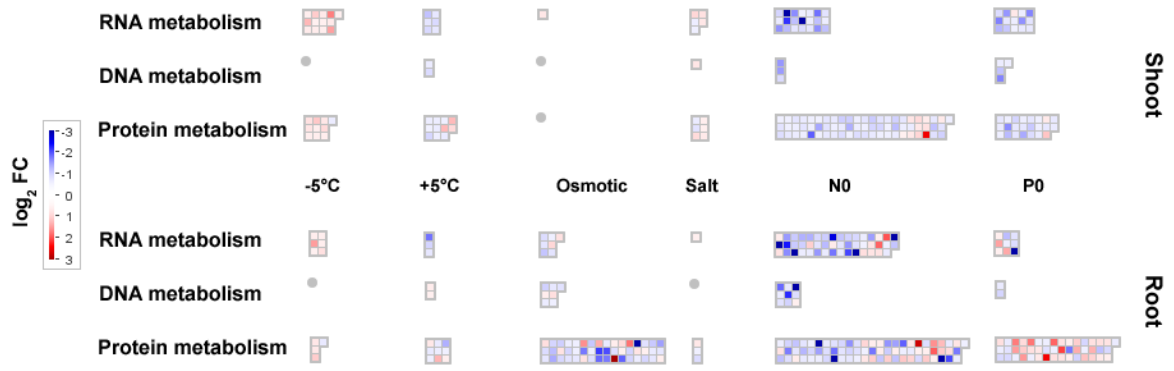

Supplementary Figure 2-3. RNA-, DNA- and protein metabolism in the shoot and the root at the end of every treatment. Heatmap was generated from MapMan based on proteins with significantly high (V≤0.05) fold change (±1.5 FC)

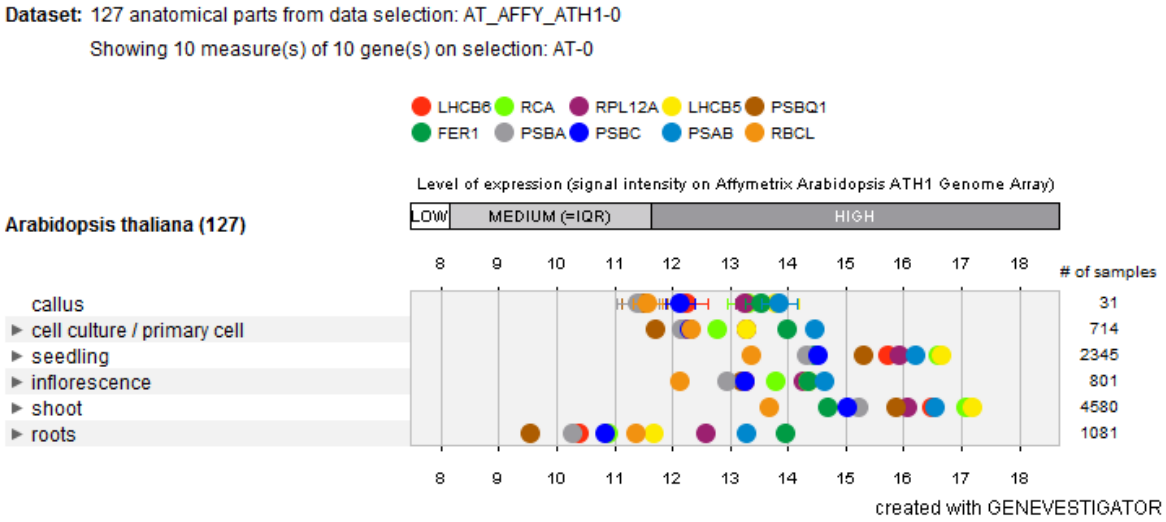

Supplementary Figure 2-4. Expression of different genes annotated as photosynthetic proteins in different tissues as displayed by Genevestigator based on transcriptomic and microarray data.

AGI	Shoot log_2FC in 25°C	log_2FC in 15°C
AT3G44750	-0.93	0.67
AT3G53460	-0.75	0.61
AT4G11960	0.98	-2.35
AT4G23670	0.74	-0.63
AT4G30720	-0.63	0.93
AT4G36390	-0.65	0.87
AT5G08610	-0.77	1.08
AT5G13930	-0.68	0.73
AT5G22580	0.76	-0.72
	Root	
AT1G13080	0.62	-0.89
AT1G65970	0.76	-1.22
AT1G73260	1.10	-0.63
AT1G77520	0.75	-1.44
AT2G01520	1.79	-0.74
AT3G05950	1.16	-1.47
AT3G16390	-1.60	1.18
AT3G18000	-1.15	1.20
AT4G32460	-1.41	0.62
AT4G38710	-0.60	0.72
AT5G43330	0.84	-1.20

Supplementary Table 2-1. Opposite behavior in protein abundance ($p \leq 0.05$), fold change (log_2FC ± 0.58 (±1.5 FC)). under changed temperature

AGI	water channel proteins	log_2FC
At2g37170	PIP2B (PLASMA MEMBRANE INTRINSIC PROTEIN 2)	-0.65
At2g39010	PIP2E (PLASMA MEMBRANE INTRINSIC PROTEIN 2E)	-0.61
At3g16240	DELTA-TIP (DELTA - TONOPLAST INTEGRAL PROTEIN)	-0.73
At3g26520	TIP2 (TONOPLAST INTRINSIC PROTEIN 2)	-0.63
At3g53420	PIP2A (PLASMA MEMBRANE INTRINSIC PROTEIN 2A)	-0.75
At3g61430	PIP1A (PLASMA MEMBRANE INTRINSIC PROTEIN 1A)	-0.91
At4g23400	PIP1;5 (PLASMA MEMBRANE INTRINSIC PROTEIN 1;5)	-0.99

Supplementary Table 2-2. Fold change of aquaporin proteins in the shoot of 15°C treatment with a significant high fold change ($p \leq 0.05$, FC ±1.5)

			Root			
AGI	**25°C**	**15°C**	**osmotic**	**salt**	**N0**	**P0**
AT3G16390	-1.60	1.18	*0.47*	*0.11*	1.23	1.87
AT4G32460	-1.41	0.62	#N/A	0.76	#N/A	#N/A
AT3G18000	-1.15	1.20	*-0.18*	1.50	1.08	1.23
AT4G38710	-0.60	0.72	*-0.18*	*0.27*	*0.03*	*0.06*
AT1G13080	0.62	-0.89	0.88	*-0.29*	*-0.68*	*-0.14*
AT1G77520	0.75	-1.44	*-0.47*	*-0.31*	*0.23*	*0.17*
AT1G65970	0.76	-1.22	-0.89	*0.64*	-2.27	*0.58*
AT5G43330	0.84	-1.20	*0.31*	*0.08*	*0.24*	*-0.17*
AT1G73260	1.10	-0.63	*0.52*	*-0.19*	-1.16	-0.76
AT3G05950	1.16	-1.47	2.04	*-0.36*	#N/A	#N/A
AT2G01520	1.79	-0.74	*0.07*	*0.00*	1.13	0.81
			Shoot			
AT3G44750	-0.93	0.67	*-0.34*	*-0.07*	-3.21	*-1.13*
AT5G08610	-0.76	1.08	*-0.11*	*-0.39*	-1.62	-1.55
AT3G53460	-0.75	0.61	*-0.13*	*-0.55*	-1.20	-0.70
AT5G13930	-0.68	0.73	*0.01*	*0.20*	1.81	0.73
AT4G36390	-0.65	0.87	#N/A	#N/A	-1.31	-1.02
AT4G30720	-0.63	0.93	-0.01	0.01	-0.36	-0.35
AT4G23670	0.74	-0.63	*0.12*	*0.39*	*0.05*	*0.43*
AT5G22580	0.76	-0.72	*-0.22*	-0.73	#N/A	#N/A
AT4G11960	0.98	-2.35	*0.51*	0.97	0.96	*0.85*

Supplementary Table 2-3. Significant ($p \leq 0.05$) high fold change ($log_2FC \pm 0.58$ (±1.5 FC)) of proteins in osmotic, salt and nutrient deficient treatments, which showed an opposite regulation in ±5°C. FC in italics are not significant.

		Log_2-ratio in transcriptomics	**Log_2-ratio in proteomics**
low nitrogen > Nutrient	low nitrogen / high nitrogen treated rosette samples	-1.09	-1.75
cold study 3 (7d) > Stress	cold study 3 (7d) / untreated seedlings	2.53	0.87
cold study 8 (Col-0) > Stress	cold study 8 (Col-0) / untreated all aerial tissue samples (Col-0)	2.86	0.87
drought study 14 (Col-0) > Stress	drought study 14 (Col-0) / untreated Col-0 rosette leaf samples	0.08	-0.30
salt study 4 (Col-0) > Stress	salt study 4 (Col-0) / Hoagland solution watered Col-0 leaf samples	3.70	0.94

Supplementary Table 2-4. Comparison of NMT1 (AT3G18000) amount on transcriptional and proteomic level in similar experimental setup. Transcriptomics data was extracted from Genevestigator.

AGI	FC	pValue
AT4G30720	1.55	0.008
AT1G12000	1.20	0.032
AT1G67090	1.15	0.031
AT1G43670	1.14	0.016
AT1G79040	1.09	0.013
AT4G09650	0.92	0.022
ATCG01100	0.91	0.024
AT3G47470	0.88	0.030
AT4G10340	0.88	0.002
AT2G40300	0.87	0.033
AT1G61520	0.86	0.009
AT3G01500	0.83	0.003
AT5G01530	0.81	0.023
AT1G76550	0.78	0.010
AT5G38410	0.77	0.004
AT4G11960	0.51	0.002

Supplementary Table 2-5. Significant (p≤0.05) fold change of proteins, which were annotated as photosynthetic proteins (GO:0015979) in 25°C. Red indicates increase in abundance compared to the plants grown in control environment.

AGI	FC	pValue
AT4G11960	5.10	0.004
AT2G34420	1.46	0.002
AT4G02770	1.42	0.005
ATCG01060	1.41	0.001
AT1G55670	1.37	0.000
AT1G31330	1.35	0.000
AT4G10340	1.33	0.000
ATCG01010	1.32	0.000
AT5G01530	1.30	0.000
AT3G47470	1.30	0.000
AT1G61520	1.30	0.000
ATCG00350	1.28	0.000
ATCG01090	1.27	0.001
AT3G61470	1.27	0.009
AT1G79040	1.24	0.001
AT5G54270	1.20	0.031
AT1G30380	1.19	0.035
AT1G15820	1.18	0.002
AT1G45474	1.16	0.005
AT3G54890	1.14	0.008
AT4G09650	1.14	0.002
ATCG01100	1.14	0.002
AT1G76550	1.12	0.049
AT1G55480	1.11	0.026
AT1G20950	0.92	0.004
AT1G43670	0.91	0.002
AT1G12000	0.77	0.005
AT3G56090	0.73	0.001
AT4G30720	0.53	0.000

Supplementary Table 2-6. Significant (p≤0.05) fold change of proteins, which were annotated as photosynthetic proteins (GO:0015979) in 15°C. Red indicates increase in abundance compared to the plants grown in control environment.

3) Cytosolic sucrose metabolism in normal and changed environmental condition in *Arabidopsis thaliana*

Dániel Á. Carrera[a], Simona Eicke[a], and Sebastian Streb[a]

a) Institute for Agricultural Sciences, Plant Biochemistry, ETH Zürich, CH-8092 Zürich, Switzerland

Reference:

Manuscript in preparation

Contribution:

I conducted most of the experiments. The creation of the knock-out library was started by Simona Eicke, the majority of the lines was isolated by me.

Abstract

Sucrose is one of the end products of photosynthesis and is transported throughout the plant supplying carbon from the source to sink tissues. Cytosolic sucrose metabolism is a complex network consisting of 16 gene families with a high redundancy of isoforms. We investigated the changes of in carbohydrate metabolism, which includes sucrose, in six different environmental condtions. Further, we created a mutant collection covering most of the proteins involved in sucrose metabolism, which were analyzed phenotypically in the control environment. Additionally, based on previous proteomic analysis, selected single mutants were grown under different long-term stress condition. By combining the different approaches, we aimed, if it is possible, to attribute new functions to cytosolic sucrose enzymes. The changes of carbohydrate metabolism to environmental perturbations were specific to the respective treatment and the tested single mutants showed often treatment dependent growth phenotypes. One of the mutants was the *frk7* homozygous knock-out, which had been downregulated during the salt-stress treatment, grew slower under normal conditions, but was not further impaired during this stress: the lack of FRK7 might provide the plant a better tolerance to salt stress. Other mutants showed an embryo lethal phenotype; SPP2 and FRK are essential for seed development. Further, we identified limiting protein isoforms, where plants lacking these showed a significant reduction in growth. The FBA8 is probably the most important isoform among the five cytosolic FBA isoforms, it has the highest contribution (three times more than the other four together) to the total enzyme activity and it may have a key physiological role in the root.

Introduction

During the day, atmospheric carbon is assimilated through photosynthesis by plants and converted into carbohydrates. Synthesis, utilization, transport, storage and remobilization of carbohydrates are tightly controlled and adapted to environmental disturbances, diurnal changes and different developmental stages to cope with changes in supply and energy demand (Bae et. al, 2005; Nishizawa et. al, 2008; Schmitz et. al, 2012, Thalmann et. al, 2016). CO_2 is incorporated into carbon skeletons in the Calvin-Benson cycle and partitioned mainly into sucrose and starch in *Arabidopsis thaliana*. During the night, when photosynthesis is not

operating, plants rely mostly on starch reserved in the leaf. Small disturbances in leaf starch turnover affect metabolism and growth and *vice versa* (Stitt and Zeeman, 2012).

The metabolic networks of the different carbohydrates are not isolated; they are highly interconnected and influence each other. As one of the end products of photosynthesis, sucrose, which is a non-reducing disaccharide, is transported throughout the plant mainly from source to sink tissues via the phloem to supply energy and carbon. Sucrose is composed of the monosaccharides glucose and fructose via a glycosidic bond between C1 on the glucosyl subunit and C2 on the fructosyl unit and it is synthetized in the cytosol.

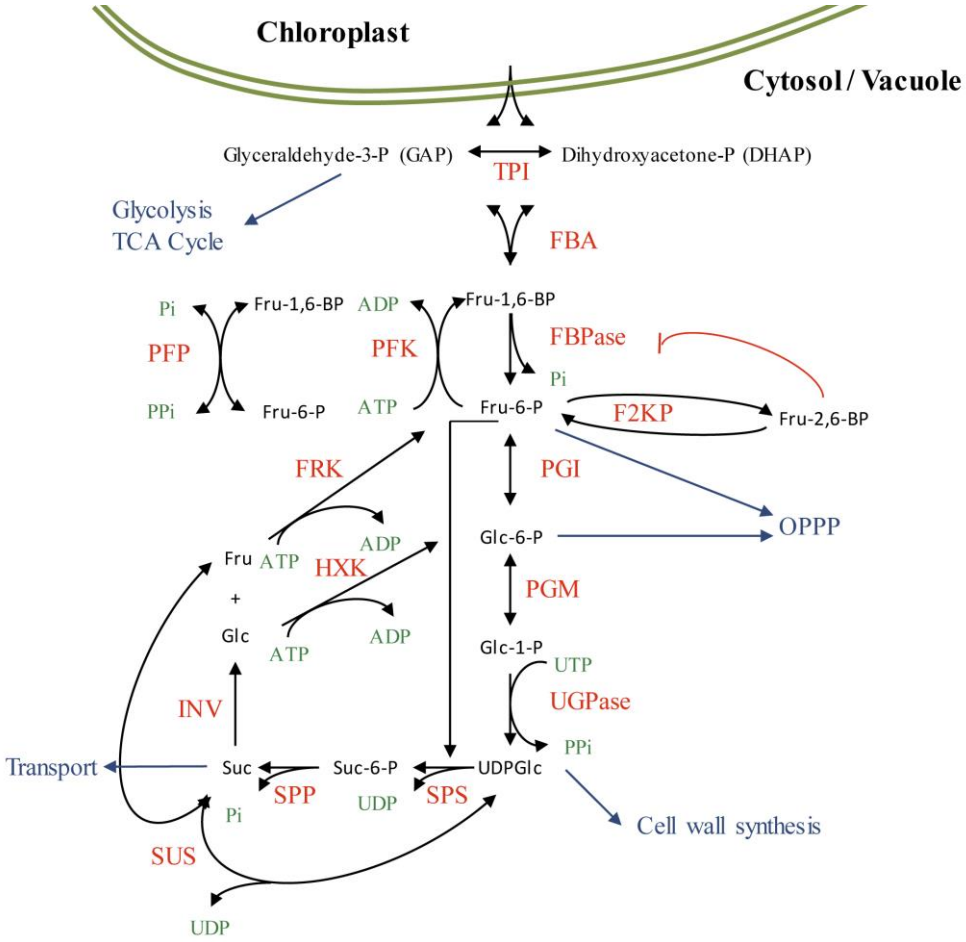

Figure 3-1. Cytosolic carbohydrate metabolism: biosynthesis and degradation of sucrose. PGI: phosphoglucoisomerase, PGM: phosphoglucomutase, TPT: triose phosphate/phosphate translocator, INV: invertases, SUSY: sucrose synthase, FRK: fructokinases, HXK: hexokinase, TPI: triose phosphate isomerase, PFK: ATP-dependent phosphofructokinases, SPS: sucrose-phosphate synthase, SPP: sucrose-phosphate phosphatase, UGPase: UDP-Glucose Pyrophosphorylase, FBA: Fructose 1,6-bisphosphate aldolase, FBPase: Fructose 1,6-bisphosphatase, F2KP: 6-phosphofructo-2-kinase/fructose- 2,6-bisphosphatase, F-1,6-BP: fructose 1,6-bisphosphate, F-2,6-BP: fructose 2,6-bisphosphate, F-6-P: fructose 6-phosphate, G-6-P: glucose 6-phosphate, G-1-P: glucose 1-phosphate, UDP-Glu: UDP-glucose, S-6-P: sucrose 6-phosphate, DHAP: dihydroxy acetone phosphate, G3P: glycerylaldehyde 3-phosphate

The sucrose metabolic network can be divided into different sub processes, which represent the metabolic steps of synthesis, breakdown or transport of sucrose (Fig. 1). First, the transport of triose-phosphates out of the chloroplast and interconversion of them into fructose-1,6-bisphosphate. Second the hexose-phosphate pool, which is followed by the actual biosynthesis of sucrose. Sucrose can be degraded into fructose and glucose by invertases or into fructose and UDP-glucose by sucrose synthases. Sucrose can be transported out of the cell or into the vacuole, where it can be stored or degraded further. A high degree

of redundancy exists among the genes participating in the sucrose metabolic network. Genome sequencing in the past decade revealed that multiple genes exist for most of the metabolic steps (i.e. six isoforms of the sucrose-synthase family, eight isoforms of the fructose 1,6 aldolases, or more than 17 invertases). There is not a well-described explanation for the high number of isoforms that we are aware of, and there might not be a single one, which can be applied to every gene family with multiple isoforms. For instance, a multiple knock-out of 4 sucrose synthases (SuSy1-4) has no phenotypical impact on plant development in normal growth environment (Barratt et. al, 2009; Baroja-Fernández et. al, 2011). Nevertheless, there are crucial metabolic steps, which are catalyzed "only" by single isoforms and the knock-out of the respective gene can causes lethality. The cytosolic hexose-phosphate pool, which consist of fructose 6-phosphate, glucose 6-phosphate and glucose 1-phosphate, is a good example. The enzyme PGI performs the interconversion of glucose 6-phosphate and fructose 6-phosphate. PGI has one cytosolic isoform and the knock-out of its activity results in an inviable plant (2010; Kunz et. al, 2014).

While the biochemical basis of sucrose metabolism in leaves is well established, several questions remain open to be answered, especially if we focus on the individual isoforms and the high degree of redundancy. To answer these questions, a collection of cytosolic sucrose metabolism related knock-out mutants was created and these mutants underwent a basic characterization. A previously performed proteomic experiment (Chapter 1), where plants were exposed to a long-term stresses (nutrient deficiencies and mild abiotic stress), revealed that the level of several cytosolic sucrose metabolic proteins changed under stress (Table 1). We sought to establish a link between the new adjusted carbohydrate metabolism and the single isoforms, and their role in the plants' stress response.

	25°C S	25°C R	15°C S	15°C R	osm S	osm R	salt S	salt R	N0 S	N0 R	P0 S	P0 R
At1g07110 (F2KP)	0.55	*ND*	-0.19	*ND*	0.09	*ND*	0.23	*ND*	0.62	0.77	0.16	0.46
At1g12000 (PFK)	-0.26	-0.22	0.38	0.15	0.02	-0.31	0.12	-0.08	-0.49	-0.23	-0.12	-0.15
At1g12240 (vINV1)	-0.33	0.39	0.41	-0.03	0.26	-0.11	0.13	-0.38	0.22	-0.75	-0.04	-0.05
At1g18270	0.03	-0.12	0.07	-0.25	-0.09	-0.15	0.16	-0.42	0.23	-0.56	0.32	-0.46
At1g20950	0.02	0.19	-0.12	-0.18	0.16	0.22	0.04	-0.10	0.34	0.12	0.09	-0.11
At1g23190 (PGM3)	-0.12	0.27	-0.15	-0.07	0.02	-0.08	-0.18	-0.10	-0.03	-0.27	0.00	0.03
At1g35580 (cINV1)	*ND*	-0.09	*ND*	0.03	*ND*	0.28	*ND*	0.08	0.32	0.60	0.08	0.24
At1g43670 (cFBPase)	0.18	*ND*	-0.14	0.21	0.11	0.21	-0.05	0.24	-0.02	0.08	-0.16	0.39
At1g47840 (HXK3)	*ND*	0.53	*ND*	-0.18	*ND*	-0.89	*ND*	0.07	*ND*	0.44	*ND*	0.88
At1g62660 (vINV2)	-0.86	-0.08	*ND*	0.16	-0.13	0.05	-0.45	0.21	0.29	-0.23	0.36	-0.29
At1g66430 (FRK)	0.15	0.12	-0.03	0.00	-0.08	-0.32	-0.10	-0.07	-0.04	0.65	-0.02	0.75
At1g70730 (PGM2)	-0.01	-0.16	0.04	0.22	0.11	0.11	0.08	0.04	-0.02	-0.02	0.03	0.20
At1g73370 (SuSy6)	*ND*	-0.74	*ND*	0.39	*ND*	-0.19	*ND*	-0.02	*ND*	-0.06	*ND*	0.43
At1g76550 (PFK)	-0.36	0.08	0.17	0.05	0.10	0.15	0.08	0.03	0.07	0.14	0.38	-0.02
At2g19860 (HXK2)	-0.07	*ND*	-0.10	0.00	0.09	*ND*	-0.06	0.25	-0.03	-0.27	-0.24	0.36
At2g31390 (FRK2)	0.02	0.06	0.05	-0.06	0.06	-0.21	-0.32	0.13	-0.26	0.15	-0.20	0.32
At2g36460 (FBA6)	-0.06	-0.27	0.06	0.33	0.02	-0.32	-0.05	0.09	0.02	0.30	-0.07	0.45
At3g03250 (UGPase1)	-0.06	0.16	-0.02	-0.06	0.05	-0.17	-0.01	-0.05	-0.03	-0.29	-0.57	-0.22
At3g13790 (cwINV1)	*ND*	0.06	*ND*	-0.07	*ND*	-0.06	*ND*	-0.05	*ND*	0.21	*ND*	0.23
At3g43190 (SuSy4)	*ND*	-0.02	*ND*	-0.12	*ND*	-2.22	*ND*	0.03	*ND*	0.20	*ND*	-0.23
At3g52930 (FBA8)	-0.22	-0.36	0.21	0.17	-0.06	0.09	0.00	0.02	-0.34	0.00	0.01	0.14
At3g55440 (cTPI)	0.05	0.01	-0.08	-0.20	-0.02	0.10	-0.11	-0.02	0.09	0.37	-0.32	-0.17
At3g59480 (FRK)	*ND*	-0.80	*ND*	1.59	*ND*	0.20	*ND*	-1.60	*ND*	2.16	*ND*	2.23
At4g04040 (PFK)	0.06	*ND*	-0.02	0.19	0.19	-0.10	0.00	0.27	-0.10	-0.38	-0.47	-0.46
At4g15530	0.63	*ND*	-0.03	*ND*	-0.05	*ND*	0.06	*ND*	1.23	*ND*	0.79	*ND*
At4g26530 (FBA5)	-0.10	*ND*	0.33	*ND*	0.02	*ND*	0.09	*ND*	0.04	*ND*	-0.24	*ND*
At4g29130 (HXK1)	-0.05	0.14	-0.08	-0.15	-0.03	0.11	-0.07	-0.10	-0.16	-0.01	-0.01	-0.03
At4g29220 (PFK1)	*ND*	*ND*	*ND*	-0.12	0.00	0.17	0.01	0.16	*ND*	-0.07	*ND*	0.42
At4g34860 (INV B)	*ND*	-0.09	*ND*	0.38	*ND*	-0.44	*ND*	0.12	*ND*	0.41	0.41	0.25
At5g11110 (SPS2)	*ND*	*ND*	*ND*	*ND*	*ND*	*ND*	*ND*	*ND*	*ND*	-1.13	*ND*	-0.72
At5g17310 (UGPase2)	-0.25	0.16	0.15	-0.19	-0.01	-0.06	0.01	-0.07	-0.01	-0.15	-0.07	0.14
At5g20280 (SPS1F)	-0.23	*ND*	0.13	*ND*	-0.09	0.36	-0.05	*ND*	-0.63	-0.77	-0.71	-1.30
At5g20830 (SuSy1)	0.24	-0.24	-0.76	0.09	-0.17	-1.09	-0.46	0.13	-1.14	-0.03	0.00	0.41
At5g22510 (pINV E)	-0.07	*ND*	0.42	*ND*	-0.22	*ND*	-0.04	*ND*	-0.11	*ND*	-0.14	*ND*
At5g37180 (SuSy5)	*ND*	*ND*	*ND*	*ND*	*ND*	*ND*	*ND*	-0.27	*ND*	*ND*	*ND*	*ND*
At5g46110 (TPT2)	-0.21	*ND*	0.28	*ND*	0.01	*ND*	0.06	*ND*	-0.37	*ND*	-0.21	*ND*
At5g56630 (PFK7)	*ND*	-0.04	-1.38	-0.18	*ND*	0.00	*ND*	0.22	0.16	-0.07	-0.71	0.02

Table 3-1 Fold change (log_2FC ± 0.58 (±1.5 FC)) of cytosolic sucrose proteins in long-term environmental changes. 15°C, 25°C, salt, osmotic (osm), nitrate (N0) and phosphate (P0) treatments were applied and protein abundance was measured in the shoot (S) and the root (R). Red indicates significant ($p \leq 0.05$) fold change. ND (not detected) stands for proteins, which were not detected in certain experiments.

Materials and Methods

Plant material

Arabidopsis thaliana plants were grown in growth chambers (Percival AR95, CLF Plant Climatics) on a nutrient rich, medium-grade, peat-based soil and plates supplied with Murashige and Skoog medium (Duchefa Biochemie) at constant 20°C, 70% relative humidity, with a 12-h light/12-h dark photoperiod. Uniform light intensity was set on 150 µmol m^{-2} s^{-1}. Sown seeds were stratified for 48 h at 4°C and transferred to the growth chambers. Single, homozygous T-DNA insertion mutants were isolated.

Arabidopsis thaliana wild-type plants (Col-0) seeds were individually distributed on cut 0.5 mL tubes containing 0.65% phytoagar for the stress treatments. They were grown hydroponically in Cramer's solution (Gibeaut et. al, 1997; Tocquin et. al, 2003) in control environment for 18 days in a Percival AR95 growth chamber (CLF Plant Climatics) with 12-h photoperiod, 20°C and 60% relative humidity. Light intensity was uniform at 150 µmol quanta m^{-2} s^{-1}. The tubes were soaked in nutrient solution (pH was adjusted to 6), which contained the following macronutrients: 1.5 mM $Ca(NO_3)_2$, 1.25 mM KNO_3, 0.75 mM $Mg(SO_4)$, 0.5 mM KH_2PO_4, 1 mM $(NH_4)_2SO_4$, 72 µM $C_{10}H_{12}FeN_2NaO_8$ and 100 µM Na_2O_3Si and micronutrients: 50 µM KCl, 10 µM $MnSO_4$, 1.5 µM $CuSO_4$, 2 µM $ZnSO_4$, 50 µM H_3BO_3 and 0.075 µM $(NH_4)_6Mo_7O_{24}$. 18 days after the germination, the plants were exposed to different stress treatments: 50 mM NaCl or 5% Poly(ethylene glycol) (M_n 6000) (PEG6000) dissolved in the hydroponic solution, ±5°C in E-41L2 growth chamber (CLF Plant Climatics) and no phosphate and nitrate content in the hydroponic solution. The plants were grown under changed conditions for additional 10 days.

Starch and sugar measurements

The hydroponic experimental setup allowed us to measure metabolites in the shoot and the root too. Samples were frozen in liquid N_2 and extracted in ice-cold 3:7 (v/v) chloroform-methanol solution. Starch and sugar concentration was measured as described earlier, modified protocol from Egli et. al, (2009). After incubation at -20°C the soluble phase was extracted with cold water and the insoluble phase was washed with 70% ethanol and water. Starch in the insoluble fraction was digested with a-amylase (pig pancreas; Roche) and amyloglucosidase (*Aspergillus niger*; Roche) and the released Glc measured

spectrophotometrically. Sugars (Glc, Fru, and Suc) in the soluble fraction were determined using high performance anion-exchange chromatography with pulsed amperometric detection. Volumes of the soluble fraction containing the equivalent of 5 mg plant fresh weight were spiked with 5 nmol cellobiose as an internal standard and applied to sequential 1.5-mL columns of Dowex50W and Dowex1 (Sigma-Aldrich). Neutral sugars were eluted with 4 mL of water, lyophilized, and redissolved in 500 µL of water. Sugars were separated on a CarboPac PA-20 column from Dionex with the following conditions: eluent A, 100 mM NaOH; eluent B, 150 mM NaOH and 500 mM sodium acetate. The flow rate was 0.5mL min-1. The gradient was 0 to 15 min, 100% A (monosaccharide elution); 15 to 26.5 min, linear gradient to 20% A and 80% B (disaccharide elution); 26.5 to 32.5 min, 20% A, 80% B (column wash step); and 32.5 to 40 min step to 100% A (column re-equilibration). Peaks were identified by coelution with known Glc, Fru, Suc, and cellobiose standards. Peak areas were determined using Chromeleon software. All peaks were normalized to the internal cellobiose standard, and the amount of each was calculated based on standard curves of the pure standards run in parallel.

Growth analysis

Rosettes were photographed to quantify the growth in leaf area. The pictures were analyzed and each leaf area of every single plant was evaluated with ImageJ software. The growth of each plant was described with a polynomial (3rd order) non-linear model: $y = ax^3 + bx^2 + cx + d$. Relative growth rate (RGR) is defined as the relative increase in leaf area over time period (GR) and was calculated by taking the difference between the polynomial transformation of the leaf area at the end (G_n) and at the beginning of the timeframe (G_{n-1}) divided by G_{n-1}: $GR_n = (G_n – G_{n-1})/ G_{n-1}$ (Hendrik Poorter, 1989; M. Heinen, 1999; Paine et. al 2012; Ruts et. al, 2013). Leaf area and RGR of each mutant was normalized to the Col-0 wild type and the normalized values was $\log_2$ transformed in order to represent them in a heatmap. Heatmaps of the transformed values were generated with R (R Development Core Team, 2010) using the gplots package, which as default uses Euclidean measure to obtain distance matrix and complete agglomeration method for clustering.

Bioinformatic/database analysis

For expression of genes and protein level values, we used the Pep2pro (Baerenfaller et. al, 2011) and Genevestigator (Hruz et. al, 2008) databases. Protein-protein interaction data and figure was provided by the STRING database (Jensen et. al, 2009).

Total FBA enzyme activity measurement

Whole rosettes from soil-grown plants were homogenized and total soluble proteins were extracted; the assay was performed as reported previously (Haake et. al, 1998; Gibon et. al, 2004).

Results

Carbohydrate metabolism in nutrient deficiency and long-term mild abiotic stress

Plant were grown on liquid media and, after 18 days in control environment, different long-term nutrient deficient and mild abiotic stress treatment were applied to them. Every long-term changed environment had an effect on carbohydrate metabolism. Starch was considered as an indicator of carbohydrate metabolism, and the starch level was changed in every

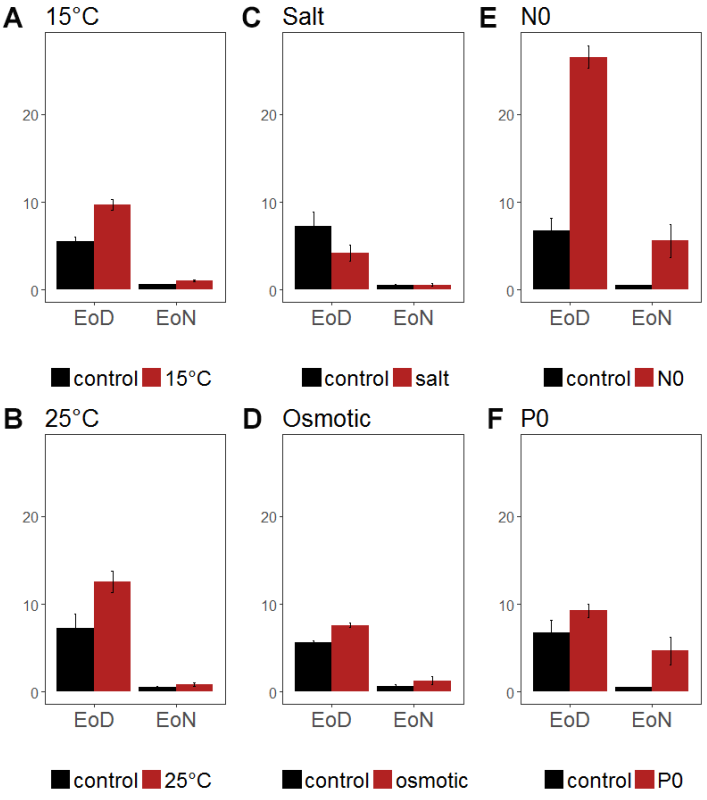

Figure 3-2. Starch metabolism in plants exposed to long-term environmental changes. Starch level at the end of the day and night in A) 15°C, B) 25°C, C) higher salt (50 mM NaCl), D) osmotic (5% PEG), E) nitrate deficient and F) phosphate deficient environment.

treatment (Fig. 2). Most of the applied treatments (5 out of 6) increased the transitory starch content in wild type leaves. The one exception is the salt treatment, where, at the end of the day, the starch level was half of the control, however, at the end of the night there was no difference. Changes in temperature generally elevate starch content, it was higher at the end of the day in 25°C and 15°C. Growth in an osmotic environment also slightly increased the starch content. The effect of nutrient deficiency is more pronounced. Especially in nitrate deficient treatment (N0), at the end of the day the starch concentration was extremely high. It decreased during the night, but it was still more elevated than in the control. Although in phosphate limitation (P0) it was not as high as under nitrate limitation (N0) at the end of the day, the breakdown of starch during the night was much lower. In P0 the difference in starch content between the end of the day and night was much lower than in N0.

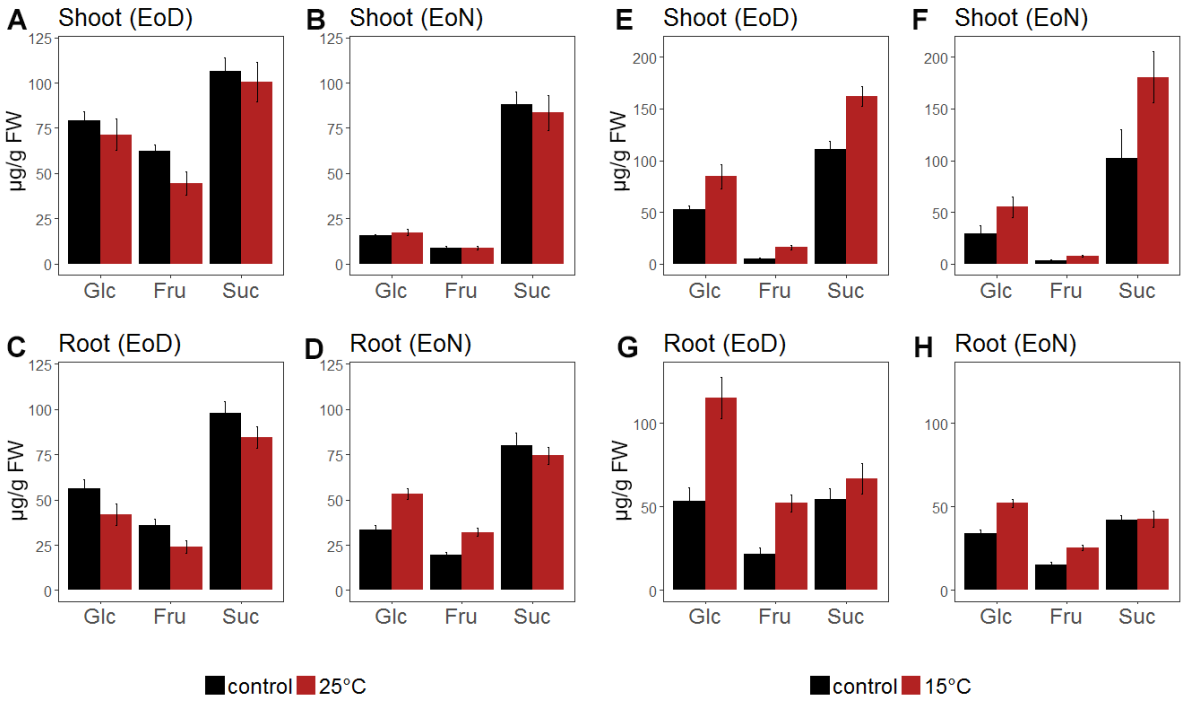

Figure 3-3. Soluble sugar metabolism in plants exposed to long-term 25°C (A, B, C, D) and 15°C (E, F, G, H) environment in the shoot and the root at the end of the day and the night. Glucose (Glc), fructose (Fru) and sucrose (Suc).

Plants respond differently to long-term abiotic stress and nutrient deficiencies (Chapter 1) and these responses involved different adjustment of the soluble sugar metabolism. Not only was the concentration of the respective sugars changed, also their proportions to each other (Fig. 3, 4 and 5). As the proteomic experiment was carried out in the shoot and the root as well,

soluble sugar content was also measured separately in both tissues. That allows to reference changes in metabolites with the changes in proteome.

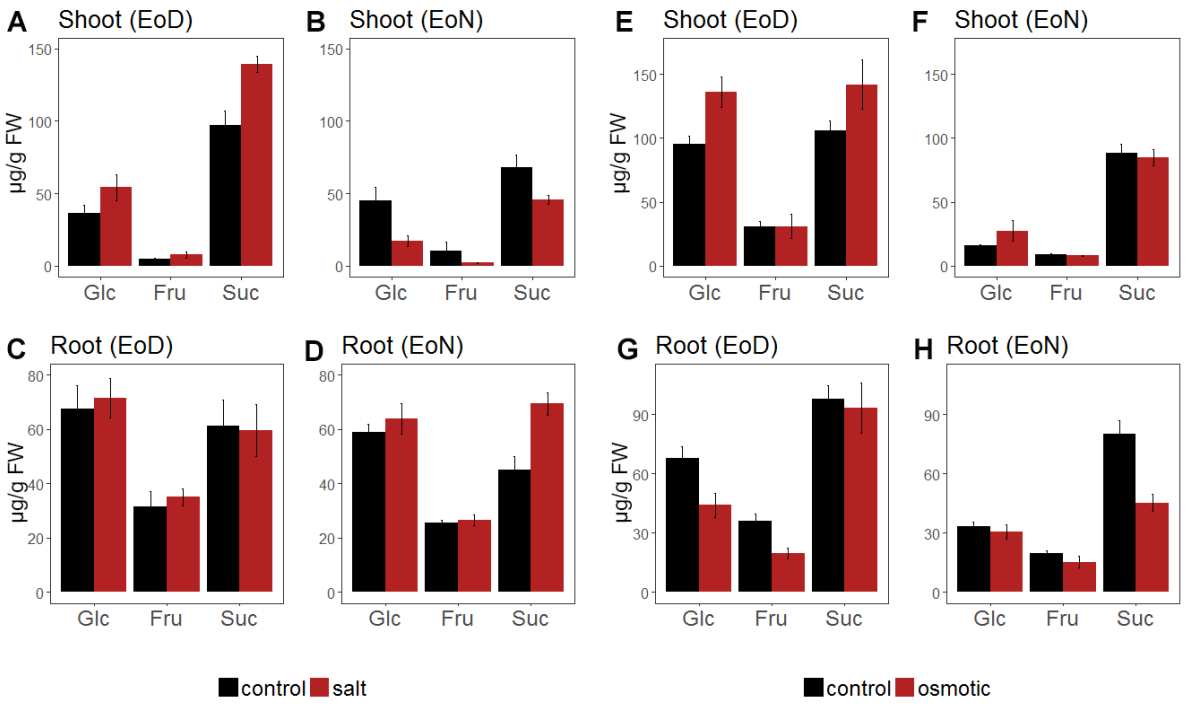

Figure 3-4. Soluble sugar metabolism in plants exposed to long-term salt (50 mM NaCl) (A, B, C, D) and osmotic (5% PEG6000) (E, F, G, H) environment in the shoot and the root at the end of the day and the night. Glucose (Glc), fructose (Fru) and sucrose (Suc).

Plants grown in 25°C showed no or minor differences in both tissues (Fig. 3). Plants exposed to 15°C had an overall higher sugar content in the shoot (Fig. 3). In the roots, the sucrose was at control level, but the glucose and fructose concentration was higher at the end of the day and night. The salt stress induced an increased sugar content in the shoot at the end of the day (Fig. 4), but interestingly, at the end of the night, the sugar pool was decreased in the leaves; all the three measured sugars were lower in amount, while in the root they were similar to the control (sucrose level might be an exception at the end of the night). Plants grown in a mild osmotic environment had a higher glucose level in the shoot, while fructose and sucrose remained similar to the control plants (Fig. 4). The root was again less affected; sucrose was reduced at the end of the night, as was the glucose at the end of the day.

The level of the neutral sugars in the shoot increased substantially compared to the control (Fig. 5), but in the root, the difference is more subtle between the treatment and the control. Compared to the plants in the control environment, the glucose level was high in the root of

N0,(Fig. 5), but interestingly, the fructose concentration was decreased. In P0, the pattern was very similar to the N0 in the shoot (Fig. 5), but in the root the differences were more subtle, the difference was not as high between P0 and control as it was in N0.

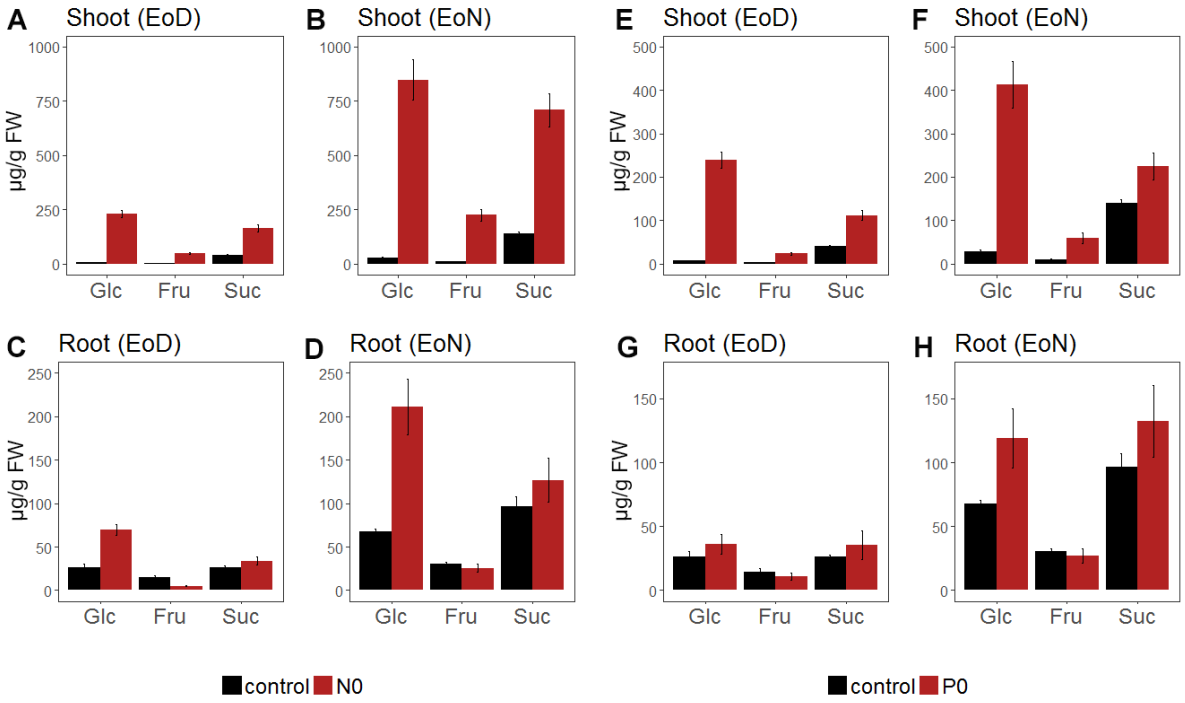

Figure 3-5. Soluble sugar metabolism in plants exposed to long-term nitrate (A, B, C, D) and phosphate (E, F, G, H) deficient environment in the shoot and the root at the end of the day and the night. Glucose (Glc), fructose (Fru) and sucrose (Suc).

Growth of cytosolic sucrose mutants in long-term changed environment

Based on the proteomic dataset several target genes from the primary carbohydrate metabolism was selected for further growth experiment in an altered environment (Table 1). The list included mainly cytosolic sucrose mutants (*susy1*, *susy4*, *f2kp*, *fba6*, *fba8*, *frk*, *pfk7*) with one cytosolic *bam5* and a plastidial *hxk3* mutant. *Susy1*, *fba8* and *pfk7* were grown in 15°C, *f2kp* and *fba6* in 25°C, *bam5* and *frk* in mild salty (50 mM NaCl) media and *susy4* and *hxk3* in media with 5% PEG6000. The growth of *sus4* and *fba6* was indistinguishable from the wild type in the control and stress (Fig. 6b and 6e). The *hxk3* and *f2kp* had already a reduced growth phenotype in control environment in our experimental setup (Fig. 6d and 6h); they were smaller than the wild type. As the mild stress treatment was applied to them, they grew even slower, but the measured leaf area was not lower when they were normalized to the respective control, which means, the stress conditions had similar relative effects on the

mutants and the wild types. *Bam5* was the only mutant, which grew faster than the wild type (Fig. 6c), and this difference was even more pronounced in salt stress. Like the *hxk3* and *f2kp*, the *susy1* and *pfk7* mutants had a reduced growth phenotype under control conditions (Fig. 6a and 6i). Interestingly, this disappeared in the long-term mild stress, they grew similarly as the wild type. The two mutants, which had another phenotype in stress environment compared to the wild type, were the *fba8* and *frk* mutant (Fig. 6f and 6g). In cold, the *fba8* almost stopped growing, but it had an overall reduced leaf area compared to the wild type under control conditions already. The impaired growth in cold might not be directly connected to the plants' stress response. The *frk* had a very high negative fold change in the salt treatment and as the mutant was exposed to 50 mM NaCl media, its reduced growth phenotype, which was observed in control environment compared to the wild type, disappeared.

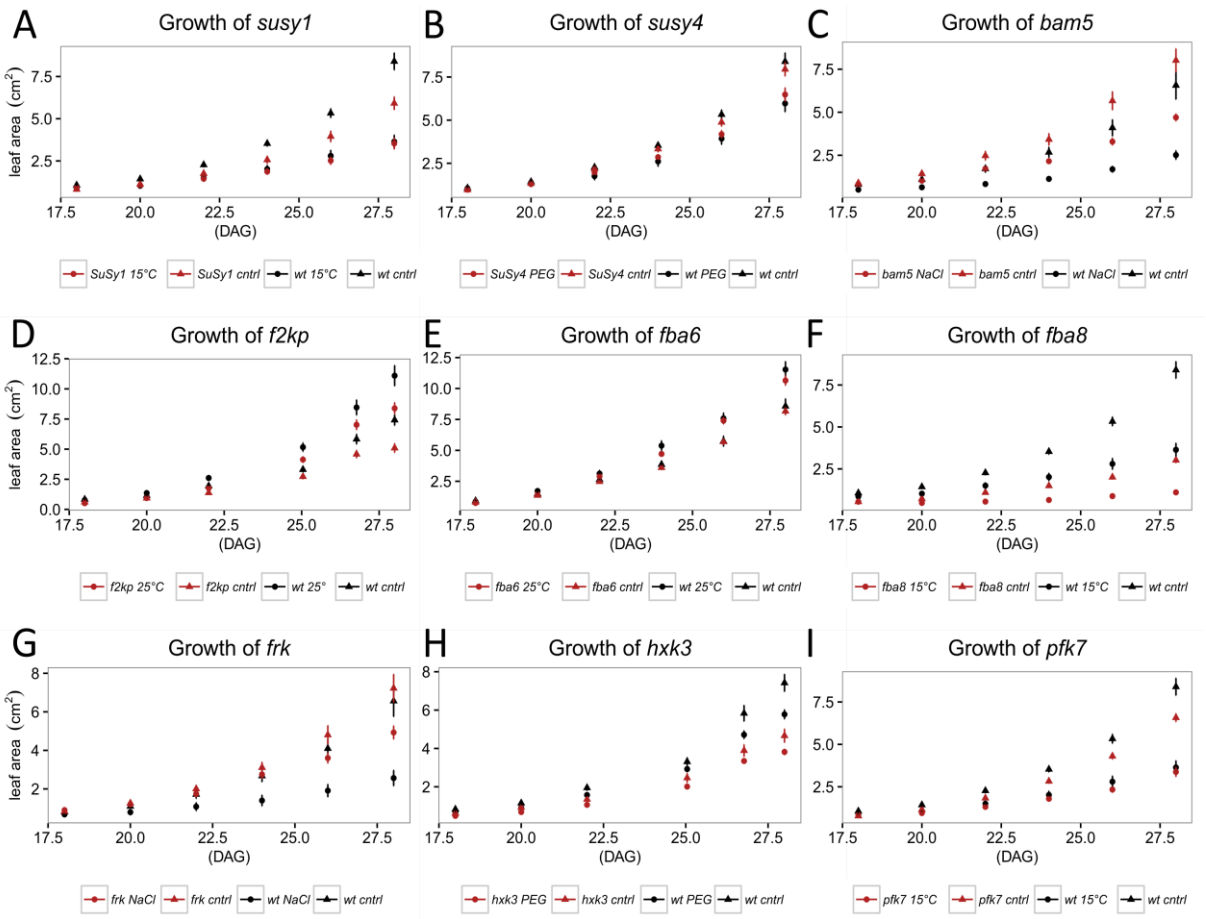

Figure 3-6. Growth of cytosolic single sucrose mutants in long-term environmental changes. A) *susy1* (At5g20830) in 15°C, B) *susy4* (At3g43190) in 5% PEG6000, C) *bam5* (At4g15210) in 50 mM NaCl, D) *f2kp* (At1g07110) in 25°C, E) *fba6* (At2g36460) in 25°C, F) *fba8* (At3g52930) in 15°C, G) *frk* (At3g59480) in 50 mM NaCl, H) *hxk3* (At1g47840) in 5% PEG, I) *pfk7* (At5g56630) in 15°C. Treatments were applied to plants of 18 days after germination (DAG), and plants were grown in changed environment until the age of 28 days after germination (DAG).

Growth of cytosolic sucrose mutants

The single knock-out plants, which lack a protein involved in the cytosolic sucrose metabolism, had most of the times no obvious growth phenotype. Nevertheless, there were some mutants, which reached even a higher leaf area at the end of their growth period: *pfk6* (At4g32840), *ugp3* (At3g56040), *sps4f* (At4g10120). On the other hand, in heatmap and clustering analysis three mutants formed a cluster, the *frk6* (At1g66430), *tpt2* (At5g46110) and *susy5* (At5g37180) plants were smaller.

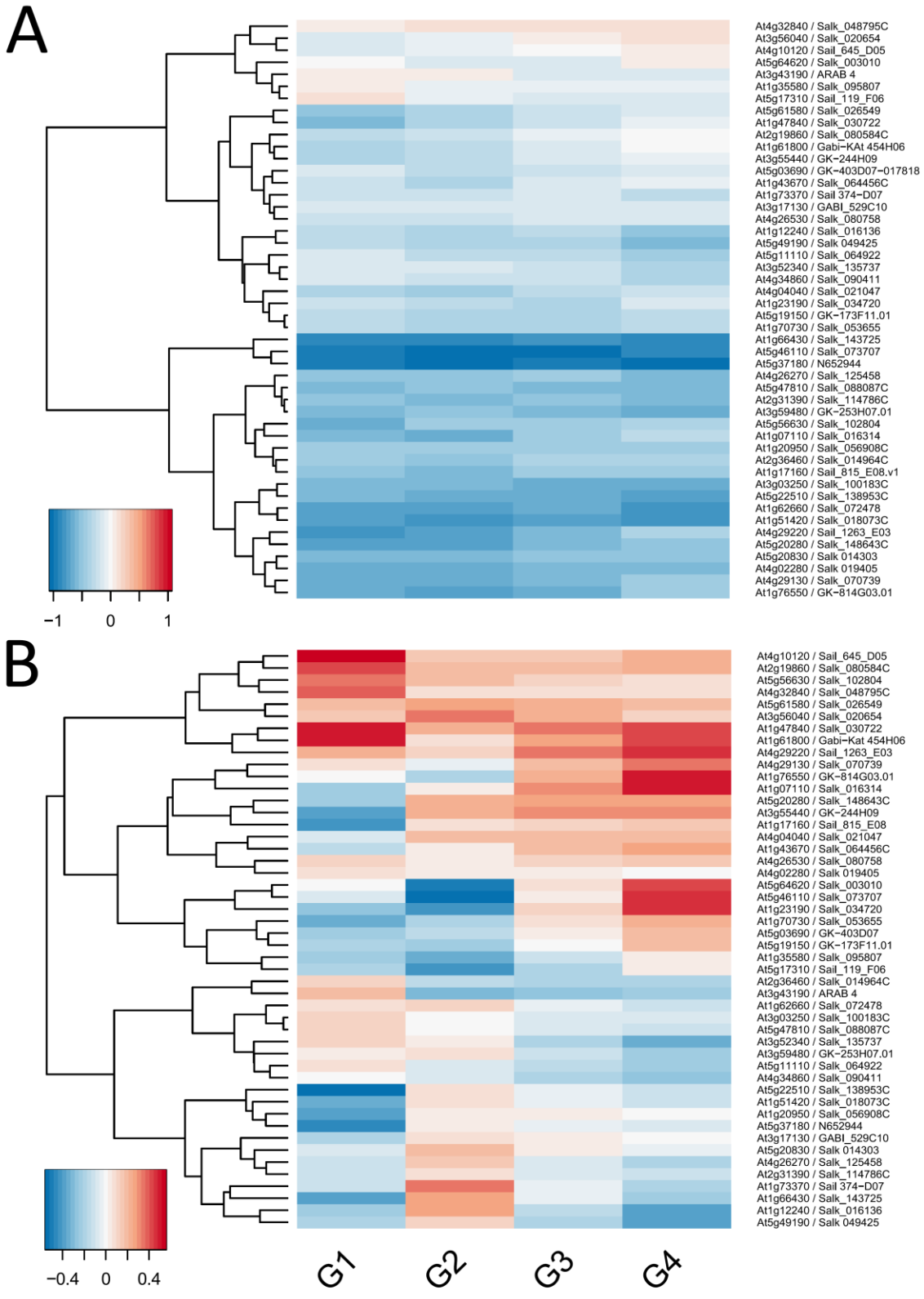

Figure 3-7. Growth of cytosolic sucrose mutants A) Heatmap and clustering of cytosolic sucrose mutants based on their growth in leaf area (cm^2). B) Heatmap and clustering of cytosolic sucrose mutants based on their relative growth rate. The leaf area and RGR values of each mutants was normalized to the wild type and log_2-transformed. 0 value equals the wild type. G1-G4 represents growth stages (21-31 days after germination). Leaf area of G0 was not included into the heatmap.

Besides the raw leaf area values, relative growth rate of each mutant was calculated, which allowed studying the growth patterns (Fig. 7b). One of them was the above-mentioned *tpt2*, which showed a significantly reduced leaf area, but together with the *pgm3* (At1g23190) and a cell wall invertase (At5g64620) mutant, they had a lower RGR (relative growth rate) in the beginning, which reversed later in development. There were a few mutants that despite their overall smaller rosette sizes had a higher RGR throughout the observed period, the top three were the *hxk3* (At1g47840), *gpt2* (At1g61800), *pfk1* (At4g29220). In our experimental setup and analysis there was no mutant identified, which had a continuous lower RGR than the wild type.

Lethal knock-out of cytosolic sucrose genes

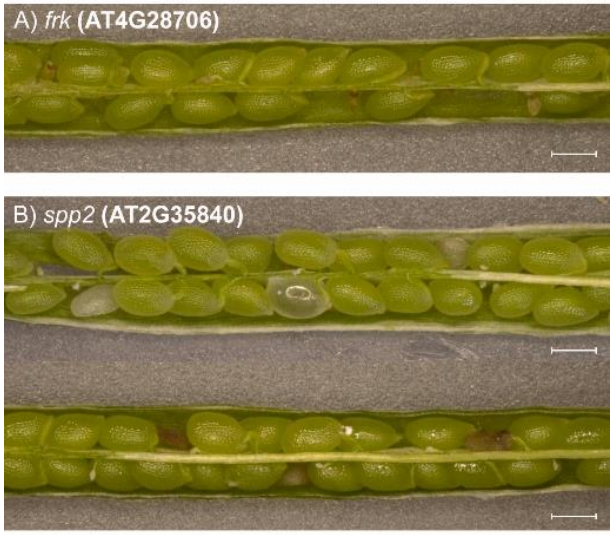

Figure 3-8. Siliques and aborted seed development of heterozygous A) *frk* and B) *spp2* mutants. Scale bar represents 1 mm.

Knocking out many of the cytosolic sucrose genes did not have a detrimental or visible effect on the development and growth of the plants; many of them were as viable as the wild type. However, there were a few, where we were not able to identify and isolate homozygous knock-out mutants: AT1G12000 (pyrophosphate-dependent PFK), At1g18270, AT2G22480 (PFK5), AT2G35840 (SPP2), At4g15530 (PPDK), AT4G28706 (FRK), AT5G42740 (cPGI). It was already reported that knocking out the cPGI was lethal for the plant (Kunz et. al, 2014). An early arrest and abortion in seed development was detected in the *frk*, and a late one in the *spp2* mutant (Fig. 8). We were not able to characterize the impact of the four other genes on

plant metabolism and no report has been published to our knowledge yet. Expression data imply that three of them (At1g18270, AT1G12000, AT2G22480) are expressed and functional in the roots (Fig. 9b). The two phosphofructokinases (AT1G12000, AT2G22480) might be a strong interaction partner of the plastidial FBA3 (At2g01140) (Fig. 9a), which is a key enzyme in heterotrophic tissues (Chapter 3). Interestingly the PPDK protein is highly expressed in the pollen.

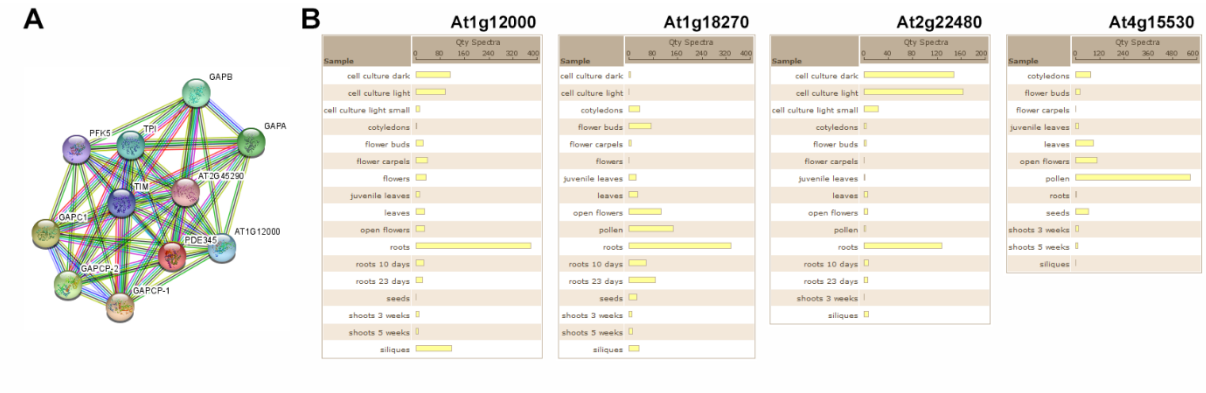

Figure 3-9. Expression and interaction data of the lethal cytosolic sucrose mutant. A) Interaction map of the plastidial FBA3 (PDE345) generated with the STRING database, PFK5 and AT1G12000 is among them. B) Expression of four presumably lethal cytosolic proteins in different tissues according to the pep2pro database.

The fba8 single knock-out mutant

The *fba8* knock-out was isolated and had a reduced growth and a slower development (Fig. 10b). According to publicly available databases, FBA8 is the most abundant of the cytosolic FBA isoforms, especially in the roots (Fig. 10a). This was confirmed by enzyme activity measurements (Fig. 10c). While knocking out the major plastidial isoforms did not significantly decrease the total FBA activity in the roots (Chapter 3), in the *fba8*, total activity dropped by over 70%.

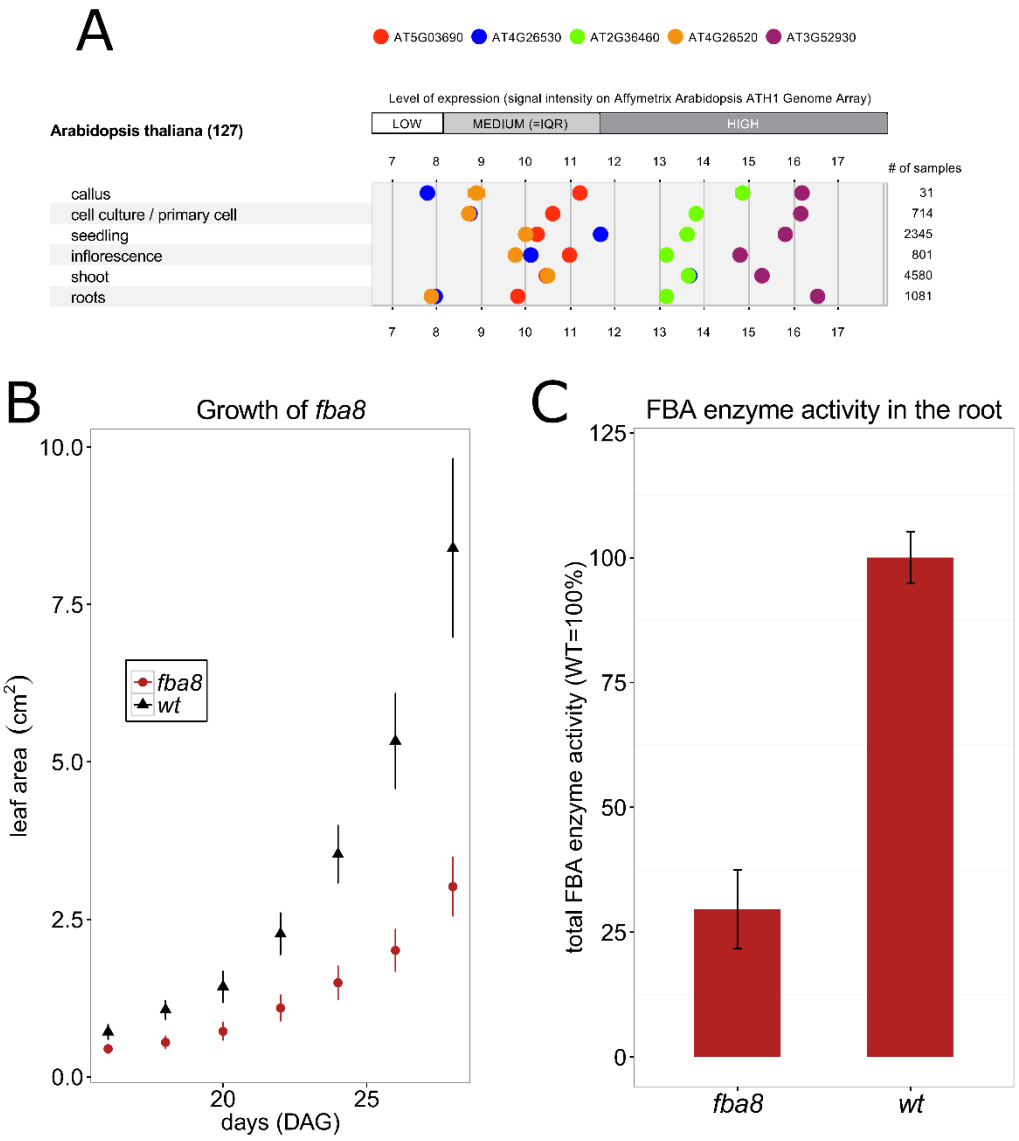

Figure 3-10. Growth of the rosettes of fba8 and FBA enzyme activity in the root of *fba8*. A) Level of gene expression (log_2 scale) of the cytosolic FBA in different tissues (created with Genevestigator). B) Leaf area of the *fba8* and wild type after 18 days of germination (DAG). C) Relative total FBA enzyme activity in the *fba8* mutant compared to the wild type.

Discussion

Redundancy of the cytosolic sucrose isoforms

The proteomic experiment suggested that several of the detected isoforms of sucrose metabolic enzymes had a tissue specific protein abundance. While certain proteins were detected ubiquitously in the shoot and the root, some appear to be specific either to the shoot (i.e. F2KP, FBA5) or in the root (i.e. SUSY6, HXK3), which might explain some of the apparent genetic redundancy. For instance, there was a difference among the sucrose-synthase gene family: SUSY1 was detected in every proteomic measurement, SUSY4 and 6 only in the roots, SUSY5 was only detected in the root exposed to salt stress. Nevertheless, the role of SUSY5 might still be crucial, because it was one of the three mutants, which had a significantly lower rosette size. The proteomic approach can be very powerful to investigate major metabolic enzymes, which are quite abundant in the plant cell. In other cases, several important proteins (e.g. those playing a role in signaling or proteins expressed in a low-abundance cell type) can be below the detection level of a non-targeted shotgun proteomic analysis, and SUSY5 might be one of them. It was previously shown that SUSY5 is expressed in the phloem (Barratt et. al, 2009). Other isoforms (i.e. SPP2, which is one the four SPP isoforms) might be crucial in the development of seeds.

Relative growth rate of the leaf area (RGR) can be useful, because lower germination rate or slower growth in early developmental stage can end up in overall smaller rosette size, but later the plant might acclimate and accelerate its growth compared to the wild type, which cannot been always detected in the single time point measurements of the leaf area. In the RGR analysis several mutants were pulled out, which had already been described as key enzymes (i.e. *gpt*, *tpt2*, *pgm3*). *Tpt2* and *hxk3* had repeatedly a significantly lower rosette size, but they had an elevated RGR compared to the wild type during the end of the recorded growth period (25-31 days after germination). They might be delayed in their growth due to different germination rates or they could have been still in exponential growth, when the wild type has started to plateau. They can have higher RGR at a specific time, even if their exponential rate is slower than the wild types earlier attained exponential rate. They could have also acclimated to the loss of enzymes thanks to metabolic changes that can compensate and accelerate development. The increased RGR can also mean that the given isoform might

have been functional only in an early temporal stage in the development and later its contribution could have decreased. Further growth analysis will be required in the future, for instance leaf area coupled fresh and dry weight measurements.

While TPT2, the major TPT isoform, is a well-described protein responsible for the export of triose-phosphates out of the chloroplast (Häusler et. al, 1998; Schneider et. al, 2002; Schmitz et. al, 2012), HXK3 is a less characterized one. TPT can be bypassed and sugars can supplied from the chloroplast by different transporters. Transporters (MEX1, GPT1), which are responsible for the export of starch degradation products (maltose and glucose) during the night (Niittylä et al., 2004; Kunz et. al, 2010), can compensate the loss of TPT2.

FBA8 might be the major cytosolic isoform in the root

Most of the cytosolic sucrose mutants had no obvious growth phenotype, but one exception was the *fba8*, which had an overall smaller rosette size compared to the wild type. The other 4 cytosolic *fba* mutants did not show any sign of reduced development. Transcriptomic and proteomic data revealed that FBA8 is a very abundant isoform, especially in the root. The plastidial isoforms (FBA1-3) contribute 90% of the total FBA enzyme activity in the photosynthesizing tissues (Haake et. al, 1998), but in the sink tissues, where the Calvin-Benson cycle is not functioning, FBA8 seems be the major isoform and contributes most to the total FBA activity: in the *fba8* mutant it dropped by ca. 80%. These are in accordance with recent findings (Garagounis et. al, 2017). We cannot exclude that it might be also a major cytosolic isoform in the leaves, because it is an abundant protein there. It might not the dominant one though, since FBA5 and FBA6 have a high expression in the shoot as well.

Carbohydrate metabolism in stress

Environmental disturbances affect growth, development and metabolism of the plants, which of course involves the primary carbohydrate metabolism. Changes in carbohydrates can be a downstream result of the plants' stress response, or it can also reflect the response of the plant to the stress in its attempt to adapt. Glucose, which is also stored temporary in starch, can serve as carbon supply in the absent of photosynthetic activity, or it can be used as osmoprotectants in stress too. Its level, either as a free sugar or as a polymer in starch, can increase depending on the nature of the treatment and the exposure period (Kaplan and Guy,

2004; Richard Sicher, 2011; Krasensky and Jonak, 2012; Prasch et. al, 2015; Thalmann et. al, 2016). We used starch as indicator for the overall carbohydrate metabolism, whether it is effected by our mild abiotic stress and nutrient deficient treatments (the latter, the nutrient deficiencies are considered a stronger treatment). Starch can be considered as temporal storage of carbon and energy and, by measuring the rates of synthesis (meaning photosynthetic activity) and degradation (necessary usage for growth in the night), it is possible to draw conclusions about the required energy and carbon a plant can or does use for growth. If some factors (may not be directly connected to carbohydrates) limits growth, starch levels often raise as they are not used. In other instances, starch level can be reduced as the carbohydrates are diverted away from starch synthesis to other relevant processes (e.g synthesis of osmoprotectants), or if the rate of photosynthesis is reduced. Overall, changes in starch always indicate changes in plant metabolism and growth (Stitt and Zeeman, 2012). In our experimental setup, at the end of the day, the starch level increased after a long-term exposure to mild changes except of the salt treatment. The latter might be the direct or indirect effect of the impaired in thylakoid and granum membrane in the presence of NaCl (Štefanić et. al, 2013). Phosphate and nitrogen starvation is known to increase not only starch, but sugar content in the plant (Rouached et. al, 2010; Stitt and Krapp 1999).

Together with the starch, the neutral sugar metabolism (glucose, fructose and sucrose) was affected too. Sugars can serve as osmoprotectants, their level are usually increased upon stress. As expected, treatments with an osmotic effect, lower temperature and additional NaCl increased their level. Interestingly, at the end of the night in salt stress their concentration dropped. It is maybe linked to lower starch level, which might be insufficient to last until the end of the night and so the sugar pool becomes depleted. Besides the actual, raw concentration data, the relation of the glucose, fructose and sucrose might be even more descriptive about regulation of sucrose degradation and its usages. As an example, in 15°C in the shoot (source) the sucrose level was higher, but in the root (sink) the sucrose was on a wild type level. On the other hand, glucose concentration was higher, which can imply that sucrose was being degraded and for other reasons the fructose was metabolized quicker or targeted more broadly into further metabolic steps. In nutrient deficiency, the root carbohydrate metabolism was not as extremely affected as the shoot. Root growth was

maintained and plants invested the limited resources into the tissues below ground (Chapter 1) and this was mirrored by the carbohydrate data as well.

Growth of single mutants in a long-term mild abiotic stress

The proteomic and metabolic measurement was carried out with the ambition of linking the two together, but to establish a direct link between the level of metabolome and proteome has proved to be difficult. Nevertheless, there were several interesting target proteins identified from these analyses. The selected mutants displayed different phenotypes in mild abiotic stress. Some of them (*fba6*, *susy4*) did not show any growth difference compared to the wild type, which implies that due to the high redundancy their role can be taken over by other enzymes without any visible growth defect. Their role might not be taken over, but there might be other processes or factors, which maintain the normal growth even in the mutants and counterbalance the loss-of-function in the mutants. Some other mutants had already a reduced growth phenotype compared to the wild type in the control environment.

The protein level of one of the FRK (following the very recent naming convention, FRK7, (Riggs et. al, 2017)) (At3g59480) decreased in the presence of salt, and the respective mutant had wild type level growth exposed to NaCl, restoring the reduced growth of the mutant in control environment (Fig. 6g). The lack of FRK7 might provide the plants an enhanced stress tolerance. FRK7 is the least active among the major 8 FRK isoforms (Riggs et. al, 2017), and knocking it out might be advantageous for the plants in a suboptimal conditions. It might not be essential in the stress response, and the other FRKs, which have higher activity in the plant metabolism (Riggs et. al, 2017), can be upregulated. Fructose level in contrast to other sugars was lower or similar to the wild type in the long-term salt treatment, which can indicate an increased FRK activity upon salt stress, but FRK7 may not contribute to it. It can be hypothesized that like one of the hexokinases, which in general catalyze a very similar reaction, the FRK7 might have a signaling role too, but this role might not linked to the stress response.

The growth phenotype of the *pfk7*, *bam5* and *susy1* correlated with the proteomics findings. Their protein abundance decrease upon the stress treatment and their growth was restored to a wild type level (*pfk7* and *susy1*) or even slightly enhanced (*bam5*). Similar speculations can be make like in the case of *frk7*. All of them belong to a gene family with many isoforms,

which in theory can compensate the lack of the proteins. However, the role of the BAM5 is still unclear, it is unlike other BAMs a cytosolic enzyme, but there are findings, which confirm its role in stress (Monroe et. al, 2014). SUSY1 is an abundant plant protein, which showed a significantly high fold change in several treatments, but it might be also a redundant one (Barratt et. al, 2009). The *susy1susy2susy3susy4* quadruple mutant had no additional phenotype suggesting that there are three other SUSY, which can take over the metabolic tasks of the SUSY1. It might be quite crucial in the metabolism of the plants to tightly control the reaction of the sucrose synthase and compensate the loss or malfunction of any SUSY, because it catabolizes the sucrose without almost any energy consumption. It provides a rapid conversion of sucrose into fructose and UDP-glucose and subsequently other carbohydrates. The isoforms of the PFK family is even less described (Mustroph et. al, 2007), the single mutants or the proteins have not been characterized yet to our knowledge.

Conclusion and outlook

Changes in carbohydrate metabolism were distinct to the respective environmental perturbation, which was confirmed by the previous proteomic results. The single proteins had specific protein abundance patterns in different treatments. There were new insights discovered about the cytosolic sucrose metabolism, but the role of many redundant isoforms remained mainly unresolved. Our treatment was relatively mild, perhaps exposure to stronger stresses can reveal more. The generation of multiple mutants, like in the case of SuSy, cannot be avoided, if we want to know more about the role of the single isoforms. Investigations about the posttranslational modifications might also provide us additional information about the regulation of the redundant genes in the future.

Those mutants, which had a smaller rosette size in the control environment (i.e. *f2kp*, *fba8*), were difficult to interpret, and the available results are insufficient to draw further biologically relevant conclusions. There are different approaches, which could allow us to dissect the role of these genes in stress responses, if we assume that they have one. In the future promoter analysis can be applied, or the stress-responsive elements, if they possess one, can be deleted. Another approach could be the complementation of these candidate mutants with the native gene driven by a non-stress responsive promoter.

Reference

Bae, H., Herman, E., Bailey, B., Bae, H. J., & Sicher, R. (2005). Exogenous trehalose alters Arabidopsis transcripts involved in cell wall modification, abiotic stress, nitrogen metabolism, and plant defense. *Physiologia Plantarum*, 125(1), 114–126.

Baerenfaller, K., Hirsch-Hoffmann, M., Svozil, J., Hull, R., Russenberger, D., Bischof, S., … Baginsky, S. (2011). pep2pro: a new tool for comprehensive proteome data analysis to reveal information about organ-specific proteomes in *Arabidopsis thaliana. Integrative Biology*, 3(3), 225–237.

Baroja-Fernández, E., Muñoz, F. J., Li, J., Bahaji, A., Almagro, G., Montero, M., … Pozueta-Romero, J. (2012). Sucrose synthase activity in the *sus1/sus2/sus3/sus4* Arabidopsis mutant is sufficient to support normal cellulose and starch production. *Proceedings of the National Academy of Sciences of the United States of America*, 109(1), 321–6.

Barratt, D. H. P., Derbyshire, P., Findlay, K., Pike, M., Wellner, N., Lunn, J., … Smith, A. M. (2009). Normal growth of Arabidopsis requires cytosolic invertase but not sucrose synthase. *Proceedings of the National Academy of Sciences of the United States of America*, 106(31), 13124–13129.

Egli, B., Kölling, K., Köhler, C., Zeeman, S. C., & Streb, S. (2010). Loss of cytosolic phosphoglucomutase compromises gametophyte development in Arabidopsis. *Plant Physiology*, 154(4), 1659–71.

Garagounis, C., Kostaki, K. I., Hawkins, T. J., Cummins, I., Fricker, M. D., Hussey, P. J., … Sweetlove, L. J. (2017). Microcompartmentation of cytosolic aldolase by interaction with the actin cytoskeleton in Arabidopsis. *Journal of Experimental Botany*, 68(5), 885–898.

Gibeaut, D. M., Hulett, J., Cramer, G. R., & Seemann, J. R. (1997). Maximal biomass of *Arabidopsis thaliana* using a simple, low-maintenance hydroponic method and favorable environmental conditions. *Plant Physiology*, 115(2), 317–9.

Gibon, Y. (2004). A robot-based platform to measure multiple enzyme activities in Arabidopsis using a set of cycling assays: comparison of changes of enzyme activities and transcript levels during diurnal cycles and in prolonged darkness. *The Plant Cell*, 16(12), 3304–3325.

Haake, V., Zrenner, R., Sonnewald, U., & Stitt, M. (1998). A moderate decrease of plastid aldolase activity inhibits photosynthesis, alters the levels of sugars and starch, and inhibits growth of potato plants. *The Plant Journal: For Cell and Molecular Biology*, 14(2), 147–57.

Häusler, R. E., Schlieben, N. H., Schulz, B., & Flügge, U. I. (1998). Compensation of decreased triose phosphate/phosphate translocator activity by accelerated starch turnover and glucose transport in transgenic tobacco. *Planta*, 204(3), 366–376.

Heinen, M. (1999). Analytical growth equations and their Genstat 5 equivalents. *Netherlands J. Agric. Sci.*, 47(1), 67–89.

Hruz, T., Laule, O., Szabo, G., Wessendorp, F., Bleuler, S., Oertle, L., … Zimmermann, P. (2008). Genevestigator v3: a reference expression database for the meta-analysis of transcriptomes. *Advances in Bioinformatics*, 2008, 420747.

Jensen, L. J., Kuhn, M., Stark, M., Chaffron, S., Creevey, C., Muller, J., … von Mering, C. (2009). STRING 8 - A global view on proteins and their functional interactions in 630 organisms. *Nucleic Acids Research*, 37(SUPPL. 1), 412–416.

Kaplan, F., & Guy, C. L. (2004). b -Amylase induction and the protective role of maltose during temperature shock 1. *Plant Physiology*, 135(July), 1674–1684.

Kircher, S., & Schopfer, P. (2012). Photosynthetic sucrose acts as cotyledon-derived long-distance signal to control root growth during early seedling development in Arabidopsis. *Proceedings of the National Academy of Sciences of the United States of America*, 109(28), 11217–21.

Krasensky, J., & Jonak, C. (2012). Drought, salt, and temperature stress-induced metabolic rearrangements and regulatory networks. *Journal of Experimental Botany*.

Kunz, H. H., Häusler, R. E., Fettke, J., Herbst, K., Niewiadomski, P., Gierth, M., … Schneider, A. (2010). The role of plastidial glucose-6-phosphate/phosphate translocators in vegetative tissues of *Arabidopsis thaliana* mutants impaired in starch biosynthesis. *Plant Biology*, 12, 115–128.

Kunz, H.-H., Zamani-Nour, S., Häusler, R. E., Ludewig, K., Schroeder, J. I., Malinova, I., … Gierth, M. (2014). Loss of cytosolic phosphoglucose isomerase (cPGI) affects carbohydrate metabolism in leaves and is essential for fertility of *Arabidopsis thaliana*. *Plant Physiology*, 166(October), 753–765.

Lastdrager, J., Hanson, J., & Smeekens, S. (2014). Sugar signals and the control of plant growth and development. *Journal of Experimental Botany*, 65(3), 799–807.

Monroe, J. D., Storm, A. R., Badley, E. M., Lehman, M. D., Platt, S. M., Saunders, L. K., … Torres, C. E. (2014). β-Amylase1 and β-Amylase3 are plastidic starch hydrolases in Arabidopsis that seem to be adapted for different thermal, pH, and stress conditions. *Plant Physiology*, 166(4), 1748–1763.

Mustroph, A., Sonnewald, U., & Biemelt, S. (2007). Characterisation of the ATP-dependent phosphofructokinase gene family from *Arabidopsis thaliana*. *FEBS Letters*, 581(13), 2401–2410.

Niittyla, T., Messerli, G., Trevisan, M., Chen, J., Smith, A. M., & Zeeman, S. C. (2004). A previously unknown maltose transporter essential for starch degradation in leaves. *Science*, 303(5654), 87–89.

Nishizawa, a., Yabuta, Y., & Shigeoka, S. (2008). Galactinol and raffinose constitute a novel function to protect plants from oxidative damage. *Plant Physiology*, 147(3), 1251–1263.

Paine, C. E. T., Marthews, T. R., Vogt, D. R., Purves, D., Rees, M., Hector, A., & Turnbull, L. A. (2012). How to fit nonlinear plant growth models and calculate growth rates: An update for ecologists. *Methods in Ecology and Evolution*, 3(2), 245–256.

Poorter, H. (1989). Plant growth analysis: towards a synthesis of the classical and the functional approach. *Physiologia Plantarum*, 75(2), 237–244.

Prasch, C. M., Ott, K. V., Bauer, H., Ache, P., Hedrich, R., & Sonnewald, U. (2015). β-amylase1 mutant Arabidopsis plants show improved drought tolerance due to reduced starch breakdown in guard cells. *Journal of Experimental Botany*, 66(19), 6059–6067.

Riggs, J. W., Cavales, P. C., Chapiro, S. M., & Callis, J. (2017). Identification and biochemical characterization of the fructokinase gene family in *Arabidopsis thaliana*. *BMC Plant Biol.*, 17(1), 83.

Rouached, H., Arpat, A. B., & Poirier, Y. (2010). Regulation of phosphate starvation responses in plants: Signaling players and cross-talks. *Molecular Plant*, 3(2), 288–299.

Ruts, T., Matsubara, S., & Walter, A. (2013). Synchronous high-resolution phenotyping of leaf and root growth in *Nicotiana tabacum* over 24-h periods with GROWMAP-plant. *Plant Methods*, 9(1), 2.

Schmitz, J., Schöttler, M. A., Krueger, S., Geimer, S., Schneider, A., Kleine, T., … Häusler, R. E. (2012). Defects in leaf carbohydrate metabolism compromise acclimation to high light and lead to a high chlorophyll fluorescence phenotype in *Arabidopsis thaliana*. *BMC Plant Biology*, 12(1), 8.

Schneider, A., Häusler, R. E., Kolukisaoglu, U., Kunze, R., van der Graaff, E., Schwacke, R., … Flügge, U.-I. (2002). An *Arabidopsis thaliana* knock-out mutant of the chloroplast triose phosphate/phosphate translocator is severely compromised only when starch synthesis, but not starch mobilisation is abolished. *The Plant Journal: For Cell and Molecular Biology*, 32(5), 685–99.

Sicher, R. (2011). Carbon partitioning and the impact of starch deficiency on the initial response of Arabidopsis to chilling temperatures. *Plant Science*, 181(2), 167–176.

Štefanić, P., Koffler, T., Adler, G., & Bar-Zvi, D. (2013). Chloroplasts of salt-grown Arabidopsis seedlings are impaired in structure, genome copy number and transcript levels. *PLoS ONE*, 8(12), 1–10.

Stitt, M., & Krapp, a. (1999). The interaction between elevated carbon dioxide and nitrogen nutrition: the physiological and molecular background. *Plant, Cell and Environment*, 22, 553–621.

Stitt, M., & Zeeman, S. C. (2012). Starch turnover: Pathways, regulation and role in growth. *Current Opinion in Plant Biology*, 15(3), 282–292.

Thalmann, M. R., Pazmino, D., Seung, D., Horrer, D., Nigro, A., Meier, T., … Santelia, D. (2016). Regulation of leaf starch degradation by abscisic acid is important for osmotic stress tolerance in plants. *The Plant Cell*.

Tocquin, P., Corbesier, L., Havelange, A., Pieltain, A., Kurtem, E., Bernier, G., & Perilleux, C. (2003). A novel high efficiency, low maintenance, hydroponic system for synchronous growth and flowering of *Arabidopsis thaliana*. *BMC Plant Biology*, 3, 2.

Tognetti, J. A., Horacio, P., & Martinez-Noel, G. (2013). Sucrose signaling in plants: A world yet to be explored. *Plant Signaling & Behavior*, 8(3), e23316.

Supplementary information

AGI	T-DNA line	Forward primer	Reverse primer
At1g07110	SALK_016314(C)®	CTACCGTATGCTCAGAGGAC	CAGATTTTACCTCGATTTGG
At1g17160	SAIL_815_E08.v1	GCTCTGTTGAATGGATGCAG	CTAAGACTTGTTTCTGGTG
At1g18270	SALK_009002C	TTTGGAAACTTGTGGAAATCG	AAACGCGGGAGATACTGTTG
At1g20950	SALK_128975	TATTTTGCGGCATACAGGTG	TAGCAAGAAAGGCGACCATC
At1g23190	SALK_034720	Egli et. al, 2010	
At1g35580	SALK_095807	TCGCTAGACCTAGCCATTAG	TTTTTCCTTACTTGCAAAGC
AT1G47840	SALK_030722	GACCACGCTCCAATTACATCG	TCGGAGTTTAGGAATTGCATGT
At1g51420	SALK_018073C	GTCATGGTTGGTTTTACGCA	GTCTTCCAGTATATAGTTTGGCTT
At1g56560	SALK_015233	GACCACGAGCGTATCTGTCA	CTCTCACAACTTTCTCACTACC
At1g61800	Gabi-KAt 454H06	Niewiadomski et. al, 2005	
At1g62660	SALK_072478	TGCAGATCCTAATGGTAAGC	CCAGTGGATAAGGTCTTTTG
At1g66430	SALK_143725	TGGAGGCTGATGAAAGTGA	CACCAACCTATACACACCATAG
At1g70730	SALK_053655	Egli et. al, 2010	
At1g73370	Sail 374-D07	Bieniawska et. al, 2006	
At1g76550	GK-814G03.01	TGGAAGGCAGGCTCCTGG	AGGTTGGTTATGAGTGTCCTAGC
At2g31390	SALK_114786C	CCTTGTCCTTCCTTACTCTCTAT	TCACGTGGTATCACGTGGATCT
At2g35840	WiscDsLox504G07	GCTCAGGAAGTTACTAAGGAGC	TTGTACATGTTCCCACACCAAT
At2g36460	SALK_014964C	TGGAAGCTACCATCACTCTCT	CTCCTGCACTCTTCAACATATCA
At3g03250	SALK_100183C	TGTGGTAGGTCAATGAGTTCA	CAGACATCACCAGACACCT
At3g17130	GABI_529C10	CAATCGCTGATCAAACATGC	TTTTGAAGGCGGATTAGACTG
At3g43190	ARAB 4	Bieniawska et. al, 2006	
At3g52340	SALK_135737	ACTTGCAGAAGAAGCGATTT	TCTCCAGCAATTGTGATAGTTC
At3g52930	SALK_124383C	CCTATATAGATGAGTTGATCGCC	TTAGCCTTGCACCTCACATAC
At3g55440	SALK_003991	TACACTCATTGCACACACACAC	CAAGACTAATAATAAGGTGCGC
At3g56040	SALK_020654	GGAGTATCTCTCCTTATCCCTC	GATTCTTCAACAAGTTGTGACC
At3g59480	GK-253H07.01	CGTGACACTAAGATCTGATGGA	CCACAAGCATTCGCAAGCCTA
At4g02280	SALK_019405	Bieniawska et. al, 2006	
At4g04040	SALK_021047	TATGATCGATGCGCGTTCCACG	CGTAACCTAATGCGTAGCAGTA
At4g10120	SAIL_645_D05	CAACTCTCGAACCACCTCGA	GCTGAAGAACAGAGCCTAGA
At4g26270	SALK_125458	GGTCTCAAGAATTATGAACCTGG	GTATCGTGACCACCTCGTGA
At4g26520	SAIL_870_A09	ATGAACGGCCCAATTATGAC	ATTCTCCTGGCAGATGATGG
At4g26530	SALK_080758	TGGCATCCTCGTCCTCTTCA	AAGCAGAGTGCCTTCGAGGA
At4g28706	WiscDsLox477-480P9	ATCCGCTGACCAGTCAACTT	AGAGACCTGCCATGAGATGAG
At4g29220	SAIL_1263_E03	CGAGGTAGGCATAACTACTTCTG	GTGCAGCATACATTGTCTGA
At4g32840	SALK_006534C	ACATTCTCGATCTCCCCGTA	AATACAGGCACGCACATCAG
At4g34860	SALK_090411	GCTCTCCATTCATCAAGAATGC	AGGTTCGTGATCTATCTACGTC
At5g03690	SAIL_1219_E07	TCCCAAATCCAAATATGAATCC	TCCCAAATCCAAATATGAATCC
At5g11110	SALK_088752	CAAATCGTTACGAATCTTCC	CCAGTGGATAAGGTCTTTTG
At5g17310	SAIL_119_F06	TTGAAGATGCTTCCGAGACC	TTCTGGATCAGGTGCTTCAAG
At5g19150	GK-173F11.01	CACCAACCTATACACACCATAG	GCGCAGAGCCAATATAGGATG
At5g20280	SALK_148643C	ACATTCACCAATTCTCTTGG	GATTCTCAGCAGCTTCCTAAG
At5g20830	SALK_014303	Bieniawska et. al, 2006	
At5g22510	SALK_138953C	TGGACCAGTCGTCACTTTACC	AGAGTTCGGATCATTAGCAGC
At5g37180	N652944	Bieniawska et. al, 2006	
At5g46110	SALK_073707.54.2	Schneider et. al, 2002	
At5g47810	SALK_088087C	CTTCTACATCACTCCTTCTGACG	AGGCCTTGAGCACGGACTTA
At5g49190	SALK_049425	Bieniawska et. al, 2006	
At5g51830	SALK_046463	ACTCAGGTTGGTGATGATGAG	TAGAAGCGCCTCTCTTAGTTTC
At5g56630	SALK_102804	CCTCATCTCATTGATTACCTTCC	ACCTCGCTGGGTTCCATCT
At5g61580	SALK_026549(AS)(BE)	TAGGCACATGGTTATTGTG	CTCATCGTTGAGATGGATG
At5g64620	SALK_003010	CTTCCTCCTCCTCGTTACCC	TTGTTCTTCTTGGCAATTTG

Supplementary Table 3-1. List of the isolated homozygous single knock-out mutants. The respective gene, which has the T-DNA insertion with the sequence of the forward and reverse primers used for the identification of the insertion

4) Characterization of the plastidial fructose 1,6-bisphosphate aldolase (FBA) isoforms in *Arabidopsis thaliana*

Dániel Á. Carrera[a], Gavin George[a], Caspar Rahm[a], Samuel C. Zeeman[a], Sebastian Streb[a]

a) Institute for Agricultural Sciences, Plant Biochemistry, ETH Zürich, CH-8092 Zürich, Switzerland

Reference:

Manuscript in preparation

Contribution:

I conducted most of the experiments. The metabolomic measurement was performed by me and Caspar Rahm together.

Abstract

In the regenerative phase of the Calvin-Benson cycle, fructose 1,6-bisphosphate and sedoheptulose 1,7-bisphosphate are both produced by the activity of fructose 1,6-bisphosphate aldolase (FBA). Three genes encoding plastidial isoforms of FBA are annotated in the *Arabidopsis thaliana* (*AtFBA1*, *AtFBA2* and *AtFBA3*) genome. However, the specific contributions of the three isoenzymes is not understood. Using T-DNA insertion mutants, we show that *fba1* single knock-out mutants are phenotypically indistinguishable from the wild type, while the *fba2* and *fba3* mutants displayed a reduction in growth. The *fba2* mutant also displayed mild chlorosis. Phylogenetic analysis indicates that FBA1 and FBA2 result from a relatively recent gene duplication within the Brassicaceae, while FBA3 has a more ancient origin during the evolution of land plants. FBA2 is the major isoform in the Calvin-Benson cycle, contributing most of the measurable activity, but redundancy with FBA1 allows both single mutants to survive. The *fba1fba2* double mutants are embryo-lethal. FBA3, on the other hand, fulfills an entirely different function. It is expressed predominantly in heterotrophic tissues of the leaf and root, especially the vasculature, but was not detected in photosynthetic tissues. We provide evidence that the loss of FBA3 causes the dysfunction of transport-associated tissues. This blocks the export of available photoassimilates from the source tissues leading to the buildup of extremely high carbohydrate levels leaves and severely retarded growth.

Introduction

CO_2 fixation in plants occurs via the Calvin-Benson cycle, where atmospheric CO_2 is incorporated into organic compounds through the action ribulose 1,5-bisphosphate carboxylase/oxygenase (RuBisCO; Fig. 1). The net assimilated carbon is used for the synthesis of carbohydrates (e.g. sucrose) that can be transported throughout the plant and metabolized for energy generation or for use as building blocks for the myriad of biosynthetic pathways that underpin growth (Christine Raines, 2011; Stitt and Zeeman, 2012). The Calvin-Benson cycle is organized into three phases: CO_2 fixation, reduction of 3-phosphoglycerate to triose-phosphaes, and regeneration of ribulose 1,5-bisphosphate (RuBP). Five out of six triose-phosphates produced in the cycle remain within the cycle for RuBP regeneration while one-sixth exits (Riesmeier et. al, 1993). The chloroplastic fructose 1,6-bisphosphate aldolase (FBA) takes part in the regeneration phase (Melvin Calvin, 1962). FBA has been demonstrated to

perform two specific reactions (i) the generation of fructose 1,6-bisphosphate (F16BP) from glyceraldehyde 3-phosphate (G3P) and dihydroxyacetone phosphate (DHAP) and (ii) the production of a sedoheptulose 1,7-bisphosphate (S17BP) from erythrose 4-phosphate (E4P) and dihidroxyacetone phosphate (DHAP). This dual function of the plastidial isoform was shown in vitro with enzymatic assays (Brooks and Criddle, 1966; Murphy and Walker, 1981; Flechner et. al, 1999) and experiments using ^{14}C-radiolabelled metabolites (Hough and Jones, 1953). Subsequent reactions in the Calvin-Benson cycle include the dephosphorylation of F16BP and S17BP by fructose 1,6-bisphosphatase (FBPase) and sedoheptulose 1,7-bisphosphatase (SBPase), respectively (Tamoi et. al, 2006; Liu et. al, 2012); FBPase generates fructose 6-phosphate, which in addition to supporting RuBP regeneration, is also a precursor for starch synthesis.

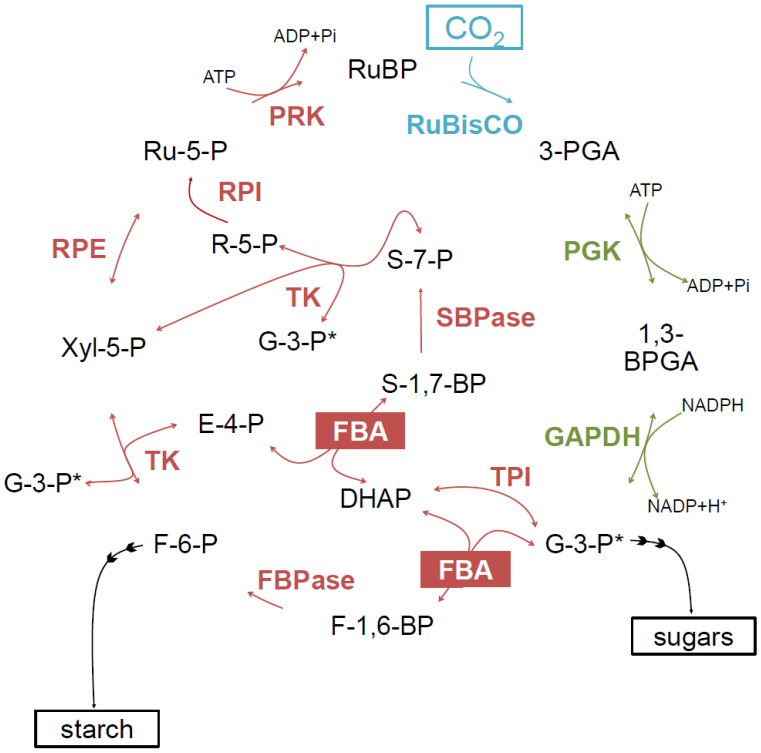

Figure 4-1. The Calvin-Benson cycle (after Christine Raines (2011)). Carboxylation, reduction of 3-PGA and regeneration of RuBP are shown in blue, green and red respectively. FBA: Fructose 1,6-bisphosphate aldolase, SBPase: Sedoheptulose 1,7-bisphosphatase, FBPase: Fructose 1,6-bisphosphatase, PRK: Phosphoribulokinase, RuBisCO: Ribulose 1,5-bisphosphate carboxylase/oxygenase, FBP: fructose 1,6-bisphosphate, E4P: erythrose 4-phosphate, SBP: sedoheptulose 1,7-bisphosphate, S-7-P: sedoheptulose 7-phosphate, F-6-P: fructose 6-phosphate, DHAP: dihydroxy aceton phosphate, G3P: glycerylaldehyde 3-phosphate, Ru-5-P: ribulose 5-phosphate, RuBP: ribulose 1,5-bisphosphate, RPI: R-5-P isomerase, TK: transketolase, TPI: triose-P-isomerase, RPE: ribulose-5-P epimerase

There are multiple fructose-bisphosphate aldolase (FBA) genes present in annotated higher plant genomes with the exact number varying amongst species (Cai et. al, 2016; Lv et. al, 2017). In *Arabidopsis thaliana* there are eight genes (Lu et. al, 2012), FBA1 and FBA2 were shown to be localized to the plastid with C-terminal GFP fusion proteins in protoplasts (Vidi et. al, 2006) and FBA3 in cell culture (Carrie et. al, 2009). Five further FBAs are predicted to be localized in the cytosol (FBA4, FBA5, FBA6, FBA7 and FBA8) (Lu et. al, 2012; Cai et. al, 2016). However, only the localization of the FBA8 was confirmed experimentally by way of the expression of a C-terminal GFP fusion protein (Garagounis et. al, 2017). In the cytosol, FBA also catalyzes the reversible condensation of triose-phosphates to F16BP (Lebherz et. al, 1984). Cytosolic FBA knock-out mutants have not yet been fully characterized. However, *fba8* single insertion mutants showed a significant reduction in the total FBA enzyme activity in roots and a reduced growth rate (Garagounis et. al, 2017).

Intermediates of the Calvin-Benson cycle supply several key metabolic processes. Their levels must be maintained to allow the cycle to function and continue CO_2 assimilation, while also supplying substrates for biosynthesis (e.g. sugar and starch production; Stitt and Zeeman, 2012). Preferentially allocating carbon to the cycle would come at the cost of export, while the opposite may lead to the restriction of assimilation due to a limiting of substrates for RuBisCO. Several metabolic control points exist within the cycle. One example is the direct regulation of RuBisCO through the RuBisCO activase, while GAPDH, FBPase or PRK enzymes have been shown to be redox regulated (Née et. al, 2009, Dietz and Pfannschmidt, 2011, Michelet et. al, 2013; Archie Portis, 2013). FBPase and PRK catalyze irreversible reactions in the Calvin-Benson cycle, but the early studies in which their activities were reduced revealed little to no effect on carbon assimilation, contrary to presumptions (Christine Raines, 2003; Stitt et. al, 2010; Christine Raines, 2011). However, metabolic modelling has suggested that RuBisCO, SBPase and pFBA could also offers potential stoichiometric-control on the photosynthetic assimilation carbon flux through the Calvin-Benson cycle (Zhu et. al, 2007).

Silencing of plastidial *FBA* expression with antisense constructs leads to a decrease in photosynthesis, starch synthesis, activity of other Calvin-Benson cycle enzymes and plant growth in potato (Haake et. al, 1998). The knock-down of the plastidial FBA protein was confirmed on a transcriptional and translational level, but the isoform specificity was not

discussed and the simultaneous impact on the cytosolic FBA could not be ruled out either. On the other hand, overexpression of pFBA in tobacco led also to an enhanced photosynthetic rate and increased biomass at elevated CO_2 levels (Uematsu et. al, 2012). The capacity to controlling the flux through the cycle was exploited in transgenic tobacco and *Arabidopsis thaliana* plants (Simkin et. al, 2015; Simkin et.al, 2016), where pFBA was overexpressed in combination with other photosynthetic enzymes (SBPase and glycine decarboxylase-H protein (GDC-H)) to increase carbon assimilation and total biomass. To reach the maximum yield, increased FBA activity was crucial yet alone it was insufficient (Uematsu et. al 2012), at least at in ambient CO_2 levels. Nevertheless, the simultaneous overexpression of the three genes resulted in a significant elevation in photosynthetic efficiency and carbon assimilation even in natural light conditions, but in higher light cditions the impact was more substantial, indicating a promising strategy for agricultural application (Simkin et. al, 2015; Simkin et.al, 2016). Surprisingly though, very little is actually known about the individual isoforms; *fba2* mutant was shown with iodine staining to have a decreased starch level, which is a visual approach, but no quantitative measurement was carried out (Lu et. al, 2012).

Not all parts of a plant perform photosynthesis, the prime example being roots. However, even within the leaves, certain regions, such as the epidermis and the tissue surrounding the veins are less, or incapable of assimilating carbon (Badeck et. al, 2009). Transport tissues, like any other heterotrophic sink tissues rely on the supply of carbon and energy from the source tissues in order to function (Bel and Knoblauch, 2000; Stitt and Zeeman, 2012). Dysfunctions in the veins and/or around them can affect transport, leading to the accumulation of sugars and starch in the source tissues, and severely affecting the growth of the plants. Such effects are observed through the direct mutation or repression of sugar transporters (i.e. *suc2-4* (Gottwald et. al, 2000) and *sweet11/12* (Chen et. al, 2012)) in leaves.

While the biochemical role of FBA has been investigated since the discovery of the Calvin-Benson cycle (Melvin Calvin, 1962) and is well-established (Penhoet et. al, 1969), several question remain surrounding the requirement for multiple isoforms in each compartment. In this paper, we aim to resolve the roles of the individual plastidial FBA isoforms. Using a series loss-of-function single and double insertion mutants, we show which isoforms are required for Calvin-cycle function, and to what extent. Interestingly, FBA3 is crucial in the metabolism

of the heterotrophic tissues especially in the vasculature and seems not to function in carbon dioxide assimilation.

Materials and Methods

Phylogenetic and bioinformatics analysis

The amino acid sequences of the proteins for phylogenetic analyses were acquired from the National Center for Biotechnology Information and Phytozome databases using pBLAST against each of the three plastidial FBA (NP_565508.1, NP_568049.1, NP_178224.1) sequences from *Arabidopsis thaliana*. The alignment was assembled with MAFFT (Katoh and Standley, 2013). The corrected Akaike Information Criterion (AICc) on the ProtTest Server (Abascal et. al, 2005) was used to choose the best suitable model (JTT) for the building of the tree. The final trees were constructed with Mega6 (Tamura et. al, 2013), branch support was tested by running 1000 bootstrap replicates. The gene duplication of the pFBAs in the *Arabidopsis thaliana* genome was checked by using the Plant Genome Duplication Database (Lee et. al, 2013).

Plant material and growth

Arabidopsis thaliana plants were grown in growth chambers (Percival AR95, CLF Plant Climatics) on a nutrient rich, medium-grade, peat-based soil or on agar plates supplied with Murashige and Skoog medium (Duchefa Biochemie) at constant 20°C, 70% relative humidity, with a 12-h light/12-h dark photoperiod. Uniform light intensity was set to 150 µmol/m^2/s. Sown seeds were stratified for 48 h at 4°C and transferred to the growth chambers. Single, homozygous T-DNA insertion mutants were isolated: *fba1-1* (SALK_063223; *Col*-0), *fba1-2* (SAIL_752_G05C; *Col*-0), *fba2-1* (SALK_000898; *Col*-0), *fba2-2* (SALK_073444; *Col*-0), *fba3-1* (GT12795.Ds5; L*er*), *fba3-2* (SALK_092715; *Col*-0). The new double mutant (*fba1-1fba2-1*) was generated by crossing the single mutants. T-DNA insertion and gene-specific primers (Suppl. Table 5) were used to check the homozygosity of the single and double mutants. *Fba3* with corresponding L*er* wild-types plants were also grown on plates with additional sucrose (0.1, 0.5, 1 and 1.5%) for root length measurements. Grafting of wild-type and *fba3* Arabidopsis seedlings was performed according to the protocol of Charles W. Melnyk (2017). Rosettes for growth measurement were photographed every third day 12-to-28 days after the germination

to quantify the growth in leaf area. The pictures were analyzed and each leaf area of every single plant was evaluated with ImageJ software.

Quantitative reverse transcription PCR measurements

Confirmation of the expression of the respective pFBA genes was measured with qPCR. Primers were designed at exon-intron borders to avoid gDNA contamination (Suppl. Table 6). Total RNA was isolated with Isol-RNA Lysis Reagent (5 PRIME); cDNA synthesis was carried out with SuperScript III first strand kit (Invitrogen) applying an oligo(dT) primer. The PCR reaction was performed with Fast SYBR Green Master Mix (Applied Biosystems) on a 7500 Fast Real-Time PCR system (Applied Biosystems) and *YSL8* (At1g48370) was used as a reference gene (45 cycles, 55°C annealing temperature).

Total FBA enzyme activity measurement

Whole rosettes from soil-grown plants or roots from plate-grown plants were homogenized in extraction buffer (50 mM HEPES-KOH, Ph 7.5, 10 mM $MgCl_2$, 1 mM EDTA, 0.25% [w/v] BSA) and total soluble proteins were extracted. The cyclic assay for FBA activity was performed as reported previously (Haake et. al, 1998; Gibon et. al, 2004). Fructose 1,6-bisphosphate (FBP) and sedoheptulose 1,7-bisphosphate (SBP) were used separately in independent experiments as a substrate.

Constructs and transformation of Arabidopsis plants

The respective FBA promoter (2000 bp upstream of the starting ATG codon) and coding sequences were amplified from genomic and complementary DNA, respectively, using iProof polymerase (Bio-Rad). The FBA promoters, the FBA coding sequences, and the sequences encoding the FLAG or HA tags, were cloned into the entry vector pDONR P4-P1r, pDONR P1-P2 and pDONR221 P2R-P3 respectively. The GUS protein was cloned into pENTR/SD/D-TOPO vector (ThermoFisher Scientific). The promoters were cloned upstream of the GUS coding sequence into the destination vector pB7m24GW, the promoter-gene swap constructs with the FLAG/HA tags were recombined into the pB7m34GW destination vector. The Multisite Gateway technique was used to build the constructs, which were introduced into *Agrobacterium tumefaciens* GV3101 strain by electroporation. *Arabidopsis thaliana* plants were transformed with the floral dip method (Clough and Bent, 1998). The *fba2* single mutants

were transformed with the *FBA2pro::FBA2:FLAG/HA* (native promoter and gene) and the *FBA2pro::FBA3:FLAG/HA* (native promoter with *FBA3*) constructs. The promoter-GUS fusion constructs were transformed into wild-type (*Col*-0) plants.

Promoter activity analysis of the pFBAs using GUS assay

Arabidopsis thaliana seedlings expressing the promoter-GUS reporter constructs were grown on ½-strength MS agar plates and the whole seedlings were destained in acetone. They were then incubated in staining solution (0.1M phosphate buffer, 0.2% [v/v] TritonX, 2 mM potassium ferrocyanide and 2 mM potassium ferricyanide) with 2mM X-GLUC in N,N-dimethlyl formamide at 37°C for 16 h. Dehydration steps were carried out with an ethanol series (20%, 35%, 50%) and the samples were fixed with FAA solution (50% ethanol, 3.7% formaldehyde, 5% acetic acid) and kept in 70% EtOH. Root samples were embedded in resin as described in Kalve et. al (2015), sectioned (80 µm) on a rotary microtome (Leica RM 2155) and visualized by light microscopy (using an Imager Z2 (Carl Zeiss) and VHX 1000D (Keyence)).

Starch and metabolite measurements

Samples comprising all the leaves of individual rosettes were frozen in liquid N_2 and ground to a fine powder using mixer mill (Retsch MM 301). Metabolites were extracted from rosettes of *fba1-1*, *fba2-1*, *fba3-1*, *Col*-0 and L*er* according to the modified protocol by Arrivault et. al (2009). Fifteen milligrams of plant powder was mixed with 300 µl chloroform:methanol solution (3:7 (v/v)). The mixture was incubated at -20°C for 2 h. Cold water (400 µl) was added, the sample mixed and separated by centrifugation. The aqueous phase was collected, dried under vacuum (Concentrator Plus, Eppendorf), and stored at -80°C. Extractions for the neutral sugar measurements via HPLC, and for starch measurements, were performed similarly except that the insoluble phase was also washed with 70% ethanol once and then with water before being stored in water at -20°C. Starch and sugars were measured by modifying the earlier protocol of Egli et. al, (2009). The fraction containing soluble sugars (glucose, fructose, and sucrose) was applied to sequential 1.5 mL columns of Dowex50W and Dowex1 (Sigma-Aldrich). Neutral sugars were eluted with 4 mL of water, lyophilized, and dissolved in 200 µL of water. The equivalent of 5 mg plant fresh weight were spiked with 5 nmol cellobiose as an internal standard and sugars were separated by a Dionex HPLC on a CarboPac PA-20 column

with the following conditions: eluent A, 100 mM NaOH; eluent B, 150 mM NaOH and 500 mM sodium acetate. The flow rate was 0.5 mL/min. The gradient was 0 to 15 min, 100% A (monosaccharide elution); 15 to 26.5 min, linear gradient to 20% A and 80% B (disaccharide elution); 26.5 to 32.5 min, 20% A, 80% B (column wash step); and 32.5 to 40 min step to 100% A (column re-equilibration). Sugars were measured using pulsed amperometric detection and peaks were identified by co-elution with known Glc, Fru, Suc, and cellobiose standards. Peak areas were determined using Chromeleon software (Thermo Scientific). All peaks were normalized to the internal cellobiose standard, and the amount of each was calculated based on standard curves of the pure standards run in parallel. Starch in the insoluble fraction was digested with α-amylase (pig pancreas; Roche) and amyloglucosidase (*Aspergillus niger*; Roche) and the released glucose measured spectrophotometrically as described previously (Smith and Zeeman, 2006). For the metabolomic measurement on UHPLC-MS/MS, the samples were resuspended in water, the amount of water was normalized to the respective plant material (250 µl/15 mg). The samples were filtered (Minisart RC4, pore size: 0.2 µm, Huberlab) afterwards. Metabolite quantity was determined with Agilent 1290 Infinity UHPLC (Agilent Technologies, USA) with Acquity T3 end-capped reverse phase column (Waters Corporation, USA) coupled to a QTRAP 5500 triple quadrupole MS (AB Sciex). Anion exchange chromatography was performed applying the gradients described in the Suppl. Table 9. and buffers with the following composition: Buffer A (10mM tributylamine, 15mM acetic acid, 5uM phosphoric acid, 5% methanol in nanopure water) and buffer B (100% isopropanol). The Calvin-Benson cycle intermediates were quantified against a standard curve prepared using commercially available compounds using the software Multiquant (AB Sciex, Switzerland). In specific cases, spiking of the plant sample with single standard components was performed to confirm the peak identity. The compound-dependent MS parameters used during data acquisition are displayed in. The metabolite amounts were $\log_2$-transformed and normalized to the wild-type for the heatmaps. PCA analysis of the metabolomics data was performed with ClustVis (Metsalu and Vilo, 2015).

Gas exchange measurements

Gas exchange experiments were carried out using four mutant and four wild-type plants in parallel. The measurement was carried out as described in Kölling et. al, (2015) and the data

processed using custom-built software described in George et. al, (2018). Plants were introduced into measurement chambers a day before measurement to allow for acclimation and prevent mechanical stress from interfering with the measurements. The plants were then measured continuously for a full day and night. Plants were subsequently harvested and fresh mass recorded. Leaf area was also recorded using leaf area measurements described above and the assimilation was normalized to fresh weight.

Recombinant expression and enzyme activity measurements of the plastidial FBA proteins in yeast

Expression of the recombinant proteins in *Pischia pastoris* was carried out as described in Weidner et. al, (2010) and Garagounis et. al (2017). The three plastidial FBA genes (*AtFBA1*, *AtFBA2* and *AtFBA3*) without the cTP sequence were cloned into empty pPICZα plasmids. Wild-type *Pichia pastoris* strain X-33 was transformed with the pPICZα constructs using electroporation. Methanol induced expression of the proteins was induced by exchanging the BMGY media to BMMY (Weidner et. al, 2010). The Pischia cells were harvested by centrifugation, re-suspended in extraction buffer (50 mM HEPES-KOH, pH 7.5, 10 mM $MgCl_2$, 1 mM EDTA, 0.25% BSA) were freeze shocked in liquid N_2, heavily vortexed for 20 min at 4°C and subject to centrifugation at 3000 g for 5 min at 4°C. The clarified culture media was assayed for aldolase enzyme activity and the presence of the recombinant protein was confirmed by SDS-PAGE and western blotting with an anti-Myc antibody. The aldolase enzyme activity assay described in Gibon et. al. (2014) was modified in order to monitor directly the changes in the product level of the FBA enzymes via UHPLC-MS/MS. The protein extract of the induced and non-induced cultures was incubated in assay buffer (0.5 M Tricine-KOH, pH 8.5, 25 mM $MgCl_2$, 5 mM EDTA, 0.25% Triton X100 [v/v]) with 20 mM FBP for 30 minutes at 25°C in 300 µl. Aliquots of 70 µl were transferred into cold chloroform:methanol solution (3:7 (v/v)) to stop the reaction after 0, 5, 15 and 30 minutes. The metabolites were extracted as described above. The increased triose-phosphate concentration was measured on UHPLC-MS/MS and normalized to the non-induced lines, protein amount and the zero time-point. The relative protein quantity was calculated with Image Studio Lite (LI-COR) image analysis software.

Results

Plastidial FBAs are conserved proteins in the plant kingdom

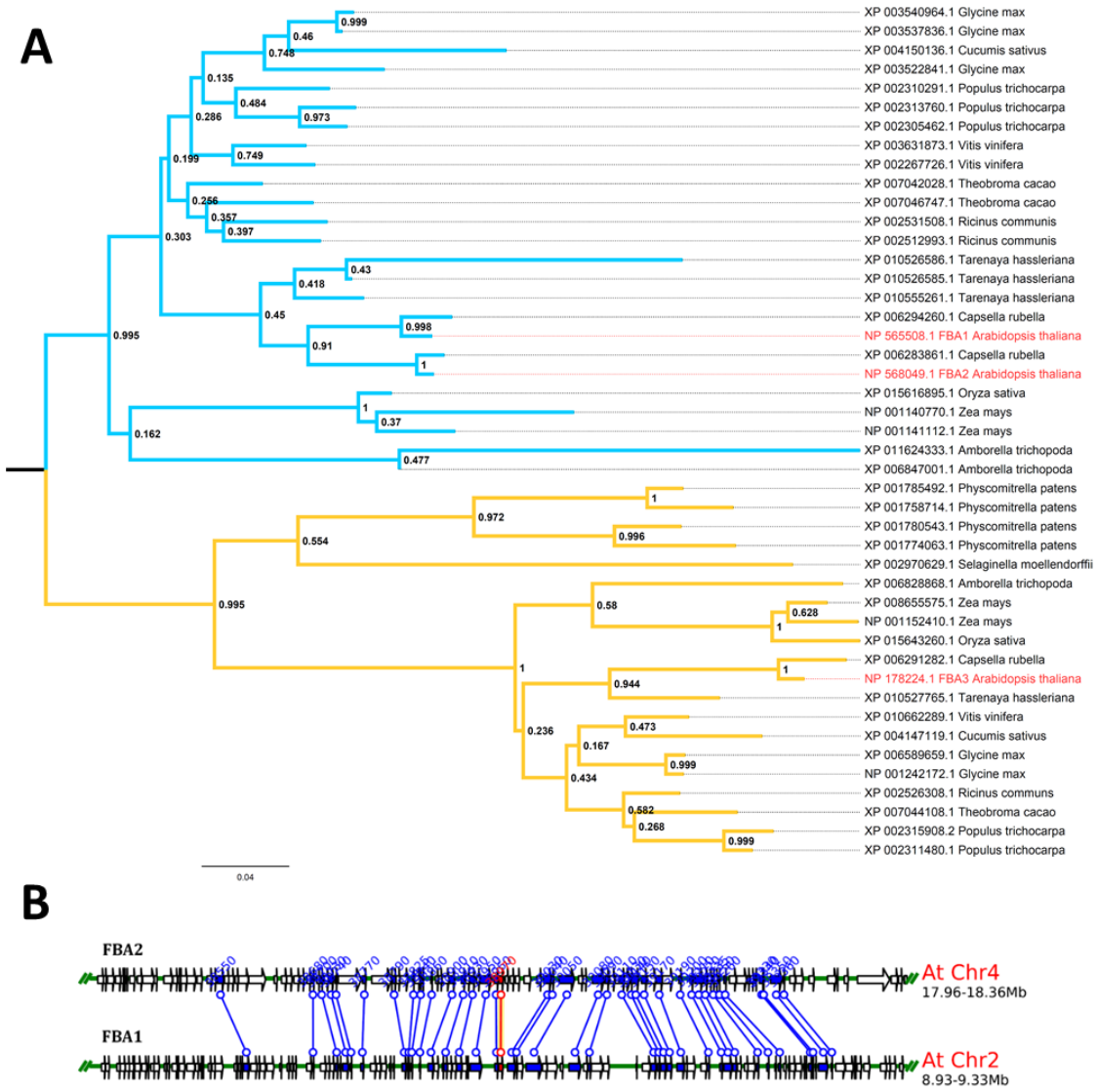

Figure 4-2. Distinct phylogenetic origin of FBA1, FBA2 and FBA3. A) Maximum likelihood phylogenetic tree with Bootstrap values of the plastidial FBA proteins from mosses and higher plant species. The Arabidopsis thaliana proteins (NP_565508.1, NP_568049.1, NP_178224.1) are shown in red. B) The duplicated chromosomal regions containing the FBA1 and FBA2 generated by the Plant Genome Duplication Database.

A phylogenetic analysis of the FBAs was performed in order to investigate their evolution. Algae, moss, lycophyte, monocot and dicot species from different clades in the plant kingdom were included in this analysis. In green algae, the cytosolic and plastidial isoforms cluster into two distinct groups suggesting an early divergence of these two clades (Suppl. Fig. 1). Within

the plastidial isoforms, similarity of protein sequences of the three plastidial isoforms in *Arabidopsis thaliana* was relatively high (above 80%). FBA1 and FBA2, are highly similar (95%) suggesting a more recent duplication and perhaps only a partial or no functional divergence (Suppl. Table 1). FBA3, on the other hand is less similar and clusters with the FBA of ancestral species such as *P. patens* and *S. moellendorffii*, suggesting that this isoform evolved first. AtFBA1 and AtFBA2 cluster with FBAs of evolutionarily more recent species such as *Amborella trichopoda* - considered the basal lineage of the Angiosperms. Subsequent duplication of this FBA is common in several species (Fig. 2a) and can be seen in most of the species included into the phylogenetic analysis. The late duplication event of FBA1 and AtFBA2 is reinforced by syntany analysis. In *Arabidopsis thaliana,* FBA1 and FBA2 are located on the chromosome II and IV respectively (Fig. 2b), the syntanic zone is approximately 0.4 Mb in length and contains the same set of 56 other genes, which are very similar and can be linked to each other.

Growth of T-DNA insertion single knock-out mutants

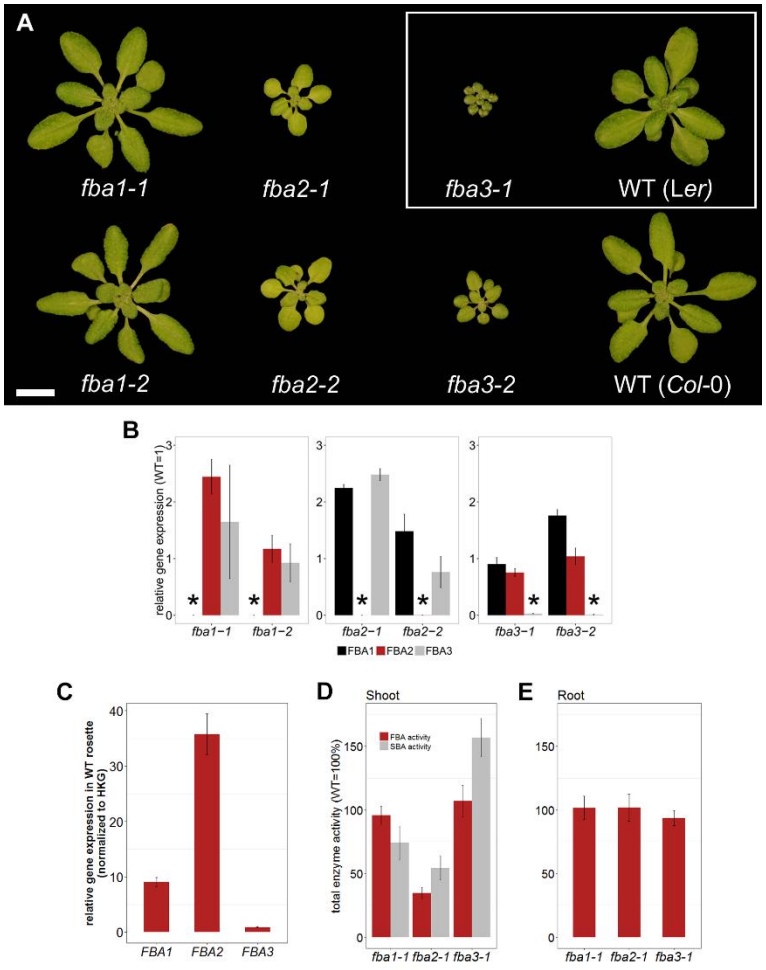

Figure 4-3. The homozygous single knock-out mutants of the three plastidial isoforms of FBA. A) Phenotype of the mutants grown 30 days after germination. The scale bar corresponds for 1 cm. B) Relative expression of the FBA1, FBA2 and FBA3 genes in the rosettes of six single knock-out mutants. Gene expression was normalized to a housekeeping gene (YLS8) and the expression of the respective FBA in the wild type was considered 1. C) Gene expression of the plastidial FBA genes in the shoot of wild-type Col-0 plants measured with qPCR at midday. Gene expression was normalized to a housekeeping gene (HKG (YLS8)). D) Total FBA and SBA enzyme activity measured in the shoot of the fba1-1, fba2-1 and fba3-1 mutants. The enzyme activity was normalized to the respective wild type. E) Total FBA enzyme activity measured in the root of the fba1-1, fba2-1 and fba3-1 mutants. The enzyme activity was normalized to the respective wild type. Bars represent mean values and the error bars standard errors (n=3).

To investigate the role of the different pFBA isoforms in the plant metabolism, two independent single homozygous knock-out lines of each isoform were isolated: *fba1-1*, (SALK_063223), *fba1-2* (SAIL_752_G05C), *fba2-1* (SALK_000898), *fba2-2* (SALK_073444), *fba3-1* (GT12795.Ds5) and *fba3-2* (SALK_092715) (Fig. 3a). The insertions were determined to be in the exons in each of the alleles (Suppl. Fig. 2) and complete elimination of normal transcript in each line was confirmed using RT-qPCR (Fig. 3b). In each *fba* mutant, the expression of the other *pFBA* genes was either increased or unaffected, with the two different alleles not necessarily behaving in the same way (Fig. 3b). The *fba1-1* and *fba1-2* had a wild-type-like growth phenotype. Mutants of *fba2*, on the other hand, were paler than the wild type and displayed a notable reduction in growth (Fig. 3a and Suppl. Table 2). Interestingly, *fba3* mutants had an even more severe reduction in growth of the rosettes and also the roots, which were stunted (Fig. 9a).

Expression and enzyme activity in the single knock-out mutants

In the leaves, *FBA2* is the most highly expressed of the three genes, followed by *FBA1*, while *FBA3* is expressed at a very low level (Fig. 3c). To see if this was also reflected at the enzyme activity level we measured total activity in both the leaves and the roots. Whole rosettes and pooled root samples were harvested and the soluble proteins were extracted (Fig. 3d and 3e). In the shoot, both reactions were determined (F16BP and S17BP production – hereafter termed FBA and SBA activity, respectively), while in the root only FBA activity was measured. In the shoot, *fba1-1* had wild-type-like FBA and SBA activity, while *fba2-1* showed a significant decrease in both reactions. FBA activity was decreased by approximately two thirds in the *fba2* mutant background, while the SBA activity was half of the wild type (Fig. 3d). In *fba3-1*, the FBA activity did not decrease. Surprisingly, the SBA activity was even somewhat increased. In the roots, no differences were detected in the enzyme activity levels between the single mutants (Fig. 3e). Thus, the major effect on total FBA and SBA activity in the shoots was consistent with the relative gene expression levels (Fig. 3c). Based on public expression data (Zimmermann et al, 2004; Winter et al. 2007; Baerenfaller et. al, 2011), *FBA1* and *FBA2* are highly expressed in the shoots but show little expression in the roots (Suppl. Fig. 5). On the other hand, FBA3 expression in the leaves remained low, but transcriptomic and proteomic databases show that it is a highly expressed and abundant protein in the roots (Suppl. Fig. 5).

Carbohydrate metabolism (sugar and starch metabolism) and photosynthetic carbon assimilation and respiration

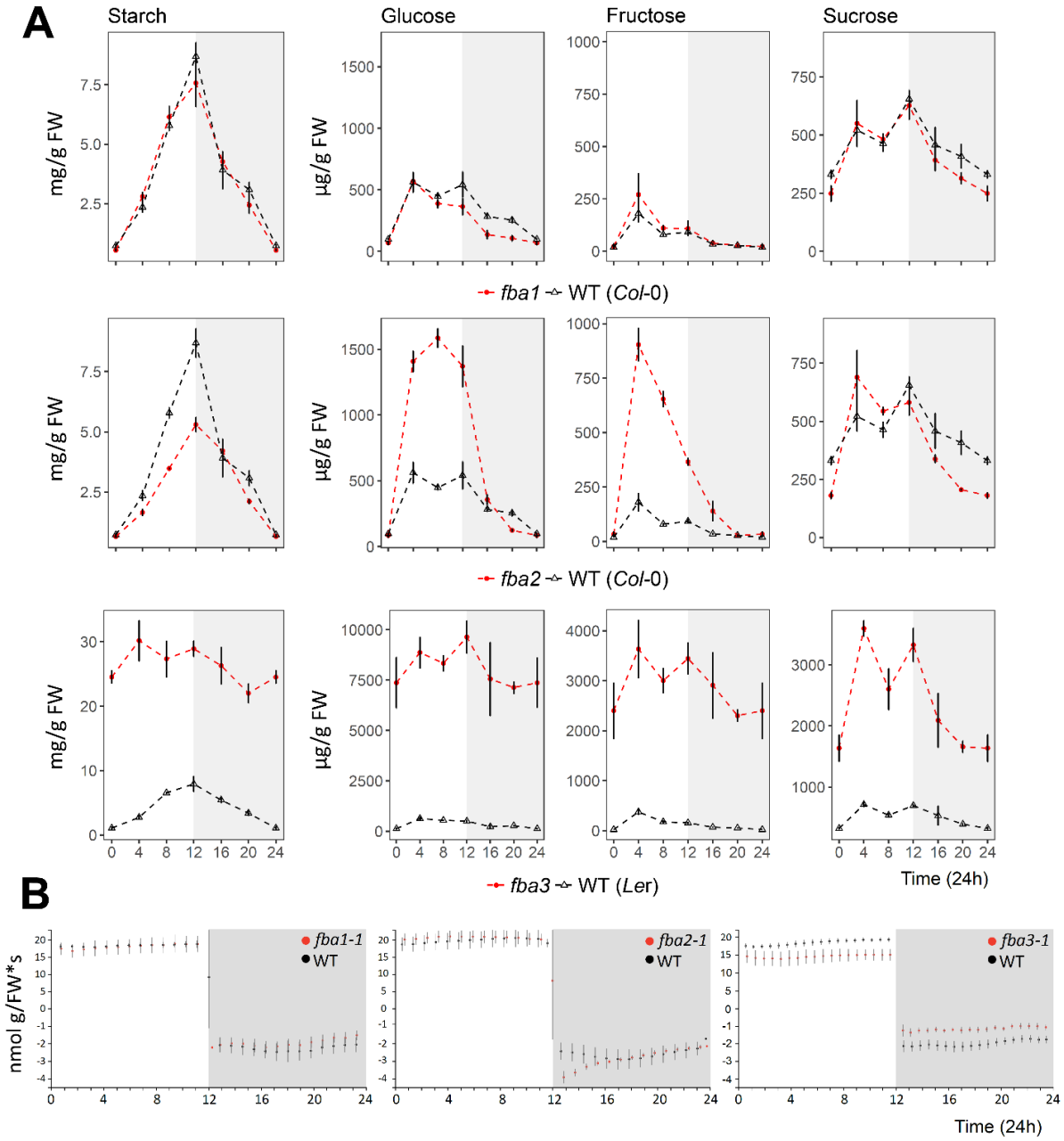

Figure 4-4. Diurnal changes of carbohydrate metabolism in the *fba1-1*, *fba2-1* and *fba3-1* single knock-out mutants with the respective wild types. Changes in A) starch and soluble sugars (glucose, fructose, sucrose) and in B) carbon assimilation. 12 h in light (white background) and 12 h in dark (grey background). The range of y-axis can be varying according to the measured data in the different mutants. The same data from the wild-type are represented in the *fba1* and *fba2* starch and sugar measurements. The points represent mean values and the error bars are the standard errors (n=4).

Primary carbohydrate metabolism is directly linked to the Calvin-Benson cycle in that assimilated carbon is partitioned directly into soluble sugars and starch. Therefore, we

measured starch and neutral sugars (glucose, fructose and sucrose) over a diel cycle (Fig. 4a). In *fba1-1* there were only minor differences to the wild type, with the content of glucose and sucrose being slightly lower during the night. In *fba2-1*, starch accumulation was reduced, with only 60% that found in the wild type produced by the end of the day. During the following night, degradation was linear and the starch reserves were not depleted earlier than in the wild type. The *fba2-1* mutant had higher glucose and fructose levels during the day, while sucrose was similar to the wild type. However, during the night, sucrose levels were lower in *fba2-1* than in the wild-type. Remarkably, the *fba3-1* mutant had a strong starch-excess phenotype. At the end of the day, starch was four times higher than in the wild type. The levels of all the three soluble sugars was also constantly high and the diel dynamics in these carbohydrate pools was lost.

Photosynthetic carbon assimilation and respiration in the plants was determined via infra-red gas analysis in custom-made chambers (Fig. 4b). The photosynthetic rate in *fba1-1* and *fba2-1* plants were similar to the wild type. At the beginning of the night, however, *fba2-1* displayed an elevated rate of respiration, which soon decreased to match the wild type. The *fba3-1* had a constantly decreased photosynthesis rate throughout the whole day and decreased respiration rate throughout the night.

Comparative metabolic profiling with UHPLC-MS/MS

We investigated the metabolic changes induced by the knock-out of the individual FBAs. Metabolic profiling in the shoots, which were harvested at midday, covered phosphorylated monosaccharides from the cytosol, the Calvin-Benson cycle and the Citric acid cycle, as well as several amino acids, nucleotides, and energetic intermediates – ATP, NAD, etc. (Fig. 5). PCA analysis of the shoot metabolite measurement revealed separated clusters of the *fba2-1* and *fba3-1* mutants, whereas both wild-type ecotypes and the *fba1-1* mutants formed one cluster (Suppl. Fig. 4). The levels of the metabolites in the *fba1* single mutants were similar overall to the wild type with few exceptions (e.g. arginine and some intermediates from the citric acid cycle. In the *fba2,* the citric acid intermediates showed a reduced abundance, but the levels of the amino acids were quite variable. The levels of the triose-phosphates - the substrates for FBAs - were elevated, while the F16BP remained unaltered, as did some other Calvin-Benson cycle intermediates, while others were slightly reduced. The metabolite levels in *fba3* were

quite different. The overall concentration of phosphorylated monosaccharides were reduced in *fba3* with few exceptions. The nucleotides and their important derivatives, coenzymes of energy and electron transfer showed an interesting pattern: uracil, uridine and especially adenine were higher, but most of their derivatives (i.e. ATP, NADH) was strongly decreased. Root metabolite profiling was carried out with *fba3-1* and L*er* samples. In the roots of *fba3-1*, there were fewer metabolites with significant changes compared to the number observed in the shoots. Unexpectedly a high ADP-glucose level was detected in the *fba3* roots, although it was virtually undetectable in the wild type.

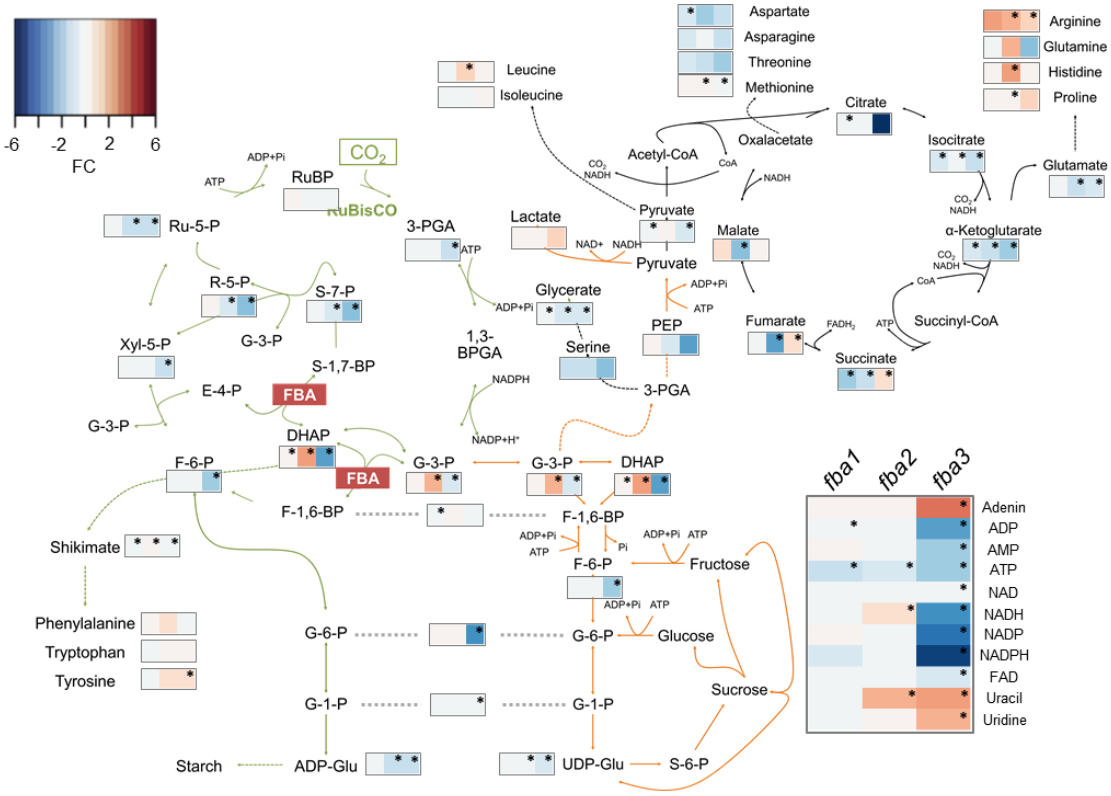

Figure 4-5. Metabolism of primary carbohydrates in the single knock-out mutants of the plastidial FBA isoforms. Schematic representation of the metabolic network of primary carbohydrates, amino acids and nucleotides. Metabolic steps illustrated in green, black and orange are in the plastid, mitochondrion and cytosol respectively. The three colored boxes represent the single mutants in the order of *fba1-1*, *fba2-1* and *fba3-1*. Metabolic values are normalized to the wild type and log_2-transformed for the heatmap analysis. Asterisk represent significant changes ($p \leq 0.05$) in the metabolite level compared to the wild type.

Enzyme activity measurement of the recombinant plastidial FBA proteins

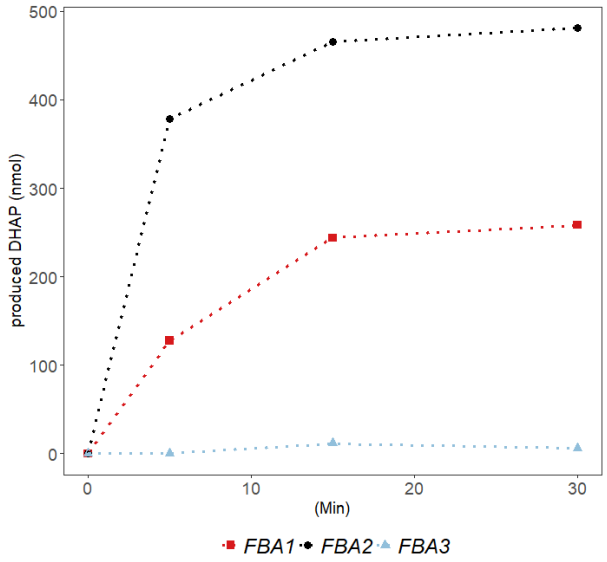

Figure 4-6. Enzyme activity of the FBA1, FBA2 and FBA3 recombinant proteins expressed in *Pischia pastoris*. The level of the product (DHAP) was monitored over 30 min and normalized to protein expression (Suppl. Fig. 12).

The FBA1, FBA2 and FBA3 recombinant proteins were expressed and assayed for aldolase enzyme activity. Product accumulation was monitored over a 30 min time period (Fig. 6). The activity of FBA1 and FBA2 was in a similar range, although the FBA2 recombinant protein had more than twice the activity of FBA1. The activity of FBA3 was below the detection limit.

Phenotype of the fba1$^{(-/+)}$fba2$^{(-/-)}$ mutant

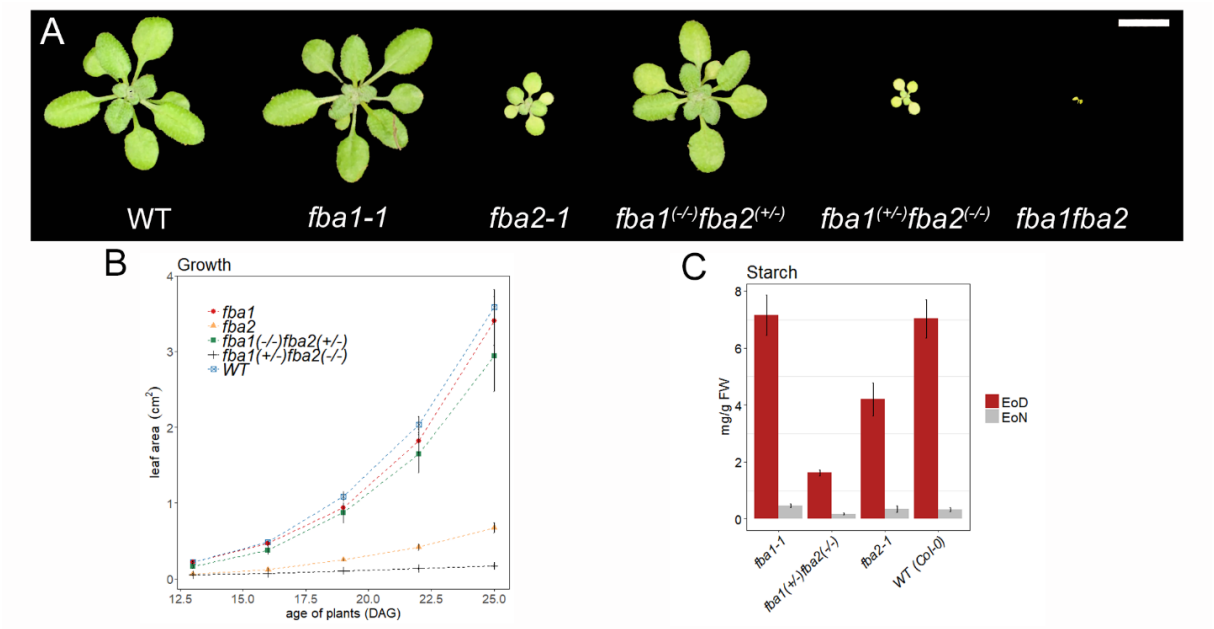

Figure 4-7. Phenotype of the *fba1$^{(+/-)}$fba2$^{(-/-)}$* double mutant. A) Phenotype of different genotypes of the *fba1fba2* F2 generation. The scale bar corresponds for 1 cm. B) Growth of leaf area of different genotypes of the *fba1fba2* F2 generation from the age of 12 to 25 days after germination (DAG). C) Starch content of the *fba1$^{(+/-)}$fba2$^{(-/-)}$* double mutant compared to the wild type, *fba1* and *fba2* single mutants. Bars and the points of the scatterplot represent mean values and the error bars standard errors (n=4)

Fba1-1 was crossed with *fba2-1* (Fig. 7). A very low number of double mutant plants could recovered at the germination stage (Suppl. Table 3) and afterwards their growth was impaired. The small, yellow seedlings that ensued were inviable. The growth of plants of the *fba1fba2* F2 segregating population was monitored and subsequently genotyped. The *fba2* homozygous single knockout plant with only one copy of FBA1 was capable of further development, but it had a very severe growth phenotype and smaller rosettes than the *fba2* single knock-out mutant (Fig. 7b). One functional copy of FBA2 was sufficient for maintaining a wild-type phenotype (Fig. 7a and 7b). The $fba1^{(-/+)}fba2^{(-/-)}$ plants had also lower starch level than the single mutants (Fig. 7c). Opening the developing siliques of either the $fba1^{(-/+)}fba2^{(-/-)}$ plants or the $fba1^{(-/+)}fba2^{(-/-)}$ plants revealed a high proportion of undeveloped or aborted seeds, explaining why so few homozygous double mutants were obtained.

Tissue localization of the pFBAs

Promoter-GUS fusion constructs were created to detect the expression and localization of the plastidial FBAs (Fig. 8); $FBA1_{pro}$*::GUS* and $FBA2_{pro}$*::GUS* showed a strong staining in the leaf lamina, especially in the green, photosynthesizing parts (Fig. 8a, 8b and 8c). On the other hand, the *FBA3* construct gave strong staining in the veins, in the middle of the stem, and in the vasculature system of the root, but no staining was visible in the photosynthetic tissues (Fig. 8c, 8d, 8e, 8f and 8g). In root cross sections, there was a strong expression of the GUS driven by the *FBA3* promotor in the stele (except for the xylem; Fig. 8f). No expression in the root was detected in plants transformed with $FBA1_{pro}$*::GUS* and $FBA2_{pro}$*::GUS* constructs (Suppl. Fig. 6).

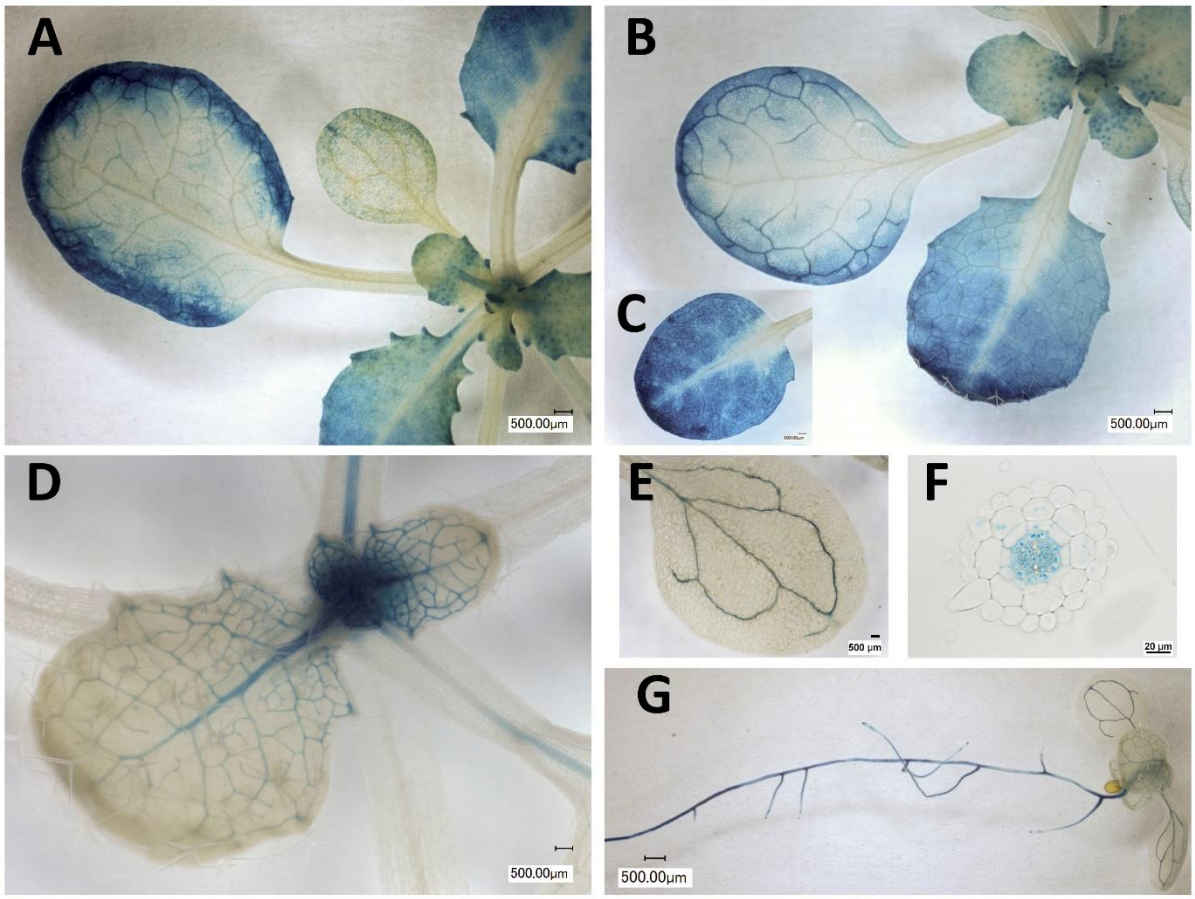

Figure 4-8. Localization of *FBA1*, *FBA2* and *FBA3* throughout the plant. Staining of seedling plants transformed with *FBA1*$_{pro}$*::GUS* (A), *FBA2*$_{pro}$*::GUS* (B and C), *FBA3*$_{pro}$*::GUS* (D, E, F and G) constructs in developing leaves (A,B, C, D and E), root cross-section (F) and the root (G).

Root growth of fba3 and grafting

The high starch phenotype of the *fba3* mutants presents in the leaf lamina, although the expression of the gene appears to be in the vasculature, suggesting a potential deficiency in sugar export. *Fba3* homozygous plants were therefore grown on ½-strength MS plates with additional sucrose (Fig. 9a and 9b). The exogenously applied sugar could slightly recover the reduced root growth of the mutant, although higher sugar concentrations inhibited the root growth again. Micro-grafting experiment were then carried out to determine if the phonotype could be tied to a dysfunction in the shoot, or in the root. To this end, chimeric *fba3*:wild-type plants were generated (Fig. 9c) where *fba3* shoot was grafted onto a wild-type root and the reciprocal, together with *fba3*: *fba3* and wild-type:wild-type controls. While the wild-type shoot grown on an *fba3* root rescued the mutant phenotype, the *fba3* shoot on a wild-type root did not, with the grafted plants still exhibiting reduced growth like the *fba3* mutant. The

roots and shoots of the chimera plants were genotyped to confirm that lateral roots were not produced at or above the graft point (Suppl. Fig. 8). These data suggest a shoot vascular dysfunction in *fba3*.

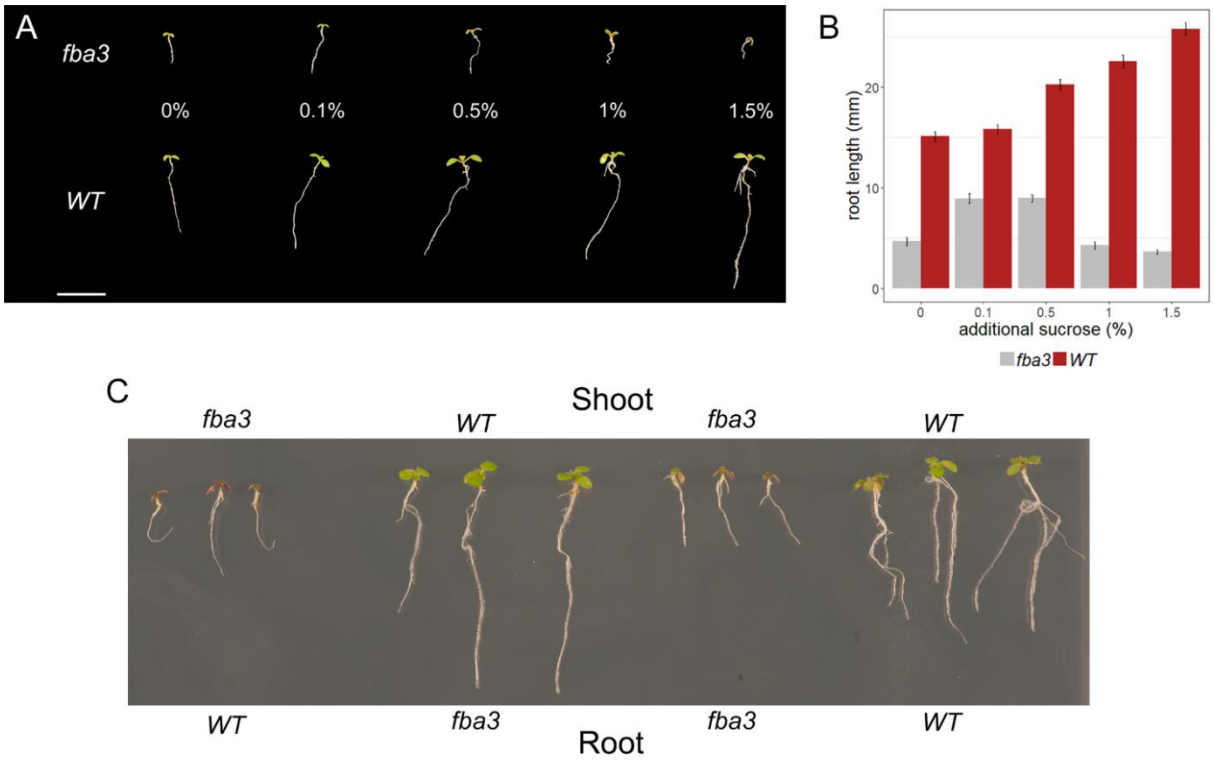

Figure 4-9. Root phenotype of the *fba3*. A) Root phenotype and B) root length of the *fba3* and wild type grown on ½ MS plates with additional external sugar (0.1, 0.5, 1 and 1.5% sucrose). Bars represent mean values and the error bars standard errors. C) Phenotype of *fba3*-wild type grafted plants. *Fba3* shoot grafted onto wild type root, wild type shoot grafted onto *fba3* roots with the *fba3* and wild type control. The genotype of the roots were determined (Suppl. Fig. 8).

Discussion

Different phylogenetic origin of the plastidial FBA genes

The enzymatic reactions of Calvin-Benson cycle, including FBA, have been characterized now for more than half a century (Linko and Calvin, 1957). This biochemical activity of this photosynthetic enzyme, participating in the regeneration phase of the cycle, is well understood. However, an in-depth characterization of each of the isoforms of FBA is still missing. Given that *Arabidopsis thaliana* has three plastidial isoforms, the question arises as to whether these isoforms are redundant in plastidial metabolism, whether they have distinct

activities, are conditionally required, or if they function in different parts of the plant. They are targeted to the same subcellular compartment (Vidi et. al, 2006; Carrie et. al, 2009; Lu et. al, 2012). Supporting the hypothesis of diversified roles is the fact that multiple plastidial isoforms exist is a wide range of land plants. For instance, monocots such as maize and rice have 3 and 2 respectively, and most dicots examined have between 2 and 4. To better understand the evolutionary basis of this multiplication of FBA we constructed two phylogenies containing all FBAs isoforms and another consisting of only the plastidial isoforms (Suppl. Fig. 1, Fig. 2). The phylogenetic analysis already implied that the plastidial isoforms may not be completely redundant. The phylogenetic tree was clustered into two classes, which was supported by high (almost 1) bootstrap values, AtFBA1 and AtFBA2 was on one branch, and AtFBA3 was on the other. While FBA1, FBA2 and FBA3 share a common ancestor gene, FBA3 might be evolutionary the closest one to that ancestor, FBA1 and FBA2 arose later during land plant evolution. FBA3 seemed to be a more conserved gene, with less duplication events in different species. There are different explanations, why certain genes undergo duplication (Panchy et. al, 2016), which do not necessarily exclude each other, dosage-sensitive genes or the ones with many interaction partners tend to be less duplicated. Together these data suggest that FBA1 and FBA2 and more closely related evolutionarily and presumable metabolically, while FBA3 is more distant, possibly fulfilling an entirely different role, which was supported by the *in silico* analysis (Suppl. Fig. 5). Gene expression (eFP Browser and Genevestigator) and proteomic (pep2pro) databases showed a clear spatial separation between FBA1/FBA2 and FBA3. While FBA1 and FBA2 are highly expressed in the leaves, FBA3 is localized to the roots, where FBA1 and FBA2 are not present at all. Between FBA1 and FBA2, FBA2 seems to a more abundant protein in the rosettes.

Function in metabolism is partially determined by localization

Our reporter constructs driven by the promoters of each of the three genes showed that FBA1 and FBA2 are expressed in the same tissues, while FBA3 has a very different expression pattern, complementing the phylogenetic analysis. Plants transformed with the *FBA1$_{pro}$::GUS* and *FBA2$_{pro}$::GUS* constructs stained mainly in the green photosynthesizing tissues, supporting the function of FBA1 and FBA2 in photosynthesis. FBA3, on the other hand, was expressed in the vasculature outside of the mesophyll tissues. Plastid metabolism varies throughout the

plant. In mesophyll tissues, plastids (chloroplasts) are predominantly associated with the processes of photosynthesis and carbon assimilation. In the roots and other heterotrophic tissues, the non-pigmented plastids have distinct roles, which can be storage, biosynthesis, energy conversion, sensing, etc. (Liebers et al, 2017). Our data strongly suggest that FBA3 is fulfilling an important role in the heterotrophic tissues of the leaf.

Mutants of FBAs reveal redundancy between FBA1 and FBA2, but not FBA3

Considering the localization of the three enzymes, it seemed likely that there would be functional redundancy between the isoforms FBA1 and FBA2. Our analysis of the phenotype of the insertional mutants supported that. Growth of *fba1* was phenotypically indistinguishable from the wild type, while *fba2* plants were small. By crossing both single mutants, we were unable to generate a viable double mutant, which implies that knocking out *FBA1* and *FBA2* simultaneously eliminates the total FBA activity in the Calvin-Benson cycle and supports their partial functional redundancy. Plants with one functional FBA1 allele (*fba1*$^{(-/+)}$*fba2*$^{(-/-)}$) were smaller than both single mutants, and their starch profile was fba2-like, but more exaggerated, implying a dosage-dependent effect. Thus, on one hand it seems that FBA1 can only partially compensate the loss of FBA2. On the other hand, even one single copy of FBA2 (*fba1*$^{(-/+)}$*fba2*$^{(-/-)}$) is sufficient to maintain the growth of the plants. In contrast, while the *fba3* mutants were even smaller that *fba2* plants, the expression pattern and the mutant phenotype were inconsistent with a role in photosynthesis.

FBA2 is the major isoform in the Calvin-Benson cycle

FBA1 and *FBA2* are highly expressed in the leaves with *FBA2* expressed at 3- to 4-fold higher levels than the *FBA1* (Fig 3C). In comparison, the expression of *FBA3* was negligible. The major contribution of FBA2 to the total activity was confirmed in the mutants. The *fba2* single mutants had the biggest and only significant decrease in the total enzyme activity level among the three. The knock-out of FBA2 reduced the FBA enzyme activity level by 75%, and plastidial FBA activity war reported to contributes ca. 90% to the total activity in leaves (Haake et. al, 1998). Thus, a complete loss was not expected in any of the mutants because of the other plastidial and cytosolic isoforms. Based on these data together, FBA2 individually has a ca. 80-85% contribution to the total FBA enzyme activity in the chloroplast, while FBA1 might have

only 15-20%. Thus, it is not surprising that loss of FBA2 has a more profound effect on plant performance, since it is probably the major photosynthetic FBA isoform. It explains why in *fba1* not all the measured physiological characteristics (enzyme activity, metabolite level, assimilation rate) were significantly different from the wild type, why FBA1 cannot compensate for the loss of FBA2 and why, when FBA2 is missing, there is a dosage-dependent effect of losing FBA1.

Fba2 had a similar carbohydrate metabolic profile like other Calvin-Benson cycle mutants (Lu et. al, 2012; Liu et. al, 2012); high sugar content coupled with lower starch level. High soluble sugar content can elevate the level of respiration at the beginning of the night (Caspar et. al, 1985) and this was detected this in the *fba2* single knock-out plants. However, the carbon assimilation in *fba2* was unexpectedly similar to the wild type level. The metabolic profiling analysis also revealed that despite the high triose phosphate levels (the substrates of FBA), the FBP concentration was maintained at wild-type levels. Further, the following metabolites in the cycle (3-PGA, F-6-P, Xyl-5-P, Ru-5P and RuBP) were only slightly or not decreased in *fba2*. The wild-type level of FBP concentration seems contradictory to the lower enzyme activity in *fba2*, but it has to be remembered that the measured FBP comes from two pools; the chloroplastic pool and the cytosolic pool. An increased flux into sugars via the cytosolic pool could mask a reduction of the chloroplastic pool. Compartment specific flux and metabolite measurements would be needed to resolve this possibility, but these are technically challenging. Regardless of the two metabolite pool issue, it seems clear that the presence of FBA1 is still sufficient to mediate a normal rate of C- assimilation, at least in the conditions we used. It is interesting that the plant partitions less fixed carbon into starch. It is not clear exactly how this change in partitioning is brought about at the biochemical level, but it may represent the ‘cost’ of maintaining the Calvin-Benson Cycle.

The growth phenotype may be partly due to the lower starch level, leading to slower growth during the night. However, this is unlikely to be the full story, because in continuous light growth is not fully restored, like other starch biosynthesis mutants. It is likely that the loss of a major photosynthetic enzyme like FBA has a more complicated negative impact on growth (Suppl. Fig. 8). Our results coincide with suggestions in previous reports that FBA might have

an important role in controlling the flux over the cycle (Zhu et. al, 2007), but further experiments are necessary in the future for a final conclusion.

FBA3 is functional in non-photosynthetic tissues, mainly in the vasculature

Among the three single mutants, the *fba3* had the strongest reduction in growth and the biggest defect in development. However, in the shoot no significant decrease was detected in enzyme activity, and only a slightly decrease was detected in the root. *FBA3* has a very low expression compared to the other two genes, but one can speculate that this might be explained if it is expressed in specific cell types. Most of the measured metabolites were decreased and *fba3* had a constant lower carbon assimilation and respiration implying that the wild-type, indicating that the whole of metabolism in *fba3* might be somehow suppressed. On the other hand, starch and neutral sugar (glucose, fructose, sucrose) levels were extremely high and no diel changes were observed. Although most of the metabolite had a lower level in *fba3* compared to the wild type, there was a few exception. While adenine had an elevated concentration, the content of its derivatives was very low. Although there is available adenine, the plant produces little of the energy-rich molecules (i.e. ATP) or cofactors (i.e. NADH, FAD) required to drive other metabolic processes. It might be that *fba3* is unable to synthetize these cofactors. Alternatively *fba3* may be able to synthetize them but, because metabolism is only partially functioning and the cofactors cannot be used, that their synthesis might be downregulated.

All the data on *fba3* suggest that the plant has available resources in terms of carbohydrates, energy and reducing power, but fails to invest them into growth and development. As FBA3 is expressed in the transport tissues from the veins of the leaves down to the roots, we speculated a role in assimilate transport, whereby the mutation of FBA3 alters plastid metabolism in the transport tissues and in some way hinders assimilate export from the source tissues. This could explain the high sugars and starch as a build-up of photoassimilates that cannot reach the sink tissues. The major site of the problem seems to be in the leaf at the site of phloem loading, because in our grafting experiment, when a wild-type shoot was put onto an *fba3* root, it restored the growth of the mutant root. However, the reverse combination (*fba3* shoot grafted onto a wild-type root) resulted in the reduction in root growth.

Mutants of sucrose transporters specific to the bundle sheath cells or phloem cells showed a similar carbohydrate-accumulating phenotype (i.e. high starch and sugar content in the leaves) (Chen et. al, 2012), supporting this hypothesized role for FBA3. One can speculate that FBA3 might be expressed in these cell types and/or other cells whose function is required for efficient functioning of the vasculature. One result points to the fact that FBA may have a broader role in the plants' physiology. In contrast to the *sweet11sweet12* double mutant (Chen et. al, 2012), *fba3* growth cannot be rescued completely with external sugar supplemented into the growth media. A small amount of additional sugar promoted growth slightly, but an increased concentration was inhibitory to *fba3* root growth. This suggests that the plants cannot effectively metabolize the exogenously provided sucrose.

Conclusion and future perspectives

In conclusion, the FBA1 and FBA2 plastidial isoforms function in the Calvin-Benson cycle. FBA1 is less abundant and less important than FBA2, which is probably the major isoform in the cycle. While FBA1 and FBA2 is active in the green photosynthesizing tissues, FBA3 has a crucial role in the vasculature ensuring the transport of carbon from source to sink tissues. The specific process that is compromised by the loss of FBA3 is not clear yet; targeted biochemical experiments will be needed to elucidate its role. FBA2 could be also a good target for further analysis of the flux regulation through the Calvin-Benson cycle. Although FBA1 seems less important, it is not completely inactive and there might be conditions (i.e. stress), where its contribution to the plant physiology might not be more relevant.

Reference

Abascal, F., Zardoya, R., Posada, D., (2005). ProtTest: Selection of best-fit models of protein evolution. *Bioinformatics* 21, 2104–2105.

Arrivault, S., Guenther, M., Ivakov, A., Feil, R., Vosloh, D., Van Dongen, J.T., et al., (2009). Use of reverse-phase liquid chromatography, linked to tandem mass spectrometry, to profile the Calvin cycle and other metabolic intermediates in Arabidopsis rosettes at different carbon dioxide concentrations. *Plant Journal.* 59, 824–839.

Badeck, F.-W., Fontaine, J.-L., Dumas, F., Ghasghaie, J., (2009). Consistent patterns in leaf lamina and leaf vein carbon isotope composition across ten herbs and tree species. *Rapid Commun. Mass Spectrom.* 23, 2455–2460.

Baerenfaller, K., Hirsch-Hoffmann, M., Svozil, J., Hull, R., Russenberger, D., Bischof, S., et al., (2011). pep2pro: a new tool for comprehensive proteome data analysis to reveal information about organ-specific proteomes in *Arabidopsis thaliana*. *Integr. Biol.* 3, 225–237.

Bel, A. van, Knoblauch, M., (2000). Sieve element and companion cell: the story of the comatose patient and the hyperactive nurse. *Aust. J. Plant Physiol.* 27, 477–487.

Brooks, K., Criddle, R.S., (1966). Enzymes of the carbon cycle of photosynthesis. I. isolation and properties of spinach chloroplast aldolase. *Archives of Biochemistry and Biophysics.* 650–659.

Cai, B., Li, Q., Xu, Y., Yang, L., Bi, H., Ai, X., (2016). Genome-wide analysis of the fructose 1,6-bisphosphate aldolase (FBA) gene family and functional characterization of FBA7 in tomato. *Plant Physiol. Biochem.* 108, 251–265.

Calvin, M., (1962). The path of Carbon in Photosyntheis. *Angew. CHEMIE* I, 65–75.

Carrie, C., Kühn, K., Murcha, M.W., Duncan, O., Small, I.D., Toole, N., et al., (2009). Approaches to defining dual-targeted proteins in Arabidopsis. *Plant J.* 57, 1128–1139.

Caspar, T., Huber, S.C., Somerville, C., (1985). Alterations in growth, photosynthesis, and respiration in a starchless mutant of *Arabidopsis thaliana* (L.) deficient in chloroplast phosphoglucomutase activity. *Plant Physiology.* 79, 11–17.

Chen, L.-Q., Qu, X.-Q., Hou, B.-H., Sosso, D., Osorio, S., Fernie, A.R., et al., (2012). Sucrose efflux mediated by SWEET proteins as a key step for phloem transport. *Science (80-.).* 335, 207–212.

Clough, S.J., Bent, A.F., (1998). Floral dip: A simplified method for Agrobacterium-mediated transformation of Arabidopsis thaliana. *Plant J.* 16, 735–743.

Dietz, K.-J., Pfannschmidt, T., (2011). Novel Regulators in Photosynthetic Redox Control of Plant Metabolism and Gene Expression. *Plant Physiology.* 155, 1477–1485.

Egli, B., Kölling, K., Köhler, C., Zeeman, S.C., Streb, S., (2010). Loss of cytosolic phosphoglucomutase compromises gametophyte development in Arabidopsis. *Plant Physiology.* 154, 1659–71.

Flechner, A., Gross, W., Martin, W.F., Schnarrenberger, C., (1999). Chloroplast class I and class II aldolases are bifunctional for fructose-1,6-biphosphate and sedoheptulose-1,7-biphosphate cleavage in the Calvin cycle. *FEBS Lett.* 447, 200–202.

Garagounis, C., Kostaki, K.I., Hawkins, T.J., Cummins, I., Fricker, M.D., Hussey, P.J., et al., (2017). Microcompartmentation of cytosolic aldolase by interaction with the actin cytoskeleton in Arabidopsis. *J. Exp. Bot.* 68, 885–898.

Gibon, Y., (2004). A robot-based platform to measure multiple enzyme activities in Arabidopsis using a set of cycling assays: comparison of changes of enzyme activities and transcript levels during diurnal cycles and in prolonged darkness. *Plant Cell* 16, 3304–3325.

Gottwald, J.R., Krysan, P.J., Young, J.C., Evert, R.F., Sussman, M.R., (2000). Genetic evidence for the in planta role of phloem-specific plasma membrane sucrose transporters. *Proc. Natl. Acad. Sci.* 97, 13979–13984.

Haake, V., Zrenner, R., Sonnewald, U., Stitt, M., (1998). A moderate decrease of plastid aldolase activity inhibits photosynthesis, alters the levels of sugars and starch, and inhibits growth of potato plants. *Plant Journal* 14, 147–57.

Hough, L., Jones, J.K.N., (1953). The synthesis of sugars from simpler substances. Part V.* Enzymic synthesis of sedoheptulose. *J. Chem. Soc.* 413–417.

Kalve, S., Saini, K., Vissenberg, K., Beeckman, T., Beemster, G.T.S., (2015). Transverse sectioning of *Arabidopsis thaliana* leaves using resin embedding. *Bio-Protocol* 5, 1–5.

Katoh, K., Standley, D.M., (2013). MAFFT multiple sequence alignment software version 7: Improvements in performance and usability. *Mol. Biol. Evol.* 30, 772–780.

Kölling, K., George, G.M., Künzli, R., Flütsch, P., Zeeman, S.C., (2015). A whole - plant chamber system for parallel gas exchange measurements of Arabidopsis and other herbaceous species. *Plant Methods* 1–12.

Lebherz, H.G., Leadbetter, M.M., Bradshaw, R.A., (1984). Isolation and characterization of the cytosolic and chloroplast forms of spinach leaf fructose diphosphate aldolase. *J. Biol. Chem.* 259, 1011–1017.

Lee, T.H., Tang, H., Wang, X., Paterson, A.H., (2013). PGDD: A database of gene and genome duplication in plants. *Nucleic Acids Res.* 41, 1152–1158.

Liebers, M., Grübler, B., Chevalier, F., Lerbs-Mache, S., Merendino, L., Blanvillain, R., et al., (2017). Regulatory shifts in plastid transcription play a key role in morphological conversions of plastids during plant development. *Front. Plant Sci.* 8, 1–8.

Linko, P., Holm-Hansen, O., Bassham, J.A., Calvin, M., (1957). Formation of radioactive citrulline during photosynthetic $C^{14}O_2$-fixation by blue-green algae. *At. Energy* 8, 147–156.

Liu, X.L., Yu, H.D., Guan, Y., Li, J.K., Guo, F.Q., (2012). Carbonylation and loss-of-function analyses of SBPase reveal its metabolic interface role in oxidative stress, carbon assimilation, and multiple aspects of growth and development in Arabidopsis. *Mol. Plant* 5, 1082–1099.

Lu, W., Tang, X., Huo, Y., Xu, R., Qi, S., Huang, J., et al., (2012). Identification and characterization of fructose 1,6-bisphosphate aldolase genes in Arabidopsis reveal a gene family with diverse responses to abiotic stresses. *Gene* 503, 65–74.

Lv, G., Guo, X., Xie, L.-P., Xie, C., Zhang, X., Yang, Y., et al., (2017). Molecular characterization, gene evolution, and expression analysis of the fructose-1, 6-bisphosphate aldolase (FBA) gene family in wheat (*Triticum aestivum* L.). *Front. Plant Sci.* 8, 1–18.

Melnyk, C.W., (2017). Grafting with *Arabidopsis thaliana*. *Plant Horm. Methods Protoc. Methods Mol. Biol.* 1497, 9–18.

Metsalu, T., Vilo, J., (2015). ClustVis: A web tool for visualizing clustering of multivariate data using Principal Component Analysis and heatmap. *Nucleic Acids Res.* 43, W566–W570.

Michelet, L., Zaffagnini, M., Morisse, S., Sparla, F., Pérez-Pérez, M.E., Francia, F., et al., (2013). Redox regulation of the Calvin-Benson cycle: something old, something new. *Front. Plant Sci.* 4, 470.

Muñoz-Bertomeu, J., Cascales-Miñana, B., Mulet, J.M., Baroja-Fernández, E., Pozueta-Romero, J., Kuhn, J.M., et al., (2009). Plastidial glyceraldehyde-3-phosphate dehydrogenase deficiency leads to altered root development and affects the sugar and amino acid balance in Arabidopsis. *Plant Physiology.* 151, 541–558.

Murphy, D.J., Walker, D.A., (1981). Aldolase from wheat leaves-its properties and subcellular distribution. *FEBS Lett.* 134, 163–166.

Née, G., Zaffagnini, M., Trost, P., Issakidis-Bourguet, E., (2009). Redox regulation of chloroplastic glucose-6-phosphate dehydrogenase: A new role for f-type thioredoxin. *FEBS Lett.* 583, 2827–2832.

Penhoet, E.E., Kochmant, M., Rutteri, W.J., Kochman, M., Rutter, W.J., (1969). Molecular and Catalytic Properties of aldolase C. *Biochemistry* 8, 4396–4402.

Portis, A., (2003). Rubisco activase - Rubisco's catalytic chaperone. *Photosynth. Res.* 75, 11–27.

Raines, C., (2011). Increasing Photosynthetic Carbon Assimilation in C3 Plants to Improve Crop Yield: Current and Future Strategies. *Plant Physiology* 155, 36–42.

Raines, C.A., (2003). The Calvin cycle revisited 1–10.

Riesmeier, J.W., Flügge, U.I., Schulz, B., Heineke, D., Heldt, H.W., Willmitzer, L., et al., (1993). Antisense repression of the chloroplast triose phosphate translocator affects carbon partitioning in transgenic potato plants. *Proc. Natl. Acad. Sci. U. S. A.* 90, 6160–6164.

Simkin, A.J., Lopez-Calcagno, P.E., Davey, P.A., Headland, L.R., Lawson, T., Timm, S., et al., (2016). Simultaneous stimulation of the SBPase, FBP aldolase and the photorespiratory GDC-H protein increases CO2 assimilation, vegetative biomass and seed yield in Arabidopsis. *Plant Biotechnol. J.* 1–12.

Simkin, A.J., McAusland, L., Headland, L.R., Lawson, T., Raines, C.A., (2015). Multigene manipulation of photosynthetic carbon assimilation increases CO_2 fixation and biomass yield in tobacco. *J. Exp. Bot.* 66, 4075–90.

Smith, A.M., Zeeman, S.C., (2006). Quantification of starch in plant tissues. *Nat. Protoc.* 1, 1342–1345.

Stitt, M., Lunn, J., Usadel, B., (2010). Arabidopsis and primary photosynthetic metabolism - More than the icing on the cake. *Plant J.* 61, 1067–1091.

Stitt, M., Zeeman, S.C., (2012). Starch turnover: Pathways, regulation and role in growth. *Curr. Opin. Plant Biol.* 15, 282–292.

Tamoi, M., Nagaoka, M., Miyagawa, Y., Shigeoka, S., (2006). Contribution of fructose-1,6-bisphosphatase and sedoheptulose-1,7- bisphosphatase to the photosynthetic rate and carbon flow in the Calvin cycle in transgenic plants. *Plant Cell Physiol.* 47, 380–390.

Tamura, K., Stecher, G., Peterson, D., Filipski, A., Kumar, S., (2013). MEGA6: Molecular evolutionary genetics analysis version 6.0. *Mol. Biol. Evol.* 30, 2725–2729.

Uematsu, K., Suzuki, N., Iwamae, T., Inui, M., Yukawa, H., (2012). Increased fructose 1,6-bisphosphate aldolase in plastids enhances growth and photosynthesis of tobacco plants. *J. Exp. Bot.* 63, 3001–9.

Vidi, P.-A., Kanwischer, M., Baginsky, S., Austin, J.R., Csucs, G., Dörmann, P., et al., (2006). Tocopherol cyclase (VTE1) localization and vitamin E accumulation in chloroplast plastoglobule lipoprotein particles. *J. Biol. Chem.* 281, 11225–34.

Weidner, M., Taupp, M., Hallam, S.J., (2010). Expression of Recombinant Proteins in the Methylotrophic Yeast *Pichia pastoris*. *J. Vis. Exp.* 1–5.

Winter, D., Vinegar, B., Nahal, H., Ammar, R., Wilson, G. V., Provart, N.J., (2007). An "electronic fluorescent pictograph" Browser for exploring and analyzing large-scale biological data sets. *PLoS One* 2, 1–12.

Zhu, X.-G., de Sturler, E., Long, S.P., (2007). Optimizing the Distribution of Resources between Enzymes of Carbon Metabolism Can Dramatically Increase Photosynthetic Rate: A Numerical Simulation Using an Evolutionary Algorithm. *Plant Physiology* 145, 513–526.

Zimmermann, P., Hirsch-Hoffmann, M., Hennig, L., Gruissem, W., (2004). GENEVESTIGATOR. Arabidopsis Microarray Database and Analysis Toolbox. *Plant Physiology* 136, 2621–2632.

Supplementary information

(%)	*FBA1*	*FBA2*	*FBA3*
FBA1	100		
FBA2	94.9	100	
FBA3	84.8	85	100

Supplementary Table 4-1. Similarity of the plastidial FBA proteins

genotype	leaf area	fresh weight (g)	dry weight (g)	FW/DW
fba1-1	6.961 ±1.191	0.168 ± 0.021	0.015 ± 0.002	11.50
fba1-2	7.493 ±1.908	0.205 ± 0.051	0.019 ± 0.004	11.09
fba2-1	1.421 ± 0.187	0.028 ± 0.005	0.003 ± 0.001	9.70
fba2-2	1.209 ± 0.226	0.023 ± 0.005	0.002 ± 0.001	11.28
fba3-1	0.476 ± 0.056	0.012 ± 0.002	0.002 ± 0.001	7.55
fba3-2	1.395 ± 0.372	0.022 ± 0.003	0.003 ± 0.001	8.09
Col-0	7.351 ± 1.499	0.171 ± 0.046	0.015 ± 0.004	11.42
L*er*	7.416 ± 1.510	0.187 ± 0.050	0.017 ± 0.005	11.03

Supplementary Table 4-2. Leaf area, fresh weight and dry weight of every plastidial FBA homozygous single T-DNA knock-out mutant lines.

%	n=268	*FBA2*		
		FBA2FBA2	***fba2FBA2***	***fba2fba2***
	FBA1FBA1	11.2	11.9	5.2
FBA1	***fba1FBA1***	18.7	34	3
	fba1fba1	7.1	8.6	0.4

Supplementary Table 4-3. Segregation rate of the F2 generation of the *fba1fba2* double mutant

Metabolite	*fba1*	*fba2*	*Col-0*	*fba3*	*Ler*
Adenin	32.11	29.32	28.00	138.58	18.88
ADP	925.79	829.25	1128.91	96.82	737.00
ADP-Glucose	52.09	29.11	68.20	21.75	47.94
AMP	697.27	466.68	612.88	115.89	360.80
Arginine	829.40	583.97	143.00	815.63	309.57
Asparagine	9084.20	12014.50	14300.00	2129.33	5662.92
Aspartate	21592.89	14114.50	43306.00	4296.33	9790.57
ATP	2170.56	3066.00	4896.78	786.37	3220.67
Citrate	194911.11	232716.67	254700.00	4091.33	283900.00
DHAP	1590.33	7653.33	1259.22	117.42	941.91
FAD	87.34	94.44	93.71	51.37	104.89
Fructose-1,6-Bisphosphate	1653.78	1688.83	1615.56	1418.67	1445.78
Fructose-6-Phosphate	2861.44	3031.83	3056.78	830.70	2645.00
Fumarate	527.20	99.33	689.59	222.57	137.36
Glucose-1-Phosphate	502.83	604.38	599.68	374.77	472.50
Glucose-6-Phosphate	3742.67	4211.00	3517.00	173.94	1847.89
Glutamate	101248.89	52126.67	130088.89	75450.00	112352.22
Glutamine	58379.11	221479.17	64923.11	7724.00	43199.56
Glyceraldehyde-3-Phosphate	81.09	274.50	68.50	24.56	44.62
Glycerate	3810.00	2642.67	4199.11	3541.00	5128.78
Histidine	437.83	2004.00	338.04	309.13	264.31
Isocitrate	2524.00	3637.17	4652.33	1558.00	3913.67
Isoleucine	581.59	717.98	725.61	891.73	594.82
Ketoglutarate	2051.33	1428.50	4055.78	1055.67	3335.78
Lactate	3870.11	5221.50	3506.33	10631.67	3471.00
Leucine	542.62	1782.17	610.13	681.83	481.62
Malate	1354.07	173.23	876.68	206.97	197.42
Methionine	884.26	1140.18	827.08	845.93	1173.00
NAD	688.98	664.68	796.36	656.57	859.71
NADH	25.21	62.36	32.56	4.44	54.09
NADP	206.82	168.33	169.59	5.37	78.46
NADPH	265.29	352.54	422.03	5.02	155.71
PEP	44.92	16.65	33.90	1.32	9.89
Phenylanaline	1740.67	2734.50	1600.44	909.47	1243.21
Proline	5829.11	6171.83	4280.22	33337.00	14624.06
Pyruvate	3623.33	4867.67	4708.22	2558.67	4561.67
Ribose-1,5-Bisphosphate	1055.27	919.52	996.84	807.70	881.17
Ribose-5-Phosphate	229.97	142.52	221.44	45.65	223.19
Ribulose-5-Phosphate	1163.09	436.62	1229.10	591.20	1411.56
Sedoheptulose-7-Phosphate	2025.22	1553.17	2330.67	297.01	1778.89
Serine	8259.27	7675.33	19129.51	2803.00	15999.83
Shikimate	820.42	1290.50	934.46	652.97	810.83

Succinate	2263.22	2996.17	8417.78	8774.00	4673.89
Threonine	4609.87	3853.92	8814.89	1403.90	5188.23
Tryptophan	192.28	262.70	208.96	292.80	206.26
Tyrosine	163.54	261.08	167.10	324.20	188.74
UDP-Glucose	2907.22	2345.67	3293.33	1352.00	2239.56
Uracil	5.43	26.08	6.83	4.01	0.73
Uridine	96.67	147.97	119.49	514.70	148.39
Xylose-5-Phosphate	164.59	148.62	175.74	71.06	148.43

Supplementary Table 4-4. Concentration (nmol/g FW) of the metabolomic measurement of the *fba1*, *fba2*, *fba3* and the respective controls. Concentration values highlighted in red stand for significant changes (p≤0.05) compared to their respective wild type.

Name		Primer sequence
fba1-1 LB	SALK_063223	TTGTTGGGAATTGTCGATTTC
fba1-1 RB	SALK_063223	CTTGTTGGTAGTAAGCAGCGG
	TDNA (SALK LBB4)	GCGTGGACCGCTTGCTGCAACT
fba1-2 LB	SAIL_752_G05C	GCTCGCTACGCAGCTATTTC
fba1-2 RB	SAIL_752_G05C	TTTTGAGCTCAGAGAGCATAATGT
	TDNA (SAIL LB1)	GCCTTTTCAGAAATGGATAAATAGCCTTGCTTCC
fba2-1 LB	SALK_000898	TCCATCCAACAAGATCTCTGG
fba2-1 RB	SALK_000898	TGTTCTGTTTTGCCCTGTTTC
	TDNA (SALK LBB4)	GCGTGGACCGCTTGCTGCAACT
fba2-2 LB	SALK_073444	GTGCCTTTTGAATGGGAATG
fba2-2 RB	SALK_073444	CAAGTTGAGTGTTGCCTCC
	TDNA (SALK LBB4)	GCGTGGACCGCTTGCTGCAACT
fba3-1 LB	GT12795.Ds5	GTGCTTACTCCGACGAGCTT
fba3-1 RB	GT12795.Ds5	CGTTGTTCTGTGCCAAGTAG
	TDNA (Ds5-4)	TACGATAACGGTCGGTACGG
fba3-2 LB	SALK_092715	TCGTTTTGCCAAGTGGTATG

fba3-2 RB	SALK_092715	GAGAGAACGAGGATGCCAAG
	TDNA (SALK LBB4)	GCGTGGACCGCTTGCTGCAACT

Supplementary Table 4-5. Primers for the genotyping of the *fba* homozygous single knock-out mutants. Primers were designed upstream (left border (LB)) and downstream (right border (RB)) of the insertion together with the TDNA specific primer.

Gene	Name	Sequence
FBA1	AT2G21330_FW01	GAAGGTATTCTCCTGAAGCCA
FBA1	AT2G21330_RV01	CACCAGACAAGAACATGATTCC
FBA2	AT4G38970_FW01	TGTCATGTTTGAAGGTATCCTC
FBA2	AT4G38970_RV01	TTCAAGTTGAGTGTTGCCTC
FBA3	AT2G01140_FW01	CAGAACATGGCAAGGCAAGC
FBA3	AT2G01140_RV01	TCCCTCGGCTGAGTATTTGC
YSL8	AT1G48370_FW	ATGACTGGGATGAGACCTGTATGC
YSL8	AT1G48370_RV	CATGGTGTTGAAGTCTGGAACCTC

Supplementary Table 4-6. Primer sequences of oligonucleotides to quantify the gene expression level of the respective FBA genes with quantitative reverse transcription PCR.

Name	Sequence
pr*FBA1*_FW01	GGGGACAACTTTGTATAGAAAAGTTGAGCGTTGTTTTCATGTTGGAG
pr*FBA1*_RV01	GGGGACTGCTTTTTTGTACAAACTTGTCGTGCTTTTCGGTGGTTTG
pr*FBA2*_FW01	GGGGACAACTTTGTATAGAAAAGTTGAGACGCAGCAGAGGTTTCTC
pr*FBA2*_RV01	GGGGACTGCTTTTTTGTACAAACTTGCCTTATCTCTCACTCCTCCCTC
pr*FBA3*_FW01	GGGGACAACTTTGTATAGAAAAGTTGAAGATCTACCGAAAGCAAGG
pr*FBA3*_RV01	GGGGACTGCTTTTTTGTACAAACTTGATCACCTACTCCCACCACC
*FBA1*_CDS_FW01	GGGGACAAGTTTGTACAAAAAAGCAGGCTCCATGGCGTCAAGCACTGCGACTATG

*FBA1*_CDS_RV01	GGGGACCACTTTGTACAAGAAAGCTGGGTAGTAGGTGTAGCCTTTTACAAAC
*FBA2*_CDS_FW01	GGGGACAAGTTTGTACAAAAAAGCAGGCTCCATGGCATCAACCTCACTCCTCAAG
*FBA2*_CDS_RV01	GGGGACCACTTTGTACAAGAAAGCTGGGTAATAGGTGTACCCTTTGACGA
*FBA3*_CDS_FW01	GGGGACAAGTTTGTACAAAAAAGCAGGCTCCATGGCGTCTGCTAGCTTCGTTAAG
*FBA3*_CDS_RV01	GGGGACCACTTTGTACAAGAAAGCTGGGTAGTAGGTGTAACCCTTGACAAAC

Supplementary Table 4-7. Primer sequences of oligonucleotides with gateway recombinant sites used for amplification of the respective FBA promoter and coding sequences sequence.

Name	Sequence
FBA1ch fw EcoR1	GAATTCATGGCTTCTGCTTACGCCGATGAG
FBA1ch rv NotI	GCGGCCGCTGTAGGTGTAGCCTTTTACAAAC
FBA2ch fw EcoR1	GAATTCATGGCCGCTTCCTCCTACGCCGA
FBA2ch rv NotI	GCGGCCGCTATAGGTGTACCCTTTGACGAAC
FBA3ch fw EcoR1	GAATTCATGGCCGGTGCTTACTCCGACGAG
FBA3ch rv NotI	GCGGCCGCTGTAGGTGTAACCCTTGACAAAC

Supplementary Table 4-8. Primer sequences of oligonucleotides used for amplification of the plastidial FBA protein chains without their chloroplast transit peptides. The forward primers were designed with EcoR1, the reverse primers with Not1 restrictions sites.

Time [min]	Flow rate [ul/min]	%A	%B
0	400	100	0
5	400	100	0
10	400	98	2
11	350	91	9
16	250	91	9
18	250	75	25
19	150	50	50
25	150	50	50
26	150	100	0
32	400	100	0
40	400	100	0

Supplementary Table 4-9. Gradients for anion exchange chromatography step.

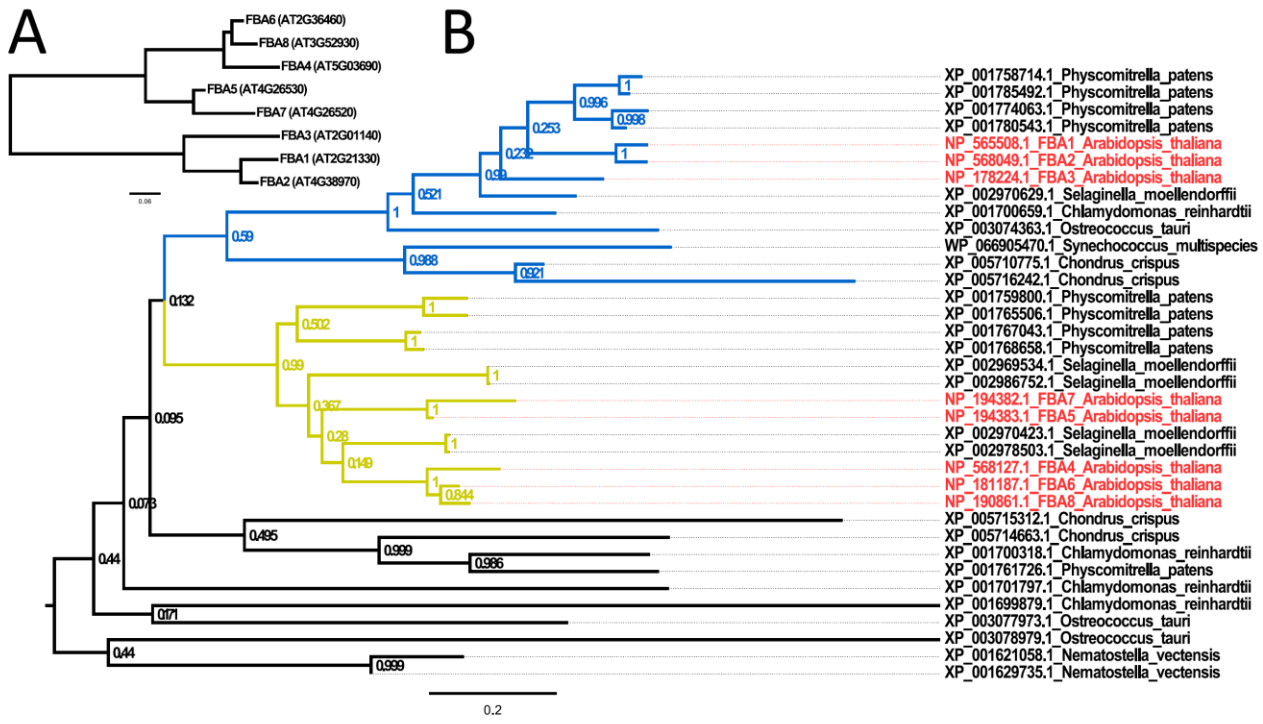

Supplementary Figure 4-1. A) Phylogenetic tree of the Arabidopsis FBA proteins (NP_565508.1, NP_568049.1, NP_178224.1, NP_568127.1, NP_194383.1, NP_181187.1, NP_194382.1, NP_190861.1). B) Maximum likelihood phylogenetic tree with Bootstrap values of the FBA proteins from green algae, mosses, higher plant species and one Metazoan species. The *Arabidopsis thaliana* proteins are shown in red.

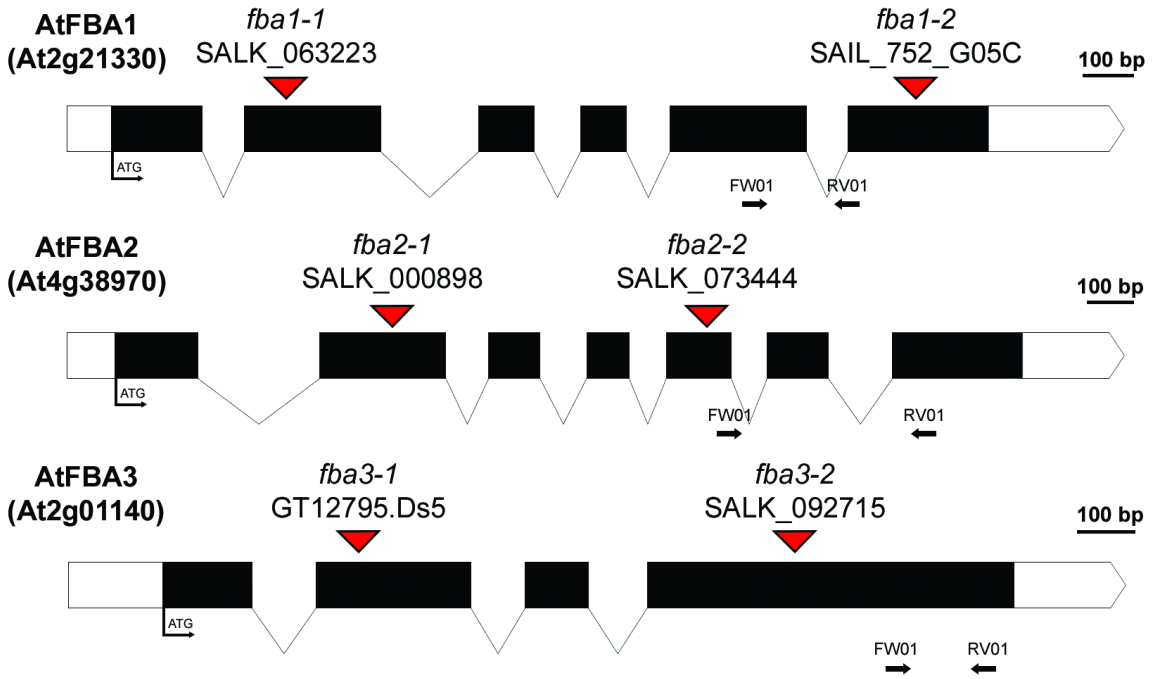

Supplementary Figure 4-2. Exon-intron structure of the plastidial FBA genes with the location of the T-DNA insertions. Black and white rectangulars represent the exons and the UTR regions respectively and two exons are connected with introns represented as single lines. Red arrows pointing the location of the insertions and the black arrows are the primers used for quantitative gene expression measurements.

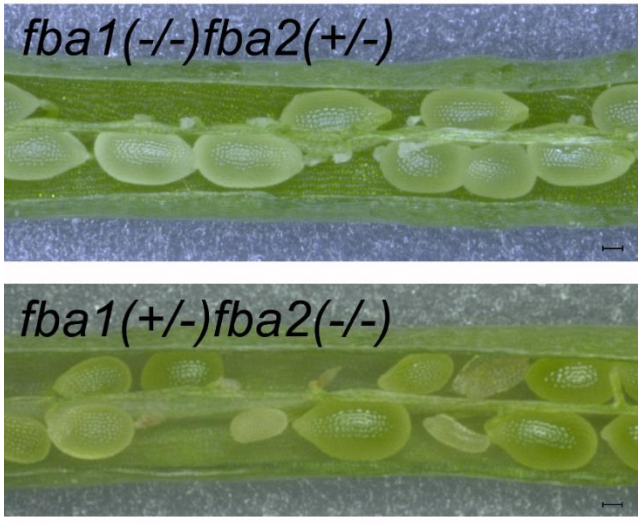

Supplementary Figure 4-3. Opened siliques and aborted seeds of A) *fba1*$^{(-/+)}$*fba2*$^{(-/-)}$ and B) *fba1*$^{(-/+)}$*fba2*$^{(-/-)}$. The scale bar represents 500 µm.

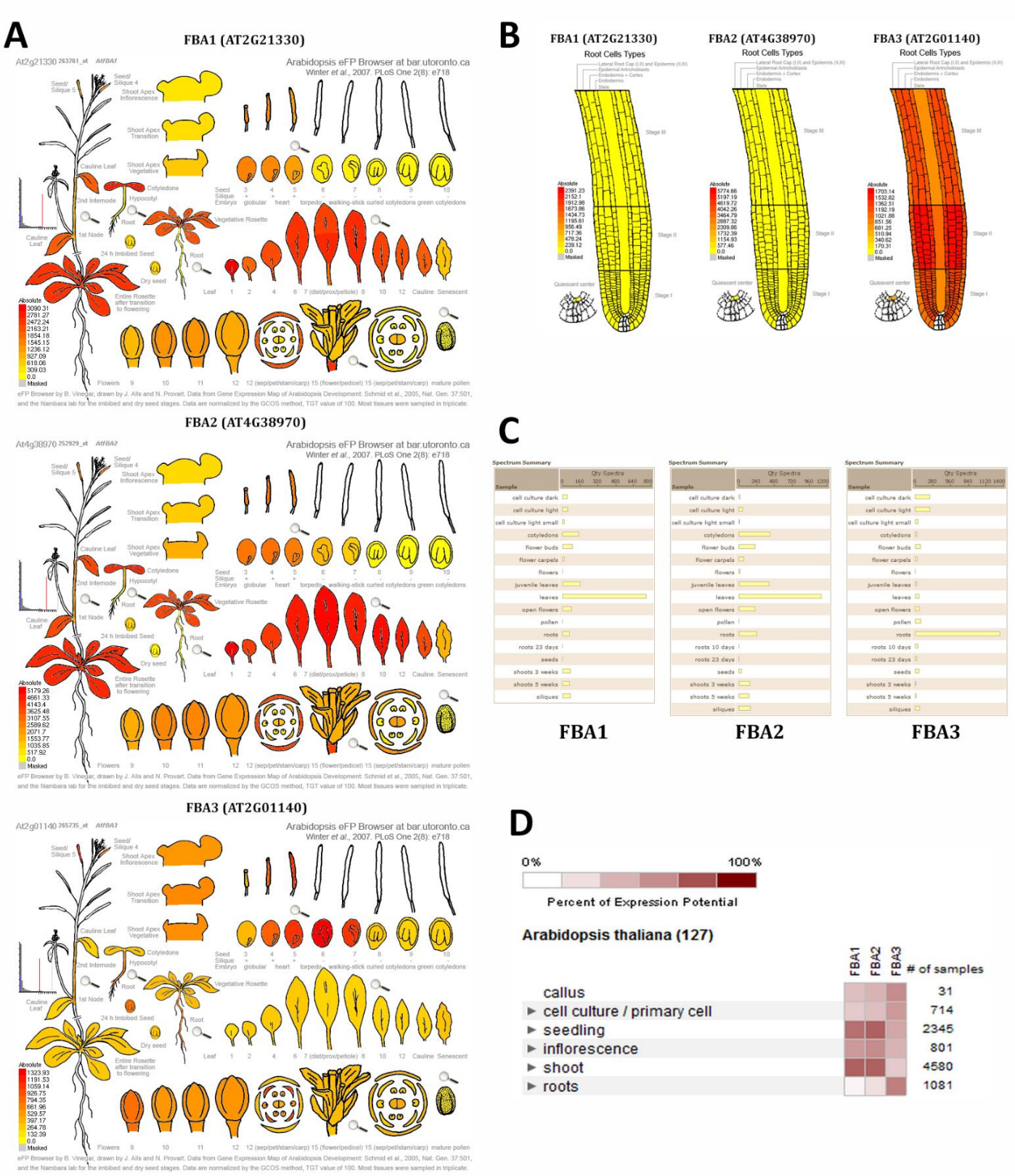

Supplementary Figure 4-4. Expression and protein level of FBA1, FBA2 and FBA3 throughout the plant. A) Expression level in the shoot and the reproductive tissues B) Expression level in the root. (Arabidopsis eFP browser (Winter et al. 2007)). C) Number of identified peptides detected in proteomic experiment (pep2pro ((Baerenfaller et. al, 2011)). D) Expression level in different tissues (Genevestigator)

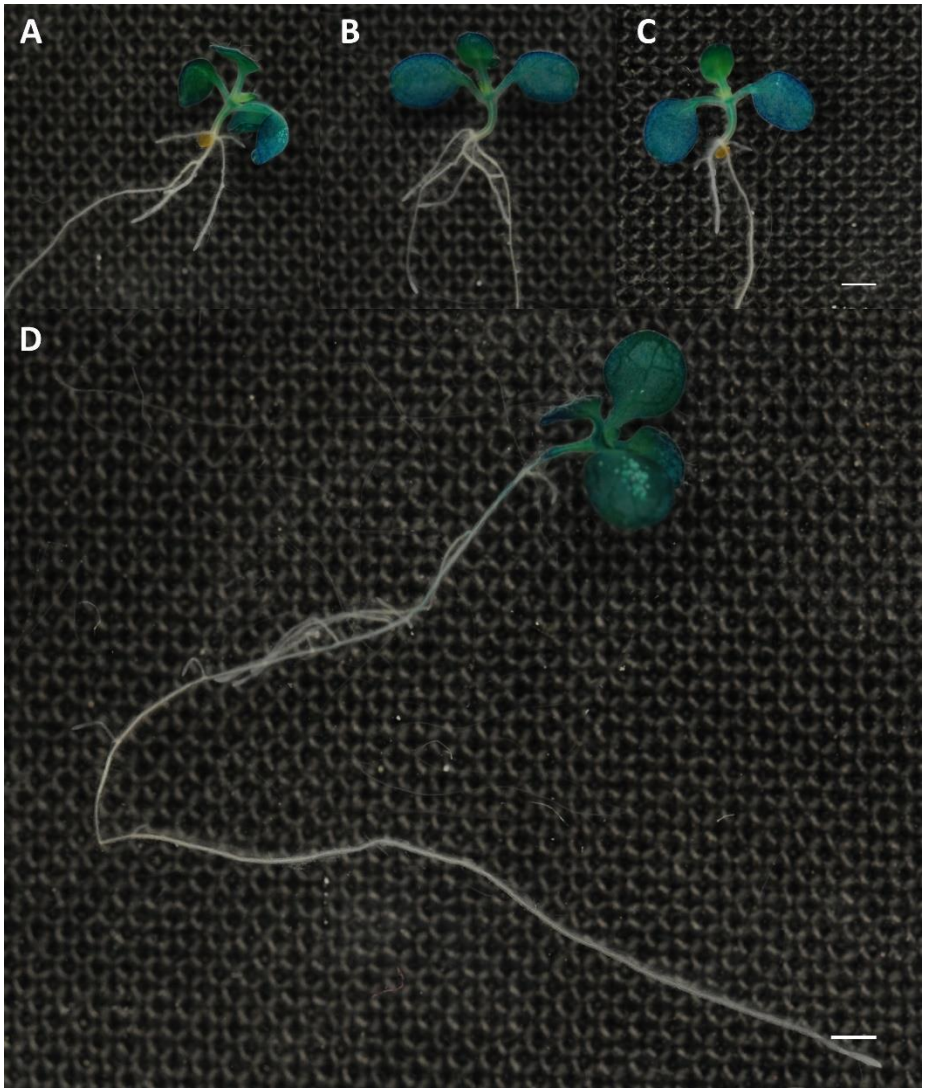

Supplementary Figure 4-5. Localization of FBA1 and FBA2 throughout the plant. Staining of seedling plants transformed with *FBA1$_{pro}$::GUS* (A, B, C) and *FBA2$_{pro}$::GUS* (D).

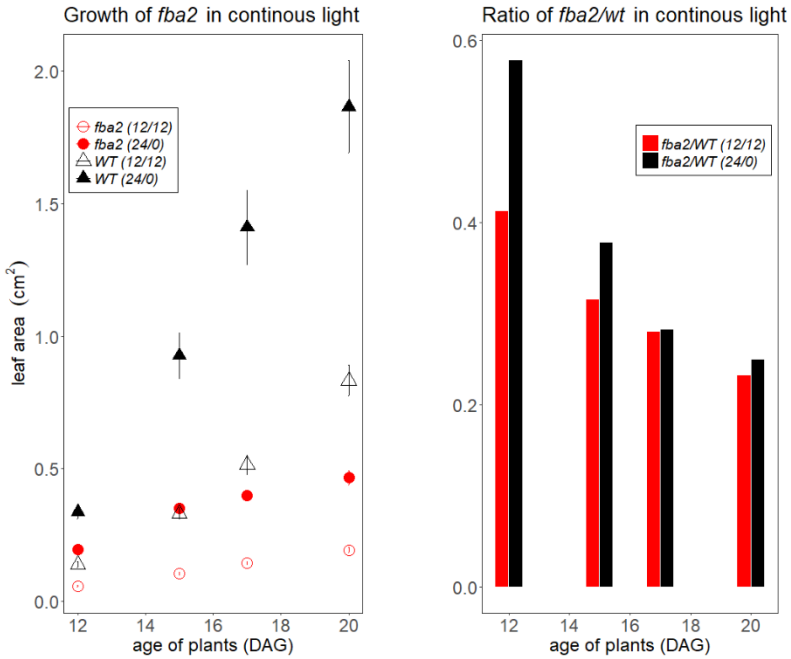

Supplementary Figure 4-6. Growth of *fba2* single mutants in continuous light 12 days after germination (DAG). A) Leaf area and B) ratio of the *fba2* and *Col*-0 plants in 12h light and 12h dark and 24h light and 0h dark

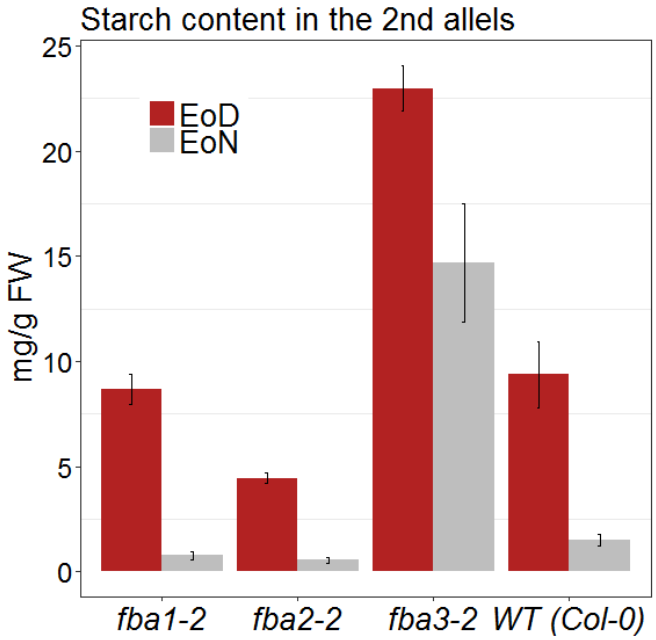

Supplementary Figure 4-7. Starch content in the *fba1-2*, *fba2-2*, *fba3-2* and *Col*-0 plants at the end of the day (EoD) and night (EoN)

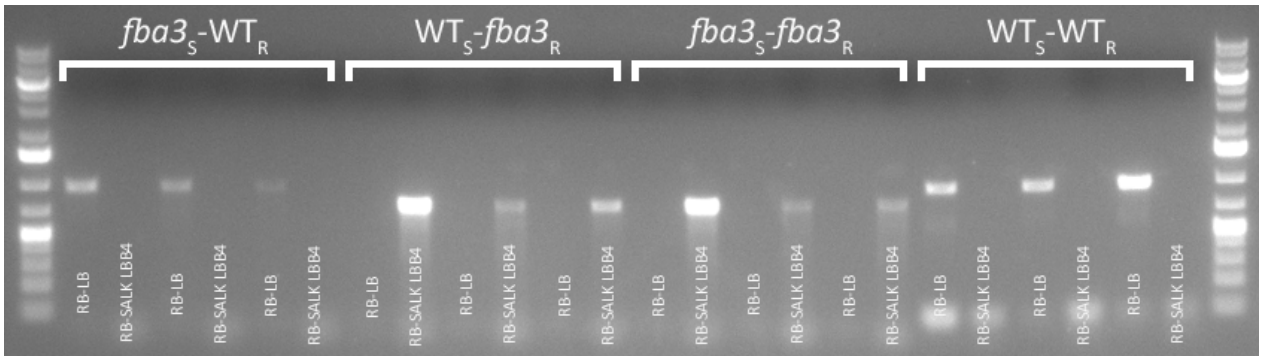

Supplementary Figure 4-8. Genotyping of the roots of the grafted wild type and *fba3* plants. Each root sample was amplified with the native FBA3 primer combination (right border (RB)-left border (LB)) and the RB and T-DNA specific LB primer.

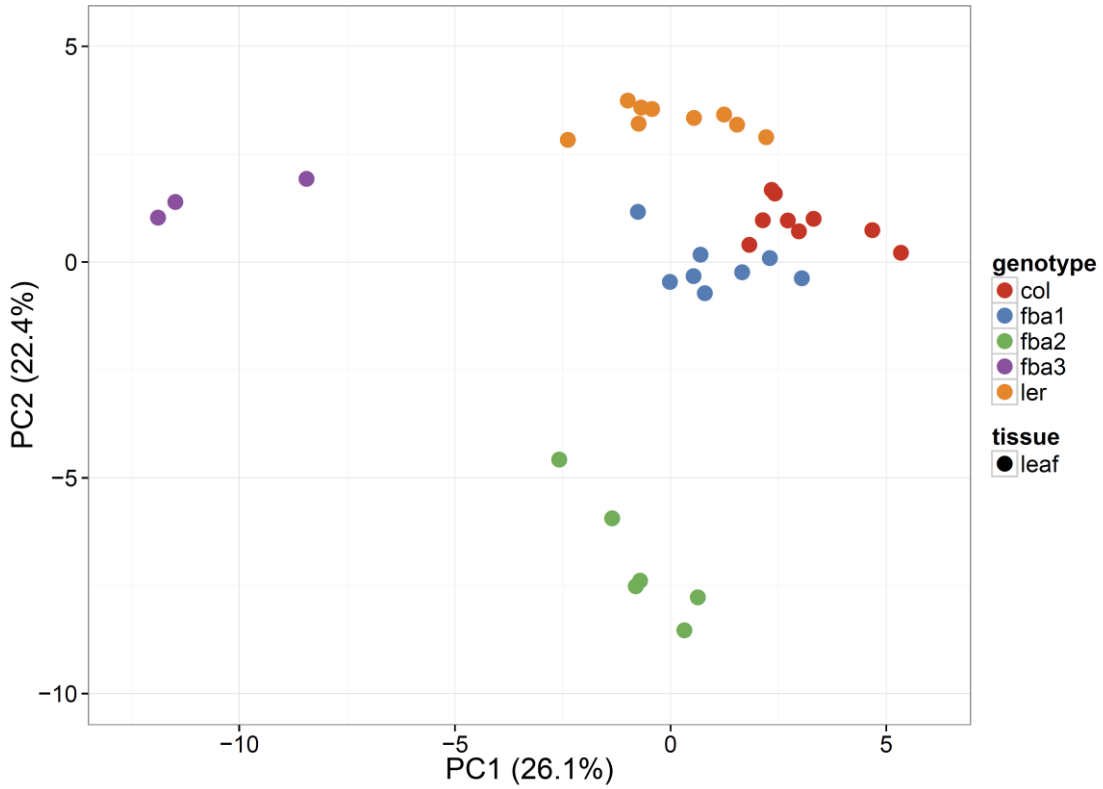

Supplementary Figure 4-9. PCA analysis of the metabolomic measurement of the *fba1-1*, *fba2-1* and *fba3-1* mutants with the respective wild types. The analysis was carried out with ClustVis (Metsalu and Vilo, 21015).

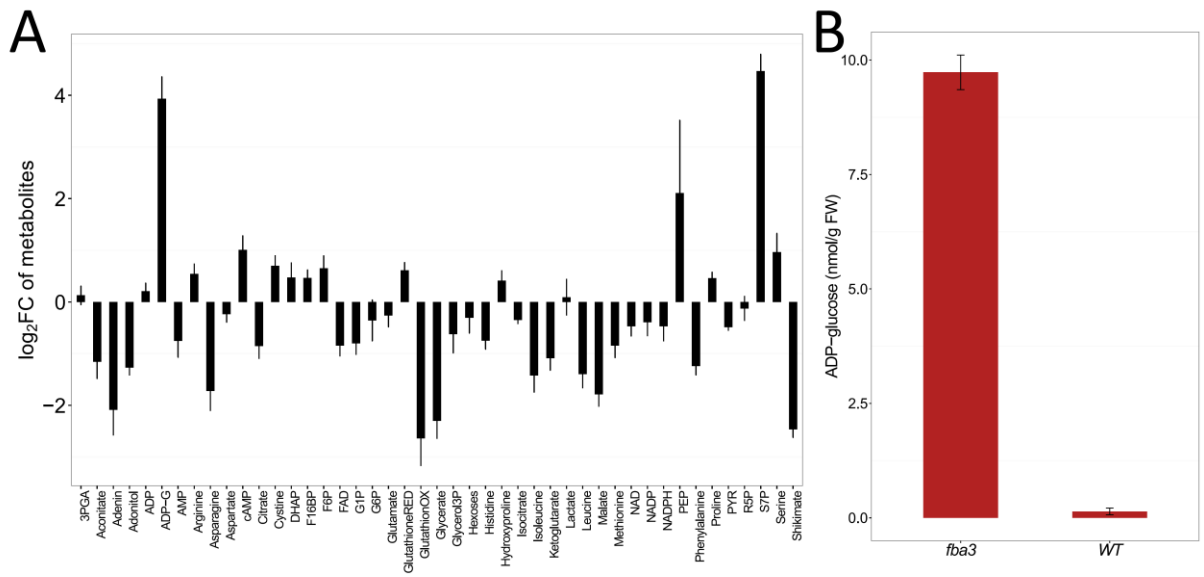

Supplementary Figure 10. Metabolomic analysis of *fba3-1* root. A) Metabolite level in *fba3-1* normalized to the wild type. The values were log_2-transformed. B) ADP-glucose absolute concentration in the root of *fba3-1*

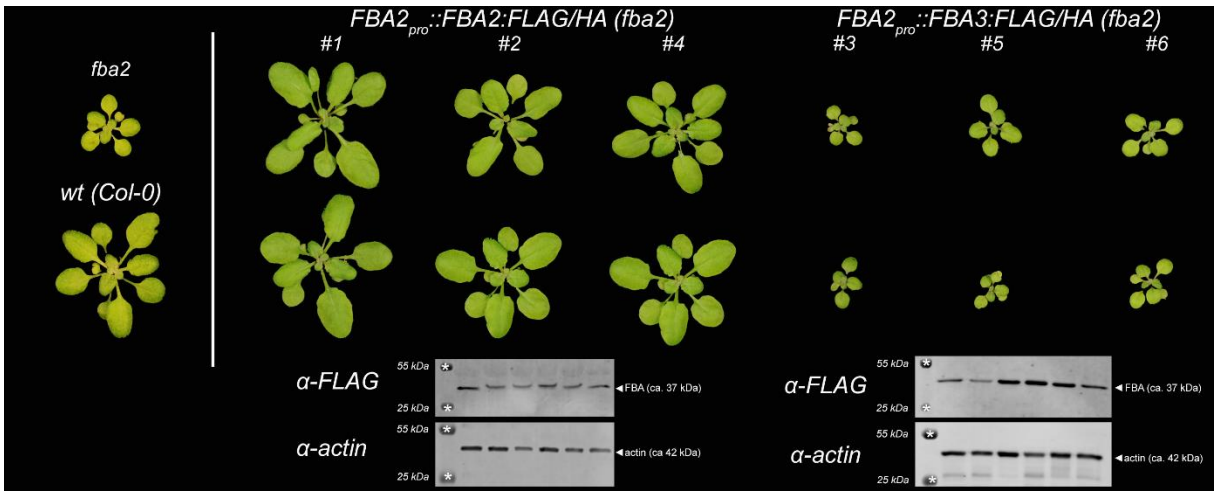

Supplementary Figure 4-11. Phenotype of three-three independent lines of *fba2* plants transformed with *FBA2$_{pro}$::FBA2:FLAG/HA* and *FBA2$_{pro}$::FBA3:FLAG/HA*. Expression of the FBA proteins (with a supposed weight of 37 kDa) detected with the antibody of the FLAG-tag and the level of expression of the actin protein (42 kDa).

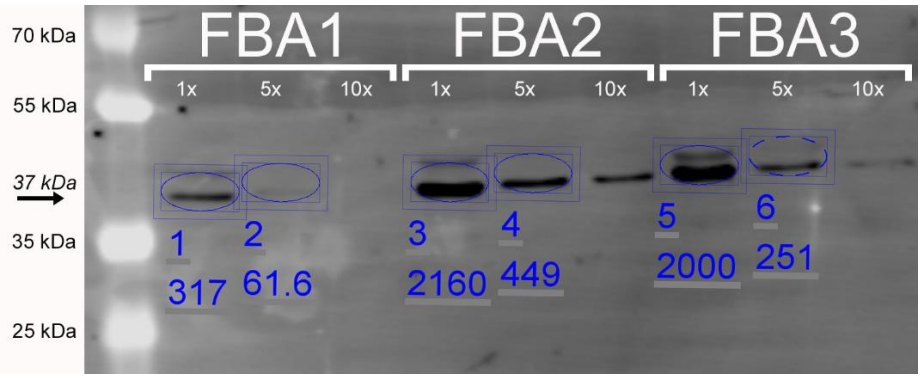

Supplementary figure 4-12. Detection and relative quantification of the pFBA recombinant proteins on western blot using α-Myc antibody. A dilution series (1x, 5x and 10x) of each pFBA was loaded onto the SDS-PAGE. The approximate size of the pFBA proteins without cTP is 37 kDa. The relative quantity was calculated with LI-COR Image Studio Lite image analysis software.

5) General Discussion and Outlook

Two of the major characteristics of the terrestrial plants are that they are sessile and autotrophic organisms. The production of complex organic compounds provides them enough supply for growth and development and the necessary driving energy is derived from the sunlight. They do not rely on other living organisms as a source of energy, linking the sessile lifestyle and photosynthetic capability deeply together. Atmospheric carbon dioxide is fixated through the Calvin-Benson cycle, the initial carboxylating reaction step in the cycle is catalyzed by the RuBisCO, which is the most abundant protein on the planet. The incorporated carbon is first partitioned mainly into starch or sucrose. Starch serves as a storage and sucrose is transported throughout the plant supplying carbon and energy from the photosynthesizing source tissues to the sink tissues. The primary carbohydrate metabolism establishes entry points for further metabolic processes too.

The focus of this work was the Calvin-Benson cycle in the chloroplast and the cytosolic sucrose metabolism. These complex and interconnected networks consist of several metabolic steps, which are catalyzed by different enzymes. There is a high frequency of redundancy, genome sequencing and the subsequent annotations revealed that multiple genes exist for most of these metabolic reactions. While the biochemical basics of these reactions are relatively well-described, the role of most of the different isoforms are still unclear. The number of different isoforms ranges from one (e.g. F2KP) to 17 (e.g. sucrose invertases) or more. I aimed to unravel the function of the numerous isoforms and identify key proteins of the primary carbohydrate metabolism and, if possible, attribute them new function.

Internal or external perturbations and limitations impact the carbohydrate metabolism directly or indirectly. Therefore, in the beginning of my PhD research, two approaches were combined: a stress-proteomic experiment was carried out and a single homozygous knock-out mutant library was created. These top-down approaches were followed by an in-depth characterization of selected gene families. Plants are robust systems, knocking out one isoform of a bigger gene family did often not result in visible or detectable changes in phenotype. Although a complete knock-out of a gene might not occur regularly in the nature, the duplication or multiplication of genes might provide a genetic protection against random mutations or malfunctioning protein folding. Increase in number of isoforms might also enable

the plant to fine-tune the enzyme amount or activity depending on the external stimuli, developmental stage and/or tissue localization. Due to their sessile lifestyle, plants cannot avoid actively the external damaging impacts, they are anchored to one location. Therefore, they have to adjust their metabolism, including the primary carbohydrate metabolism, to minimize the loss and the isoforms might have an important role in the adjusted physiology of the plants. Hence, a long-term moderate stress experiment was designed, where *Arabidopsis thaliana* plants were grown in hydroponic culture for 10 days under controlled moderate abiotic stress (15°C, 25°C, salt and osmotic) and in nutrient deficiency (deprivation of nitrate and phosphate), growth was monitored and proteomic experiments were performed at the end of the treatment. Through the hydroponic setup, I were able to monitor the specific changes of the proteome of the shoot and the root and carbohydrates (sugars and starch) were also measured in both tissues.

Different adapted strategies of the plants' stress response

The stress response was investigated on three physiological levels: proteome, metabolites and growth. The acclimation of plants to the different environmental changes was specific to the applied treatments, the changes of the proteome and growth pattern were quite distinct. There were differences in the carbohydrate metabolism of the plants among the stress experiments too, but it was difficult to link the changes in growth, proteome and metabolite level directly.

The application of several stress treatment and their direct comparison was enabled by the technological advances of the gel-free, single tube proteomic approach (Wisniewksi et al. 2009). The comparative analysis allowed us to raise the question, whether there is a core response, which might be regulated by masterregulators independently from the nature of the stress. Plants might sense the external stimuli, enhance several downstream signaling routes, but the actual stress responses to different treatments might converge into certain shared core pathways. Our proteomic analysis could not confirm this hypothesis, the overlap of the changed proteins was low, which might be a strong argument against a core stress response with a few masterregulator gene. The plants might have specific adapted evolutionary strategies and physiological tools to acclimate, tolerate and mitigate the effects of different stresses. However, I determined the proteomics status only at the end of a longer

(10 days) period of changed environmental conditions. It could be that the disturbance at the start of new conditions are regulated similarly by key fast responding regulators. At the stage of the newly established metabolic balance, these overlaps might have diminished and the plants established a unique and specific solution for the growth conditions. This differentiation between early transient response and late stable balance might also explain the observed discrepancies between experiments investigating plant responses to similar stresses. Studies investigating the response to similar environment changes, show regularly different results and propose alternate hypotheses. This is likely due to several factors, which are seldom identical between these studies (Dupae et. al, 2014). Special care has to be laid on in future experiments to use the same developmental stage of plants, the same treatment, same treatment length, same methodology to measure changes. The last is especially important, because results from proteomics approaches are difficult to compare with transcriptional approaches, which are again often influenced by diurnal changes.

Phospholipid metabolism linked to the stress response

There might not be a universal stress response in the plants, nevertheless, there are cellular components and/or organelles, which are almost always affected by external stimuli. Cell membranes might be one of them, they must be constantly protected and maintained, the integrity of the them are crucial, damaged membranes can be fatal for the cells. It is also one of the location of sensing the stimuli and any osmotic changes affect the membranes directly. The N-Methyltransferase 1 (NMT1, At3g18000) is a key protein in phospholipid biosynthesis, which is essential for the construction of eukaryotic cell membranes (BeGora et. al, 2010; Eastmond et. al, 2010). It was one of the few proteins, which was found in several treatment, and it was the only one, which had a significantly high fold change in five (out of the six) different stress experiment. Interestingly, the one exception was the osmotic treatment, which might be counterintuitive. I would have assumed that an osmotic stress could affect the membranes severely, which cannot be excluded, but the NMT1 might not have a major role in this specific stress response, however, its exact role is still unknown. It was not simply a stress-responsive protein, the protein level of NMT1 seemed to be regulated by the nature of the environmental impact and it was also dependent on the spatial expression. A good

example for that were the nutrient deficient treatments, where it had an elevated abundance in the root, but it had a strong negative fold change in the shoot.

Temperature shift

Increasing the temperature by 5°C may not have been a stress for the plants. Leaf area and biomass were increased, there was only a minor group of stress-related proteins, which increased their abundance and other similar response proteins even decreased their concentrations. While the starch level was elevated at the end of the day in 25°C, it was almost completely broken down till the end of the night, and the soluble sugar content remained on a wild type level. The higher starch level was probably not the result of a stress response process, it could be considered more as sign of a better photosynthetic efficiency. A bigger starch reservoir for the night could have promoted the increased growth. The proteome and growth analysis revealed an interesting antagonistic response between the plants exposed to 15°C and 25°C. It was less reflected in the carbohydrates, however, the soluble sugar content was increased in 15°C, but they may have served rather as osmoprotectants, they might have not been supplied for growth, because it was almost immediately slowed down as the temperature dropped. The elevated carbon pool (starch and sugar) was not invested in growth at 15°C suggesting that temperature optimum of *Arabidopsis* might be much narrower as we earlier anticipated. The antagonistic changes of the proteome and the specific proteins appeared to be temperature-dependent. The identified proteins can be interesting for follow up experiments, some of them might be even temperature sensors. The in-depth characterization of these target proteins might also provide insights about rate-limiting enzymes, which can be differently regulated depending on the temperature.

Overwhelming part of cold stress research focuses on low or even freezing temperatures, but as our research indicates, even a subtle drop in temperature can drastically affect the physiology of the plants, which in the case of crop plants can ultimately decrease the yield. While there are cold-tolerant crops (i.e. barley), there are cold-sensitive ones (i.e. maize), which are widely spread in temperate climate, where similar temperature changes happen regularly.

Impact of osmotic stress and nutrient deficiency

As expected, plants exposed to nutrient deficient environment displayed a distinct phenotype; growth, proteomic changes and metabolite levels compared to the wild type were quite different from the other moderate abiotic stress treatments. The observed biomass allocation and carbohydrate metabolism in phosphate and nitrate deficiency had been reported before confirming our observations.

Interestingly, in some aspects the osmotic stress had a nutrient deficient-like effect, as it was revealed in the proteomic clustering analysis. The PEG-treatment might have hindered the uptake of nutrients, which are present in the surroundings of the roots inducing a similar effect as if these nutrients would have been deprived. It had been hypothesized that the salt and osmotic stress would invoke a similar response, but our analysis could not confirm this hypothesis. The overlap between the proteins with significantly high fold change was low, the sugar concentration was different at the end of the night and starch level was decreased at the end of the day in the elevated salt concentration, which was an exception among the six treatments. The additional large PEG molecules in the growth media, which probably did not enter into the plant cells, might have induced rather a local, root-specific response, while the salt ions were taken up by the plants and reached the distant source tissues inducing a systemic response.

Tissue specificity

The tissue specific proteomic experiment also revealed that some of the isoforms might be ubiquitously expressed in the whole plant. On the other hand, some are only present in the shoot or the root and the regulation of the proteins in the two organs turned out to be quite distinct. The biomass and the carbohydrate measurements showed that the plants in an unfavorable environment allocates the limited resources preferably into the roots

Changes of protein concentration of the primary carbohydrate enzymes

While the concentration of certain proteins changed dramatically, the carbohydrate enzymes were less affected, however, the starch and sugar level changed at the end of every treatment. The lesser number of major metabolic carbohydrate proteins in our proteomic experiment might imply that their regulation does not necessary include changes in abundance, their

enzyme activity can be increased or decreased without changing their protein amount, which can involve posttranslational modifications (i.e. phosphorylation, methylation, acetylation), formation of protein complexes, etc. It might be more efficient to adjust these factors to modify enzyme activity than enhance protein synthesis or breakdown, which are slower and more costly. A phosphoproteomic approach might be a more suitable way to investigate, how the proteins of the carbohydrate metabolism are affected and regulated in environmental perturbations.

The plastidial Fructose 1,6-Bisphosphate Aldolases

The tissue specificity can be a strong driving factor to promote multiplication of genes in the plant genome, which can further result even in different intracellular function. Or the multiplication of genes might have allowed the formation of tissues in the plants. Evolutionary-linked proteins may not be only expressed in different organs and still responsible for the same metabolic process, but over the time they might have gained an alternate function. Our analysis of the plastidial fructose 1,6-bisphosphate aldolase (FBA) gene family, which has three different isoforms in the plastid of Arabidopsis thaliana (AtFBA1, AtFBA2 and AtFBA3), showed a tissue specific expression. While FBA1 and FBA2 are functional in the green photosynthesizing tissues, the FBA3 is localized mainly in the vasculatory. The phylogenetic analysis implied that FBA3 might be the ancestral form and after unknown events, which involved at least one duplication process, FBA1 and FBA2 evolved with the vascular plants. The single plastidial FBA gene in the photosynthesizing ancient algae and later in the early terrestrial plants (i.e. mosses) might have proven enough to fulfill different physiological roles, but in the vascular plants one copy might have not been sufficient.

The colonization of the lands by the plants ca. 470 Ma years ago was an incomparable event in the history of the planet, which gave rise of three-dimensional multicellular organisms, and subsequently included the specialization of tissues and organs, like the vasculature and photosynthesizing leaves together with the root, seeds and flower (Pires and Dolan, 2013). The first colonizing plants may have had the necessary minimal genetic pool, but these genetic resources must have been re-used, reassembled or expanded for the subsequent adaptation to the terrestrial lifestyle (Pires and Dolan, 2013). The spatial separation might have allowed the intracellular specialization too, although the order of the evolutionary processes could

have also occurred the other way around. In the case of the plastidial FBAs, FBA1 and FBA2 participate in the Calvin-Benson cycle in photosynthetic cells and FBA3 might have a role outside the Calvin-Benson cycle, in a glycolytic-like process in the plastid of the transport tissues. The exact role of the FBA3 is still unclear, further experiments could be carried out in the future. However, this functionalization was conserved in every plant species, which were involved into the phylogenetic analysis, suggesting the essential role of this spatial and metabolic separation from the early evolution of the plants.

Intracellular compartmentalization

On a cellular level, compartmentalization can have a similar effect as tissue specificity. Some isoforms can even lose their catalytic activity and acquire a different physiological role (i.e. signaling). Enzymes of the carbohydrate metabolism are good subject of this switch in cellular function, because sugars act as signaling molecules too. The hexokinase and β-amylase gene family are well-described examples (Jang et. al, 1997; Reinhold et. al, 2011). For example, there are nine β-amylases in Arabidopsis thaliana, and two of them are localized to the nucleus and act as a transcription factor.

One can speculate that the FRK7 protein can be a candidate for further analysis in signaling. It was a relatively abundant protein, but it had been reported that it had a low catalytic capability (Riggs et. al, 2017). Nevertheless, the growth of the respective single knock-out mutant was restored to the wild type level in elevated salt concentration indicating that it might not be a simple pseudogene, but this hypothesis must be further tested.

Reference

BeGora, M. D., Macleod, M. J. R., McCarry, B. E., Summers, P. S., & Weretilnyk, E. A. (2010). Identification of phosphomethylethanolamine N-methyltransferase from Arabidopsis and its role in choline and phospholipid metabolism. *Journal of Biological Chemistry*, *285*(38), 29147–29155.

Dupae, J., Bohler, S., Noben, J.-P., Carpentier, S., Vangronsveld, J., & Cuypers, A. (2014). Problems inherent to a meta-analysis of proteomics data: a case study on the plants' response to Cd in different cultivation conditions. *Journal of Proteomics*, *108*, 30–54.

Eastmond, P. J., Quettier, A.-L., Kroon, J. T. M., Craddock, C., Adams, N., & Slabas, A. R. (2010). PHOSPHATIDIC ACID PHOSPHOHYDROLASE1 and 2 regulate phospholipid synthesis at the endoplasmic reticulum in Arabidopsis. *The Plant Cell*, *22*(8), 2796–2811.

Jang, J. C., León, P., Zhou, L., & Sheen, J. (1997). Hexokinase as a sugar sensor in higher plants. *The Plant Cell*, 9(1), 5–19.

Pires, N. D., & Dolan, L. (2012). Morphological evolution in land plants: new designs with old genes. *Philosophical Transactions of the Royal Society B: Biological Sciences*, 367(1588), 508–518.

Reinhold, H., Soyk, S., Šimková, K., Hostettler, C., Marafino, J., Mainiero, S., … Zeeman, S. C. (2011). β-Amylase–Like proteins function as transcription factors in Arabidopsis , controlling shoot growth and development. *The Plant Cell*, 23(4), 1391–1403.

Riggs, J. W., Cavales, P. C., Chapiro, S. M., & Callis, J. (2017). Identification and biochemical characterization of the fructokinase gene family in *Arabidopsis thaliana*. *BMC Plant Biology*, 17(1), 83.

Wisniewski, J. R., Zougman, A., Nagaraj, N., & Mann, M. (2009). Universal sample preparation method for proteome analysis. *Nat Methods*, *6*(5), 359–362.